Spring 2014

Synthesis of polymers with the potential to release H2S: polydicyclopentadiene nanoporous membranes

Tyler Richard Long
University of Iowa

SYNTHESIS OF POLYMERS WITH THE POTENTIAL TO RELEASE H_2S: POLYDICYCLOPENTADIENE NANOPOROUS MEMBRANES

by

Tyler Richard Long

A thesis submitted in partial fulfillment
of the requirements for the Doctor of
Philosophy degree in Chemistry
in the Graduate College of
The University of Iowa

May 2014

Thesis Supervisor: Associate Professor Ned B. Bowden

Graduate College
The University of Iowa
Iowa City, Iowa

CERTIFICATE OF APPROVAL

_____

PH.D. THESIS

_____

This is to certify that the Ph.D. thesis of

Tyler Richard Long

has been approved by the Examining Committee
for the thesis requirement for the Doctor of Philosophy
degree in Chemistry at the May 2014 graduation.

Thesis Committee:_____
Ned B. Bowden, Thesis Supervisor

_____
Mark A. Arnold

_____
James B. Gloer

_____
F. Christopher Pigge

_____
Aliasger K. Salem

To my family Emmett, Madalyn, Brian, Jessica, Rebecca, and my wife Sarah.

Success is not final, failure is not fatal: it is the courage to continue that counts.

Winston Churchill

ACKNOWLEDGMENTS

First, I would like to thank my adviser Dr. Ned Bowden for bringing me into his group and turning me into a scientist. I would also like to thank our collaborator Dr. Aliasger Salem, for the work on the H_2S project, the rest of my committee members, and Dr. Hien Nguyen. I would like to thank my professors from undergrad, especially Dr. Charles Cornett for sending me to Japan.

Second, I would like to thank all the Bowdenites past and present for being a great group and team. Some other grad students that I used to bounce ideas off of included Joe Topczewski and Ross Bemowski. Also, Amaraporn Wongrakpanich for make the microparticles and doing the degradation experiments, and I would like to thank Justine Olson for proofreading.

Next, I would like to thank my family for their support and encouragement. Especially my parents for the love and support, and for all the extra time, effort and money needed to get me through school. It is much easier to take risks, especially when you have someone making sure you land on your feet. Also a special thanks for my siblings Brian, Jessica, and Rebecca for keeping me from becoming too nerdy, and my cousin Jonathan for not letting me die in undergrad.

Last but not least I would thank my wife Sarah for all the love and support during graduate school.

TABLE OF CONTENTS

LIST OF TABLES

LIST OF FIGURES

CHAPTER 1

INTRODUCTION

Hydrogen Sulfide and Its Role in the Body

In the past few decades much research has gone into the pathophysiological and pharmacological role of gasotransmitters. The most well-known gasotransmitter is nitric oxide (NO), but more recently hydrogen sulfide (H_2S) has been gaining recognition as an important signaling molecule. H_2S has been shown to have numerous physiological effects and to play an important role in a variety of biological systems and diseases.[1-7] For these reasons, H_2S is being actively explored for its possible beneficial and therapeutic effects. This chapter will focus on the role that H_2S plays in the body and the positive effect a therapeutic dose of H_2S has on fighting numerous diseases. This chapter will also explore new H_2S releasing prodrugs and drug hybrids currently being investigated, as well as methods for detecting H_2S *in vivo* and *in vitro*. Finally, this chapter will discuss the importance of developing of a system that releases H_2S *in vivo* over one day to several weeks.

Chemistry of H_2S

H_2S is best-known for its horrible smell and toxicity, but the unique chemistry of H_2S *in vivo* is what makes it an exciting drug candidate. The structure of H_2S is similar to the structure of water, but differences between sulfur and oxygen yield different bond lengths and angles as seen in Figure 1.1. Differences in electronegativity and size also yield vastly different physical properties for H_2S and H_2O. For example, the boiling point of H_2S is -60.7 °C compared to 100 °C for water. H_2S will dissolve readily in water up to about 117 mM and is a weak acid with a pK_{a1} of 6.77.[4] This is significantly lower than the

pK_a of 15.7 for water, and even lower than alkylthiols which have pKa values around 10.[4] Approximately 80% of H_2S in solution exists as HS^- under normal physiological conditions at a pH of 7.4[2], because the pKa_2 of H_2S is 12, the concentration of S^{2-} under negligible in physiological conditions.[6] H_2S is also 5 times more soluble in lipophilic solvents than in water, which increases the ability of H_2S to pass through cell membranes.[5]

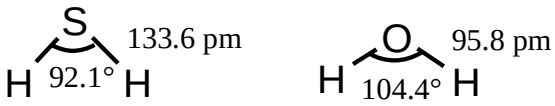

Figure 1.1. The structures, bond angles, and bond lengths of H_2S and H_2O.[7]

The toxic effects of H_2S are well known and the physical effects at different concentrations are described in Table 1.1. H_2S is considered a broad-spectrum poison because it is able to affect all systems of the body similar to hydrogen cyanide and carbon monoxide. H_2S becomes poisonous when it reaches a concentration (approximately 50 µM), at which point it overwhelms the body's natural ability to oxidize it to safe sulfur species. When the concentration of H_2S surpasses 50 µM, H_2S will complex to the iron in mitochondrial cytochrome enzymes. This prevents cell respiration and leads to cell death.[1] At lower concentrations (such as less than 20 µM), the mitochondria are able to safely oxidize H_2S indefinitely.[1] One of the challenges in this field is that the reported concentration of H_2S *in vivo* can vary by several orders of magnitude depending on which detection method is used. The challenge of accurately measuring the concentration of H_2S will be discuss at length later in this chapter, but the growing consensus is that its *in vivo* concentration is less than 1 µM.

Table 1.1. Toxic effects of H_2S

Ambient H_2S, ppm	Equivalent Total Plasma Sulfide, μM[a]	Effects
0.01-0.3	0.003-0.1	Threshold for detection
1-3	0.3-1	Offensive odor, headaches
10	3.3	8-h occupational exposure limit in Alberta, Canada
15	4.9	15-min exposure limit in Alberta, Canada
20-50	6.5-16.2	Eye and lung irritation
100	32.5	Olfactory paralysis
50-500	162.3	Pulmonary edema
500	162.3	Sudden unconsciousness, death within 4 to 8 h
1000	324.5	Immediate collapse, breathing ceases within several breaths

Source: Table 1.1 was taken from Olson.[3] a) Equivalent plasma calculated after Whitfield et al.[8] Assuming H_2S equilibrates across the alveolar membranes,[9] Henry's Law constant for H_2S at 37°C, at 140 mM NaCl is 0.0649 $Matm^{-1}$,[10] and 20% of total sulfide exists as H_2S gas.[2]

H_2S: The Third Gasotransmitter

Gasotransmitters are small molecules that have the ability to move across biological membranes and control biological pathways and functions, they are potentially toxic, their biosynthesis and catabolism are regulated by endogenous processes, and they possess short half-lives. H_2S has become recognized as the third gasotransmitter after nitric oxide (NO) and carbon monoxide (CO). NO is the most intensely investigated gasotranmitter because it was the first gasotransmitter discovered and has been shown to play a large role in controlling cardiovascular functions. The fundamental role of NO is to relax the blood vessels which regulate blood pressure and to reduce hypertension. Several molecules that release NO are being developed and investigated for their ability to release therapeutic amounts of NO.[11] CO, on the other hand, does not seem to be an interesting target in the pharmaceutical industry. Early studies indicated that H_2S had almost all of the beneficial cardiovascular effects of NO, but NO is

known to produce harmful Reactive Oxygen Species (ROS), whereas H_2S is known as an ROS scavanger.[1,2]

The biosynthesis of H_2S (Figure 1.2) is dependent on four enzymes: cystathionine beta-synthase (CBS), cystathionine gamma-lyase (CSE), cysteine aminotransferase (CAT), and 3-mercaptopyruvate sulfurtransferase (3-MST). Cysteine consumed in the diet is the primary source of sulfur for H_2S.[1] CBS and CSE are responsible for the majority of H_2S produced in the body and are found in a variety of different types of tissue including the liver, kidney, heart, vasculature, and brain,[6] but CBS and CSE are not found in equal concentrations in these tissues and throughout the body.[1] For example, CBS is responsible for H_2S production in the central nervous system, and CSE is more prevalent in the cardiovascular system. Some tissues require both CBS and CSE for the production of H_2S, such as the liver and kidneys.[6] The CSE in the cardiovascular system can produce H_2S at a rate of 3-6 nanomoles/min/g of tissue.[1]

H_2S is consumed in the body by several mechanisms shown in Figure 1.3. One way it is consumed is as a reducing agent that reacts with ROS – this is typically viewed as a benefical effect of H_2S. The mitochondria are responsible for the consumption of most of the H_2S produced *in vivo* through several enzymatic steps using quinone oxidoreductase, S-dioxygenase and S-tranferase to form thiosulphate $S_2O_3^-$.[1] Thiosulphate is converted to sulphite (SO_3^{2-}) with the rhodanase enzyme, the same enzyme that converts cyanide (CN^-) to thiocyanate (SCN^-).[1] Sulphite is then finally converted to sulphate by sulphite oxidase. H_2S can also interact with methemoglobin in the blood to form sulphemoglobin, and a small amount of H_2S is methylated by S-methyltransferase (TSMT) to methanethiol then to dimethylsulphide in the cytosol.[1]

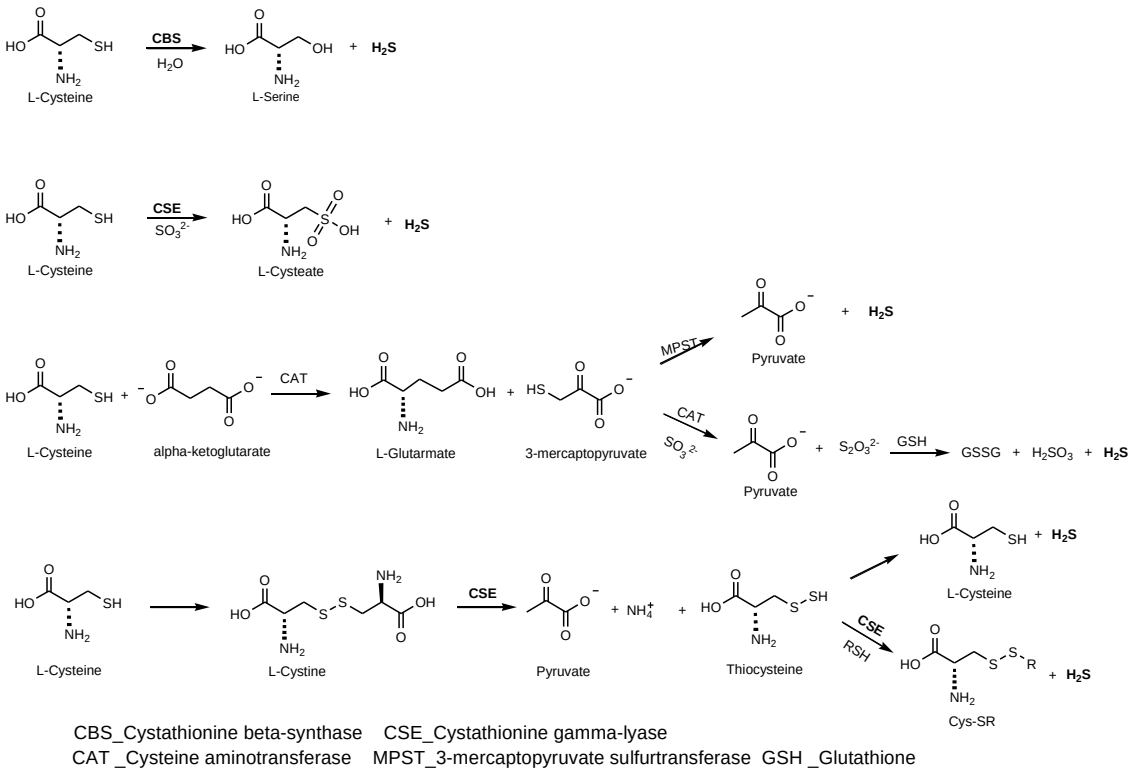

Figure 1.2. The biosynthesis of H_2S from cysteine

The beneficial biological effects attributed to H_2S are proposed to be due to at least two different mechanisms. First, H_2S has the ability to neutralize ROS. H_2S is a well-known reducing agent and reacts with at least four different reactive oxygen species: hydrogen peroxide, peroxynitrite, superoxide radical anion, and hypochlorite.[2] The neutralization of these highly reactive compounds by H_2S can protect proteins and lipids from damage. H_2S has also been shown to reduce oxidative stress in neuroblastoma cells by increasing the levels of glutathione (GSH, a major cellular antioxidant), by enhancing cysteine transport and redistribution of GSH to the mitochondria.[12] More work is needed in this field because the antioxidant mechanisms that are currently known do not fully explain the antioxidant effect of H_2S.

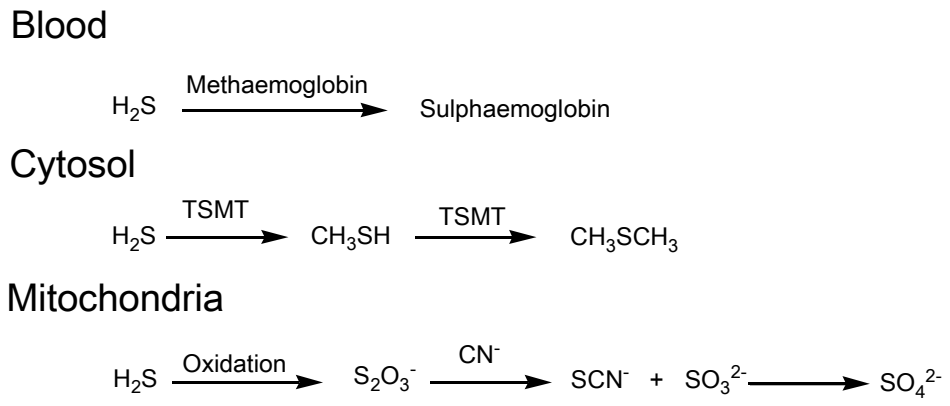

Figure 1.3. Catabolic pathways of H_2S in blood, cytosol, and mitochondria. (thio S-methyl transferase – TSMT)

The second known beneficial biological effect of H_2S is that it can mediate the activation of adenosine triphosphate (ATP)-sensitive potassium channels (K_{ATP}). K_{ATP} plays a pivotal role in regulating the biological functions in several types of tissues including pancreatic beta, neurons, myocardial, smooth muscle and skeletal cells.[13] The activation of K_{ATP} channels is dependent on the intracellular concentration of ATP and adenosine diphosphate (ADP). High levels of ATP inhibit K_{ATP} channel activity. If the cell is under reduced energetic metabolism conditions the amount of ADP increases which makes the ATP/ADP ratio drop and activates the K_{ATP} channel allowing an outward flow of potassium ions.[1] The interaction between H_2S and the K_{ATP} channel is poorly understood. It has been hypothesized that H_2S decreases the intracellular ATP concentration, consequently decreasing the ATP/ADP ratio and activating the K_{ATP} channel.[1] This metabolism-dependent activation mechanism makes the K_{ATP} channel a key factor in regulating biological functions, including heart activity, smooth muscle tone, insulin secretion, and neurotransmitter release.[14]

Initial work with H_2S has shown has it has wide potential to treat many diseases. There are a variety of different diseases that H_2S may affect including: high blood pressure, hypertension, atherosclerosis, myocardial injury, ischemia, angiogenesis, asthma, colitis, diabetes, Alzheimer's, Parkinson's, cancer, and erectile dysfunction.[2,15,16] By opening the K_{ATP} channel, H_2S causes the relaxation of vascular smooth muscle cells which has been shown to increase blood flow, lower blood pressure, decrease hypertension, and prevent atherosclerosis and ischemia. The increased blood flow may also be used to treat erectile dysfunction. The anti-inflammatory effects of H_2S could help treat asthma, Alzhemer's, and Parkinson's.[2] The opening of K_{ATP} channel by H_2S in pancreatic beta cells may be able to regulate insulin metabolism and glucose levels to treat diabetes.[2]

H_2S Donors in Medicine

The ideal prodrug to release H_2S should be non-toxic, generate H_2S at a slow and steady rate, have a localized release of H_2S, and release H_2S with other drugs if desired. The most direct source of H_2S is an aqueous solution of hydrosulphide and sulphide salts, such as NaSH and CaS, which have been used for experimental purposes but are not suitable for clinical uses. The rapid release of H_2S may have adverse effects such as a dramatic and dangerous decrease in blood pressure. In animal testing, NaSH has been used to establish some of the benefits of H_2S, such as reducing hypertension in spontaneously hypertensive rats and reducing blood pressure.[7]

Natural H_2S Donors

Garlic is one of several natural dietary supplements that are known to release H_2S. The cardiovascular benefits of garlic are well-known and have been credited with reducing several risk factors of cardiovascular diseases, including

high blood pressure, high cholesterol, an increase in ROS, platelet aggregation and blood coagulation.[17] The compound in garlic that is considered to be responsible for its pharmacological activity is allicin, which is produced from the amino acid alliin by the enzyme alliinase when garlic is crushed (Figure 1.4). In aqueous solution allicin rapidly decomposes to diallylsulfide, diallyl disulfide (DADS), diallyl trisulfide (DATS) and ajoene.[18]

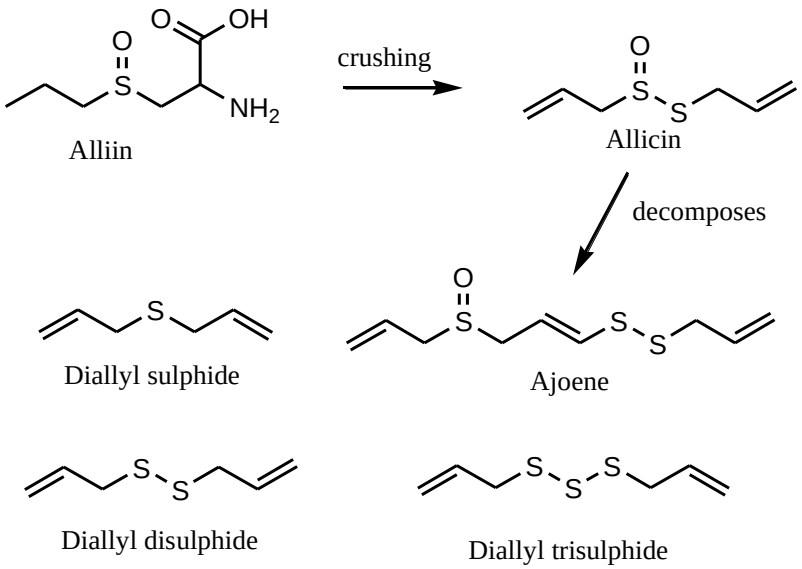

Figure 1.4. The formation of allicin and its decomposition products.[1]

The polarographic trace in Figure 1.5 show the release of H_2S from DATS and DADS in the presence of (GSH). DATS releases about three times more H_2S than DADS, whereas allyl sulphides and non-allyl disulphides do not release any measurable amount of H_2S. It should be noted that the release of H_2S is rapid, with a peak concentration of H_2S occurring in a matter of minutes.

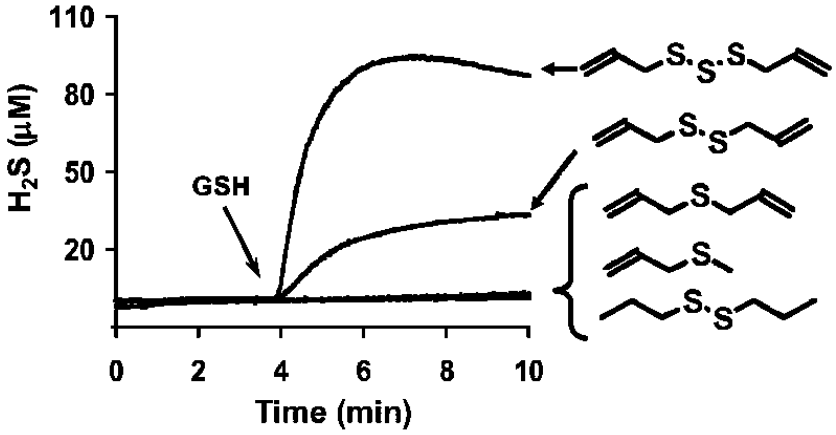

Figure 1.5. The polarographic trace of H_2S production in anoxic 10 mM PBS with 50 µM DTPA, with 100 µM each diallyl trisulphide, diallyl disulphide, diallyl sulphide, allyl methylsulphide and dipropyl disulphide and the addition of 2 mM of glutathione at the arrow. This figure was taken form Benavides et al.[19]

GSH is a tripeptide that is responsible for neutralizing ROS in the body and is required for the release of H_2S from DADS and DATS. The mechanism for H_2S release from DADS is illustrated in Figure 1.6 and occurs via multiple pathways. The two types of chemical reactions to convert DADS to H_2S are simple thiol/disulphide exchange and nucleophilic substitution. The release of H_2S from DADS requires a large amount GSH and converts GSH to GSSG. The consumption of garlic as a dietary supplement has its benefits, but it does not fit the profile of an ideal H_2S releasing drug because of the quick release of H_2S and its dependence on GSH.

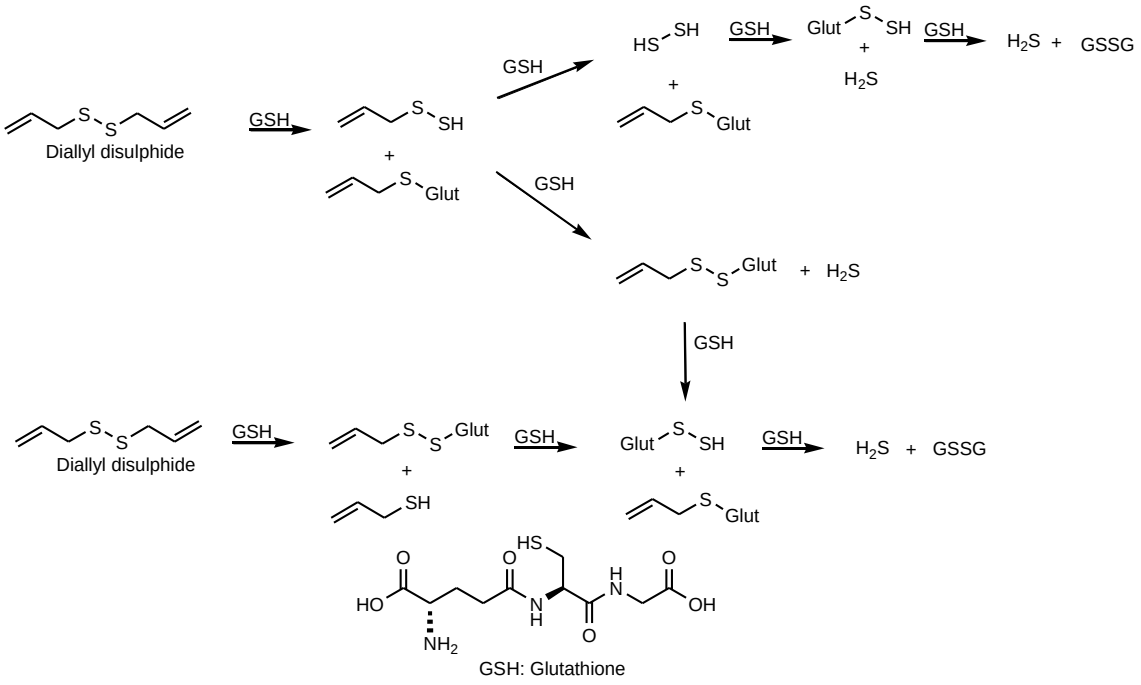

Figure 1.6. Mechanism for the production of H_2S from glutathione and diallyl disulphide

Synthetic Drugs that Release H_2S

There are several synthetic H_2S-releasing drugs that have been developed and are being used in pharmacological studies. The drug that releases H_2S over the longest period of time is GYY4137, the synthesis of which is shown in Figure 1.7. GYY4137 was originally used in the vulcanization of rubber about 50 years ago, but has recently shown promise as a water-soluble H_2S releasing drug.

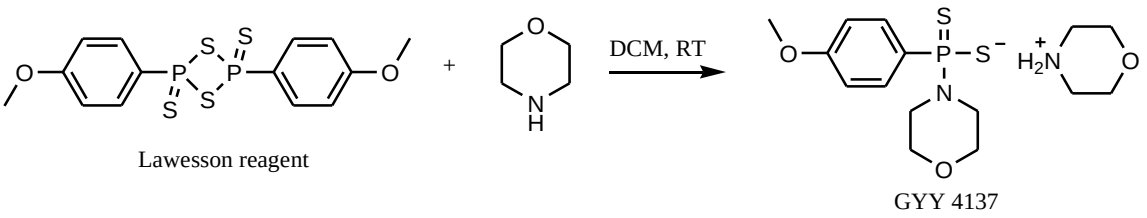

Figure 1.7. Synthesis of GYY4137 from Lawesson's reagent.

GYY4137 has been shown to release H_2S in biological systems, buffered solutions containing cysteine, or at pH 3.0.[20,21] The effectiveness of GYY4137 to act as an H_2S releasing drug was tested on rats *in vivo* and on tissue *in vitro* and compared to NaSH. The treatment of rat vascular smooth muscle cells with GYY4137 at a concentration of up to 100 µM did not show any toxicity for up to 72 hours.[20] To test the ability of GYY4137 to relax vascular smooth muscle, the aortic rings of a rat were isolated and exposed to either GYY4137 or NaSH. The use of NaSH caused a rapid and reversible relaxation of the aortic ring that only lasted about 20 to 30 seconds, whereas the use of GYY4137 caused the relaxation of aortic rings, but with a slower onset of approximately 10 min, and the effect lasted for about 40 min.[20] GYY4137 and NaSH have also been shown to lower blood pressure in anesthetized rats. The administration of NaSH caused an immediate drop in blood pressure and only lasted for 10 to 30 seconds, whereas the treatment of GYY4137 caused a slow and steady decrease in blood pressure that was apparent at 30 min and lasted for 120 min.[20]

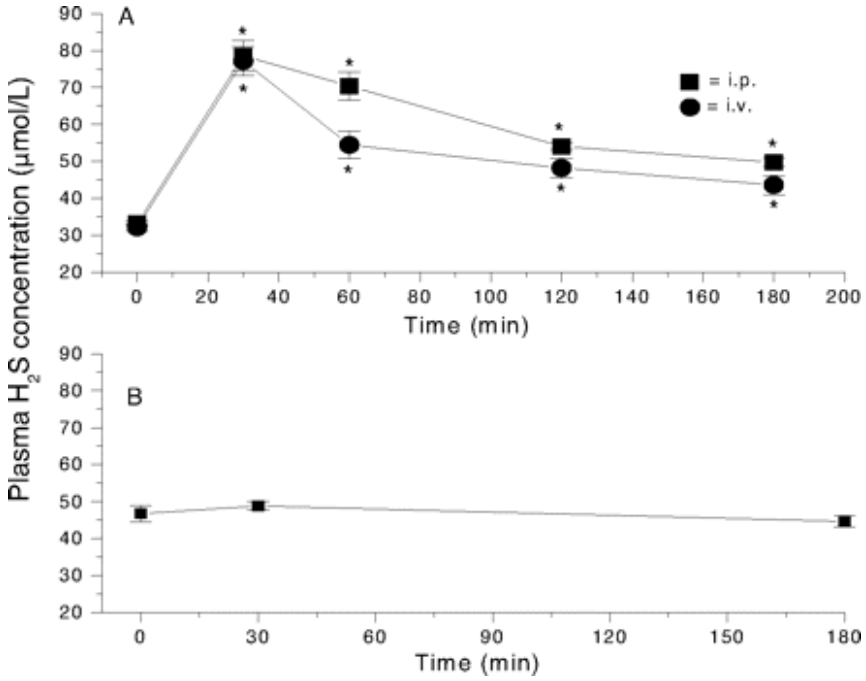

Figure 1.8. The plasma concentration of H_2S after injection (time=0)
a) GYY4137 (133 µmol/kg) ether intravenous (i.v.) or intraperitoneal (i.p.).
b) NaSH (20 µmol/kg) ether intravenous (i.v.).
Source: figure taken from Ling Li et al.[20]

The rise in plasma concentration of H_2S in rats that were injected with GYY4137 was plotted and showed an increase in concentration of H_2S over the first 30 min, but it slowly decreased for the next 150 min and remained elevated at the conclusion of the experiment (Figure 1.8).[20] The concentration of H_2S was determined by first withdrawing 0.5 mL of blood from the rat at the respective time intervals after the injection of GYY4137 or NaSH. Next, the anticoagulant heparin was added to the blood before it was centrifuged to separate the plasma. Finally, H_2S in the plasma was reacted with zinc acetate, and the concentration of ZnS was determined by spectrophotometric analysis. This method was used to determine the combined concentrations of the sulfur species H_2S, HS^-, and S^{2-}. This method of detection of H_2S is no longer believed to be as reliable as more

recent methods, but it can be used to show a relative increase in the concentration of H_2S. This study and others demonstrate that GYY4137 has promise as a drug that releases H_2S, it was non-toxic, and it has a longer release profile than other drugs that releases H_2S. One limitation is that, as a small molecule, GYY4137 would be cleared from the body rather quickly by the kidneys.

H_2S-Releasing Drug Hybrid

Other drugs that releases that have been developed include 5-(4-hydroxyphenyl)-3H-1,2-dithiole-3-thione (DTT) and 4-hydroxythiobenzamide (Figure 1.9). These H_2S releasing drugs have been mostly used in conjunction with well-known drugs as pharmacological hybrids (Figure 1.10). These hybrids release a pharmaceutical drug and DTT or 4-hydroxythiobenzamide by hydrolysis of an ester bond. The synergy of H_2S with established drugs increases its possible application in medicine. Drug synergy occurs when the combination of two or more drugs enhances the therapeutic impact or reduces side-effects. For example, when codeine is mixed with ibuprofen, it enhances the pain relief effect of codeine.

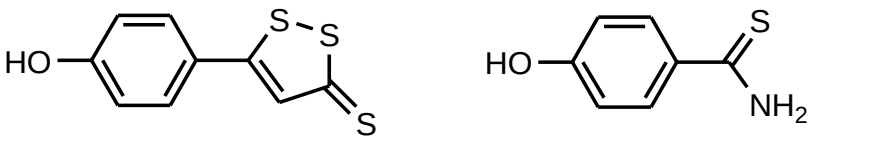

DTT 4-Hydroxythiobenzamide

Figure 1.9. Structure of 5-(4-hydroxyphenyl)-3H-1,2-dithiole-3-thione (DTT) and 4-hydroxythiobenzamide.

DTT and 4-hydroxythiobenzamide are excellent candidates for applications as drug hybrids. These molecules release H_2S in biological systems and the phenol group provides a good handle to attach to known drugs through an ester linkage that can be easily cleaved under biological conditions. Early examples of H_2S-releasing hybrids were the combination of non-steroidal anti-inflammatory drugs (NSAIDs) with DTT. H_2S can reduce gastric injury by opening K_{ATP} channels which improves mucosal blood flow and the stimulation of mucus production. The increased mucus production protects against gastric injury and may reduce some of the side effects of long term use of NSAIDs. The H_2S-releasing NSAIDs (Figure 1.10) shows a marked reduction in gastric damage score when compared to the parent NSAIDs.[22,23]

This technology has been further developed by the combination of an NO and H_2S releasing hybrid that has been investigated as a multi-target cardiovascular agents.[11] NO and H_2S both have the ability to open K_{ATP} channels and protect against gastric injury. Recently, NSAIDs that release both NO and H_2S (these NSAIDS are termed “NOSH”) have been developed to increase the effectiveness of aspirin in the cardiovascular system while reducing its negative side effects.[24] One example of a NOSH aspirin hybrid is depicted in Figure 1.11, and NOSH aspirin hybrid have also been developed with varying NO-and H_2S-releasing functional groups.

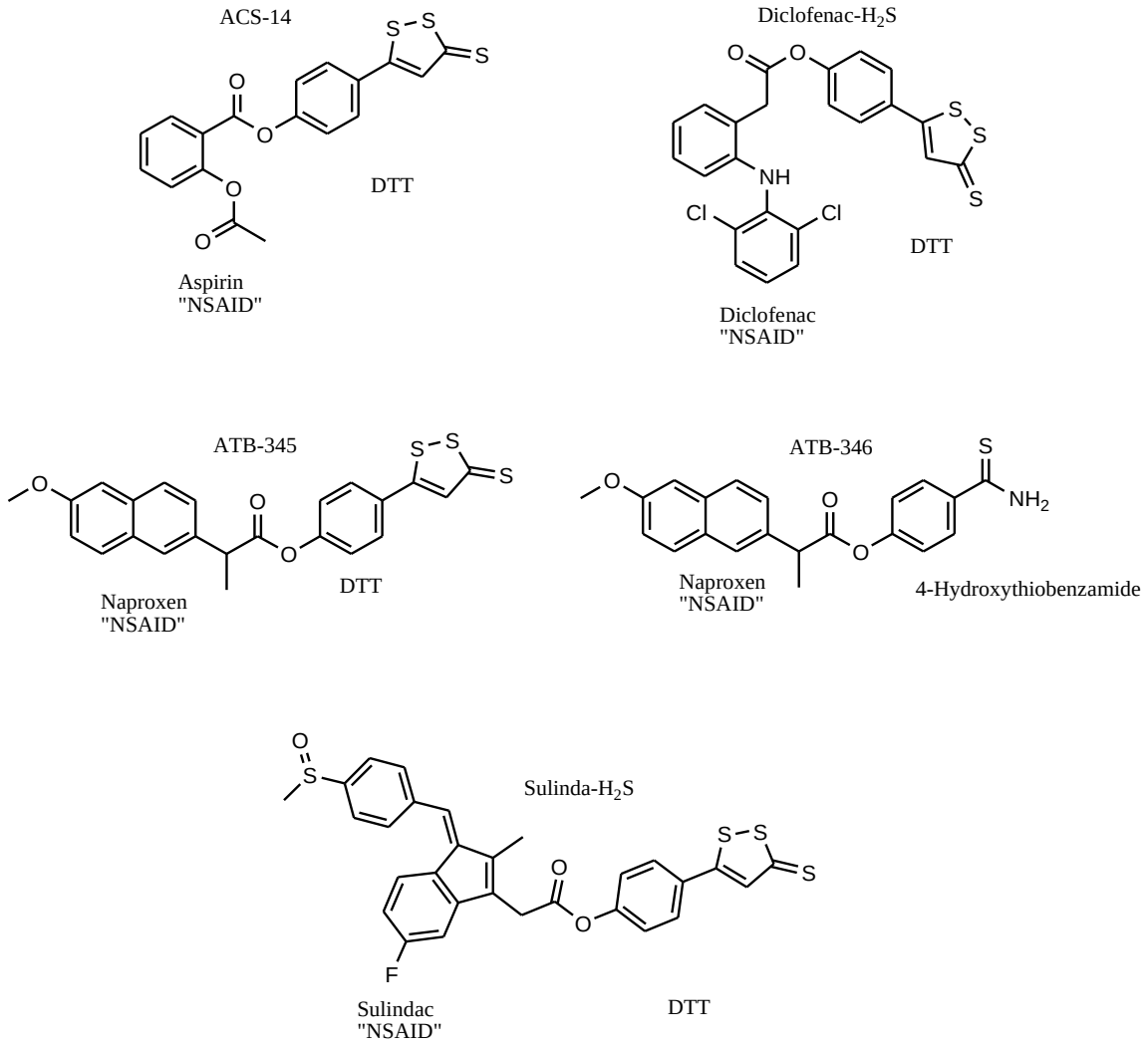

Figure 1.10. Structure of H_2S-releasing hybrids of aspirin, diclofenac, sulindac, and naproxen.

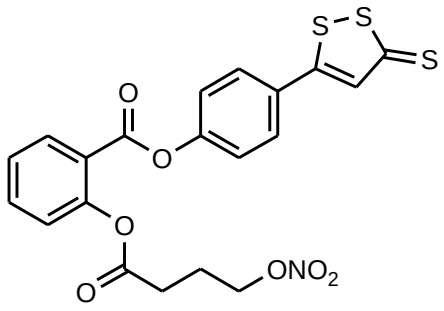

NOSH Aspirin

Figure 1.11. A pharmaceutical hybrid that can release NO, H_2S, and aspirin.

Some of the other H_2S-releasing pharmacological hybrids include H_2S-EXP3174 (the hybrid of Sartans) and ACS 6 (the hybrid of Sildenafill) (Figure 1.12). Sartans is widely used to treat hypertension, and H_2S also has been shown to treat hypertension, but by a different mechanism. The combination of these drugs has been proposed to improve the antihypertensive effects.[1] Sildenafill is well-known for the treatment of erectile dysfunction. The addition of DTT to release H_2S (which is known to relax smooth muscle cells) has shown an increased effectiveness of sidenafill in animal testing.[25] Sildenafill also has the potential to treat acute respiratory distress syndrome and H_2S may increase its effectiveness by reducing oxidative stress.[26]

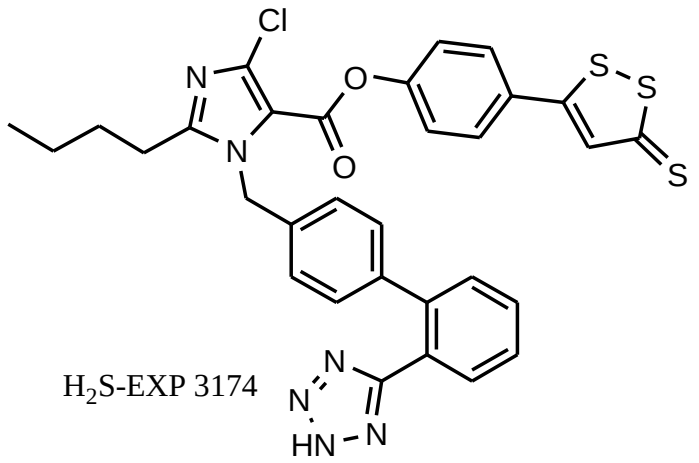

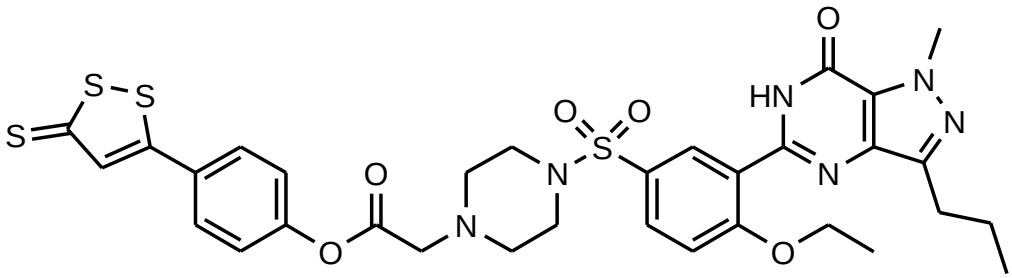

ACS 6

Figure 1.12. H_2S releasing sartans (H_2S-EXP 3174) and sidenafill (ACS 6).

The synergy of H_2S with well-known and important pharmaceutical agents makes the ability to combine them an important consideration when designing any new H_2S delivery systems. The H_2S-releasing hybrids discussed in this chapter show that benefits exist when H_2S is combined with pharmaceutical agents, but these hybrids lack the ability to release H_2S over a significant period of time. When the H_2S-releasing hybrid of aspirin (ACS-14) was given to rats, the H_2S concentration spiked at 5 minutes and only remained elevated for 40 minutes.[23] The next advance in medicinal H_2S that is needed is the development

of a system that releases H_2S slowly and can be easily coupled with a known drug without altering the drug.

Detection of H_2S

The detection of H_2S at biologically relevant concentrations and in biological systems remains a major challenge in this field. Since H_2S has emerged as an important biological signaling molecule a significant amount of effort has gone into developing new and better ways to detect H_2S both *in vivo* and *in vitro,* but there is still much work to be done. Studies published before 2000 reported the concentration of H_2S in plasma as undetectable (less than 1 µM).[3] Since 2000, the reports of concentration of H_2S in plasma have spanned over 3 orders of magnitude and have been reported as high as 300 µM.[6] The high concentrations, greater than 50 µM, are unrealistic because H_2S would be toxic at these high levels, and blood would smell of H_2S at concentrations as low as 1 µM.[3] The most common methods that were used to determine the concentration of H_2S between 2000 and 2010 were the 'methylene blue method' and 'S^{2-} sensitive electrode method' which produced a wide range of H_2S concentrations from 8 µM to 301 µM in the blood or plasma of rat, mouse, or human.[3]

The large range and unrealistically high H_2S concentrations demonstrated the need for new H_2S detection methods. Several H_2S detection methods that measure the concentration of H_2S directly have been developed more recently and have reported much lower concentrations of H_2S *in vivo*, including a polarographic H_2S sensor and gas chromatography (GC). There has also been the development of a variety of chemical detection methods that include several different fluorescent probes, colorimetric probes, and a monobromobimane

(MBB) probe. Some of the newer methods have not yet reported data for the concentration of H_2S in blood or plasma due to real or anticipated difficulties with data collection. The growing consensus however, based on the concentrations of H_2S that have been reported, is that the concentration of H_2S *in vivo* must be less than 1 µM.[3]

One of the first methods to detect H_2S is the methylene blue method which reacts *N,N*-dimethyl-*p*-phenylenediamine with the H_2S in the blood or plasma to yield methylene blue (Figure 1.13).[27] The concentration of methylene blue can be measured by UV-Vis spectroscopy to determine the concentration of H_2S. The concentrations reported in blood or plasma range from 8 µM to 301 µM.[6] These concentration could be inflated by the liberation of H_2S from acid-labile sulfur pools.[27]

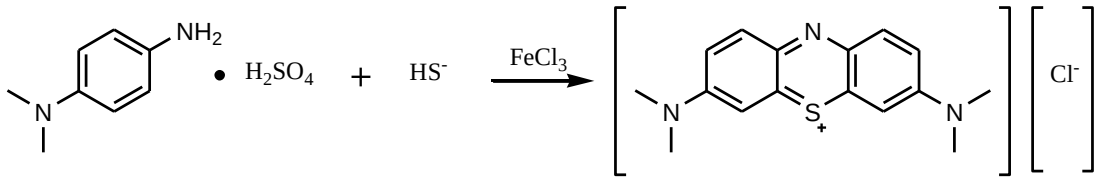

N,N-dimethyl-p-phenylenediamine sulfate salt

methylene blue

Figure 1.13. Reaction of *N,N*-dimethyl-*p*-phenylenediamine with HS^- to form methylene blue.

The S^{2-} sensitive electrode method uses a strong base and a reducing agent to convert H_2S and HS^- to S^{2-}, which is detected by a S^{2-} sensitive electrode. The lower detection limit for this method is 1 µM, and its use has yielded reported concentrations of H_2S in blood or plasma of 34 to 75 µM.[6] The basic conditions necessary to promote the conversion of sulfides to S^{2-} will artificially inflate the concentration of H_2S.[6] If the concentrations of H_2S reported

using methylene blue or the S^{2-} sensitive electrode methods were correct, fresh blood would have a strong odor of rotten eggs and H_2S would be present at toxic levels. Therefore, an artifact in these measurements that has not been accounted for must exist and these values should not be trusted.

The three H_2S detection methods that reported reasonable concentrations of H_2S in blood or plasma are the polarographic, GC, and MBB methods. The polarographic method measures only free H_2S by using a membrane on a probe that allows H_2S to freely pass through while preventing ionic species from permeating. The pH is then used to calculate the ratio of H_2S to HS^- which is used to determine total the concentration of H_2S. The polarographic method has a lower detection limit of 14 nM of H_2S or 0.1 µM total sulfide, and it showed that the concentration of H_2S in several animals, including rat and pig, was below the detection limit.[8]

In the GC method a tissue sample is taken and a phosphate buffer solution at pH 5.7 is added to convert all the HS^- to H_2S. The gas from the sample is then injected into a gas chromatograph with a chemiluminescence sulfur detector. This method gave a concentration of H_2S of 17 nM for mice liver and 14 nM for mice brain with a lower detection limit of 1 ppb.[28]

The polarographic and GC methods measure the concentration of H_2S directly whereas MBB reacts with H_2S to form sulfide-dibimane (SDB) in a buffered solution at pH 9.5 as illustrated in Figure 1.14. The derivatization of H_2S with MBB was completed after 2 min and then the solution was run through an HPLC with a fluorescence detector. The area of the peak for SDB was compared to a standard curve to determine the concentration of H_2S. This method has yielded a concentration of H_2S in the plasma of mice of 1.7 µM with a lower detection limit of 0.1 µM.[27]

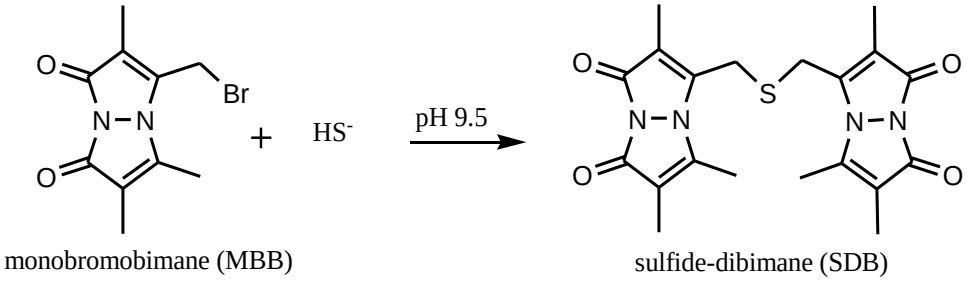

monobromobimane (MBB) sulfide-dibimane (SDB)

Figure 1.14. The derivatization of hydrogen sulfide with monobromobimane to form sulfide-dibimane.

Fluorescent and Colorimetric Detection of H_2S

The polarographic, GC, and MBB methods all give much more reasonable concentrations of H_2S than what was previously reported. The next advance in H_2S detection in biological systems was the development of fluorescent probes. The advantages that fluorescent probes have over the previous methods are that they are potentially fast, accurate, and able to determine H_2S concentrations in real-time. Fluorescent probes are also highly desirable because they are typically very sensitive which is required to determine low concentrations of H_2S. An ideal probe should react with H_2S in seconds and show little interference with other anions or molecules in the blood. The florescence probes developed to detect H_2S take advantage of the nucleophilic and reducing properties of H_2S. This chapter will discuss five of the known fluorescent probes but there are several others.[29,30]

The fluorescent probe dansyl azide (DNS-Az) can be easily synthesized from commercially available dansyl chloride (DNS-Cl) as seen in Figure 1.15. DNS-Az is reduced by H_2S to yield dansyl amide which is fluorescent. Importantly, this reaction is completed in 10 seconds.[31] The fluorescence can be measured and fitted to a standard curve to determine the concentration of H_2S. This method has a lower detection limit of 1 μM and shows little or no

fluorescence when exposed to 17 different anions, but it was not tested around cysteine or GSH.[31] The concentration of H_2S in the blood of mice using DNS-Az was determined be 32 µM.[31] This concentration might be high because of the interference of cysteine, GSH, or other biological thiols that are potent reducing agents.[6]

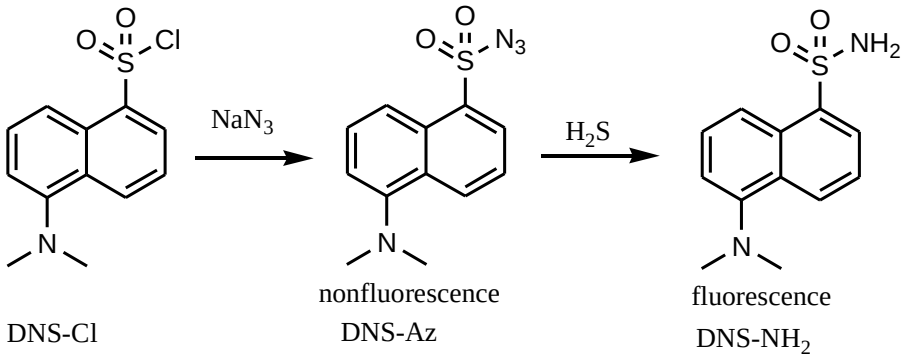

Figure 1.15. Dansyl azide synthesis and reduction with H_2S.

C-7Az reacts similarly to DNA-Az by the reduction of the azide by H_2S, which causes fluorescence as seen Figure 1.16. C-7Az can be synthesized from commercially available 7-amino-4-methylcoumarin using the Sandmeyer reaction.[32] The reduction of C-7Az by H_2S takes an hour to reach maximum fluorescence intensity so it cannot be a quick measure of the concentration of H_2S. The fluorescence intensity was not effected by biologically relevant anions, GSH, and cysteine.[32] The detection limit for this probe was less than 0.25 µM, but it was not used to determine the H_2S concentration in blood or plasma.[32] Instead, it was used to detect H_2S in living cells via two-photon laser scanning fluorescence microscopy, and the *in situ* visualization of H_2S in cardiac tissues.

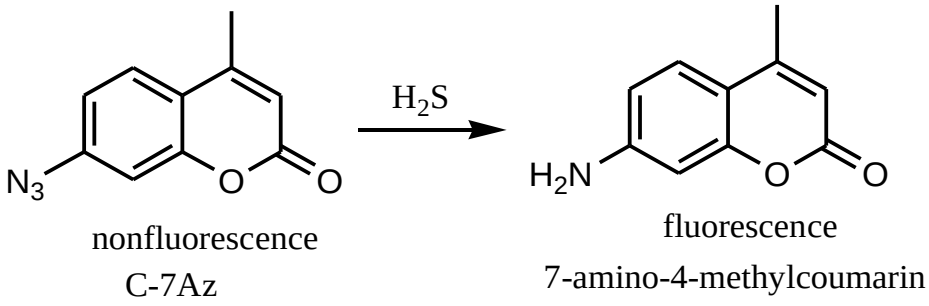

Figure 1.16. Reduction of C-7Az by H_2S.

The final three fluorescent probes that will be discussed in this chapter are diagramed in Figure 1.17. Sulfidefluor-1 (SF1) and Sulfidefluor-2 (SF2) are reduced by H_2S in a similar fashion to DNZ-Az and C-7Az. SF1 and SF2 take an hour to reach the peak fluorescence intensity and have a lower detection limit of 5-10 μM.[33] SF1 displayed about 3 times greater fluorescence when exposed to H_2S compared to exposure to GSH, cysteine, and other biologically relevant species. Similarly, SF2 has 5 times greater fluorescence when exposed to H_2S then after exposure to the same biologically relevant species.[33]

Sulfidefluor-3 (SF3) reacts with H_2S different than the other fluorescent probes discussed in this chapter. SF3 takes advantage of the nucleophilicity of H_2S rather than its reductive ability. H_2S breaks the disulfide bond in SF3 which then spontaneously undergoes cyclization resulting in the cleavage of two ester groups. This induces fluorescence as seen in Figure 1.17. The reaction that induces fluorescence takes an hour to reach completion which limits the usefulness of this probe. Also, its fluorescence intensity was much high than SF1 and SF2 which gave SF3 a lower detection limit of 2.5 μM.[34] SF3 does not react with any biological thiols including GSH and cysteine, but it could not detect H_2S

in plasma.[35] SF1, SF2, and SF3 all have been used to detect H_2S released in living cells.

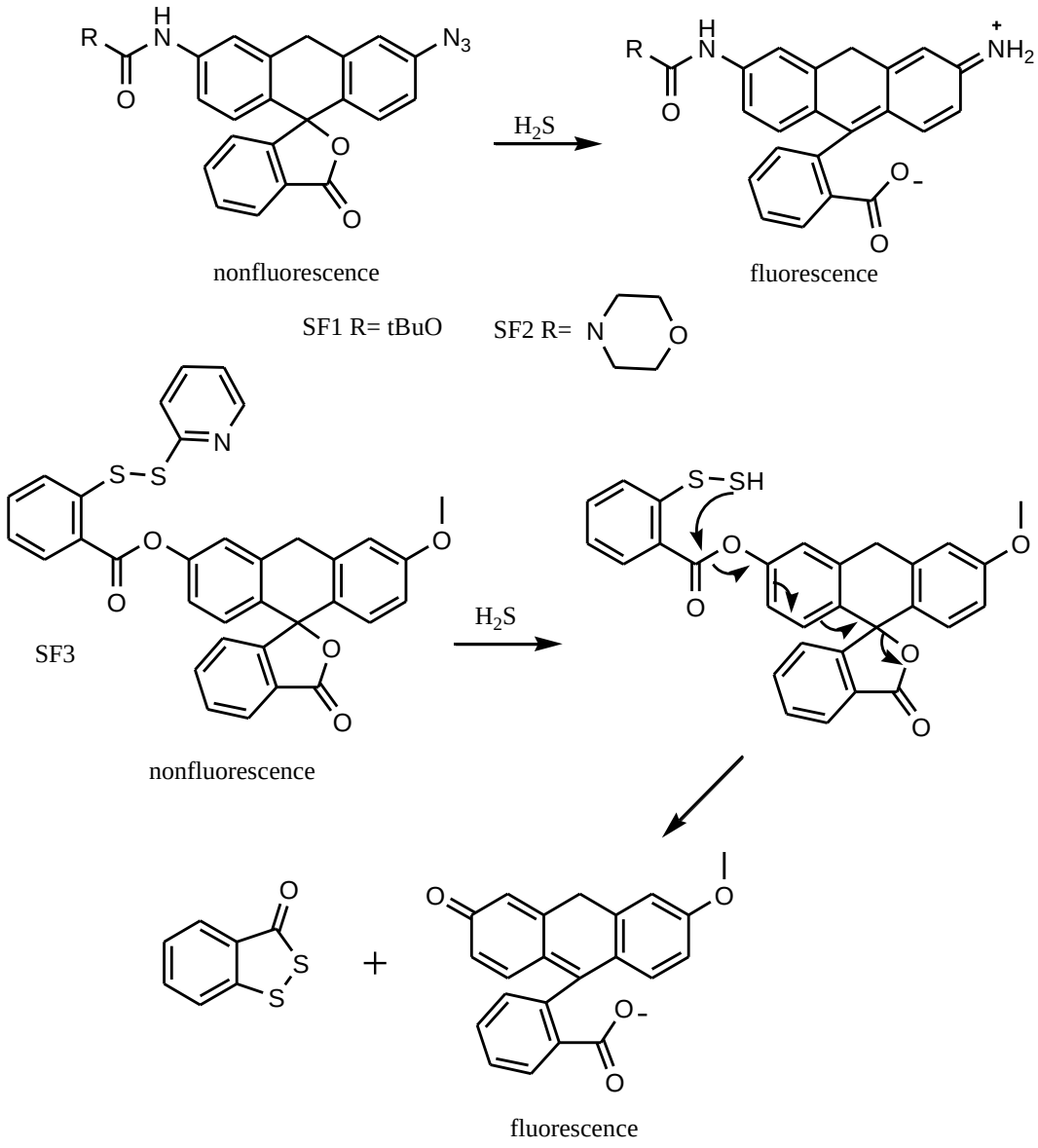

Figure 1.17. Reaction of Sulfidefluor-1 (SF1), Sulfidefluor-2 (SF2), and Sulfidefluor-3 (SF3) with H_2S.

One of the newly developed H_2S detection reagents is a commercially available colorimetric probe 4-chloro-7-nitrobenzofurazan (NBD-Cl). Similar to other electron-deficient arenes with good leaving groups, NBD-Cl undergoes nucleophilic aromatic substitution when exposed to suitable nucleophiles. NBD-Cl reacts quickly with H_2S or other thiols to produce NBD-SH or NBD-SR. The thiol group on NBD-SR can be exchanged with other thiols or H_2S, however, the production of NBD-SH is irreversible. NBD-SH is highly colored, cannot exchange with other thiols, and can be detected by UV-Vis spectroscopy, which allows for the detection of H_2S in the presence of thiols. The reaction between NBD-SH and an excess of NDB-Cl to form $(NBD)_2S$ decreases the concentration of NBD-SH which will affect the accuracy of this method. Another challenge is that $(NBD)_2S$ can also react with H_2S to produce NBD-SH, as seen in Figure 1.18. The reaction of NBD-Cl with H_2S occurs quickly and this method has a lower detection limit of 0.210 µM.[36] NBD-Cl has not yet been used to determine the concentration of H_2S in blood, plasma or other biological systems but has shown promise. Other electron-deficient arenes are also being explored as well.

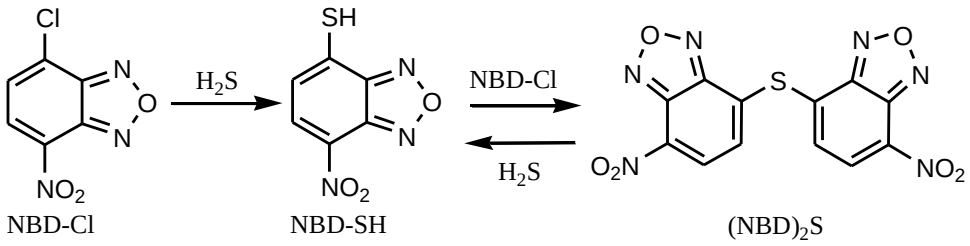

Figure 1.18. The nucleophilic aromatic substitution of 4-chloro-7-nitrobenzofurazan by H_2S.

Measurement of the *in vivo* concentration of H_2S at the biologically relevant concentrations has proven to be a challenging undertaking. The exact concentration of H_2S in the blood or plasma of mice or humans is still uncertain, but growing evidence indicates that the concentration of H_2S is less than 1 µM. If the GC and polarographic methods are correct and the concentration of H_2S is around 14 nM, it will be difficult to find a fluorescent or colorimetric probe with a suitably low detection limit. If the concentration of H_2S is closer to 1 µM as determined by the MBB method, a fluorescent or colorimetric probe will likely yield accurate values for the concentration of H_2S. An ideal fluorescent or colorimetric probe will react with H_2S in seconds and not react with other species in a complex biological matrix including thiols. This ideal fluorescent or colorimetric probe has not been discovered yet, and more research is needed.

The recent increase of interest in H_2S as a signaling molecule is due to its potential beneficial and therapeutic effects. Recent discoveries have led to the development of new H_2S releasing drugs and drug hybrids. These drugs have shown to be potentially effective in treating a variety of different diseases including cardiovascular disease, but the effects of H_2S are short-lived and these small drug molecules are quickly cleared by the kidneys. The field of H_2S in medicine lacks a long-term method to release H_2S. A biodegradable polymer that slowly releases a prodrug of H_2S as it degrades in the body may directly address this challenge. A biodegradable H_2S releasing polymer would not be easily cleared by the kidneys and would stay in the body and release H_2S for days or weeks. The polymer could encapsulate known pharmaceutical agents that have synergy with H_2S and release them at the same time.

CHAPTER 2

LONG-TERM RELEASE OF H_2S FROM POLYMERS BASED ON POLY(LACTIC ACID) AND 4-HYDROXYTHIOBENZAMIDE

Abstract

The first long-term release of molecules that react to yield H_2S *in vivo* is described. A series of polymers were synthesized by the copolymerization of L-lactide and a lactide functionalized with 4-hydroxythiobenzamide. A new method to attach functional groups to a derivative of L-lactide was described based on the addition of a thiol to an α,β-unsaturated lactide using catalytic I_2. This reaction proceeds under mild conditions and does not ring-open the lactone. The copolymers had molecular weights from 8 to 88 kg mol^{-1} with PDIs below 1.50. Two sets of microparticles were fabricated from a copolymer; the average diameters of the microparticles were 0.53 and 12 μm. The degradation of the smaller microparticles were investigated in buffered water to demonstrate the slow release of thiobenzamide over 1 week. Based on the ability to synthesize polymers with different loadings of thiobenzamide, these particles provide the first method to deliver H_2S over days to weeks. This research addresses a critical need in the field of H_2S in medicine where no other method exists to release H_2S *in vivo* at times over a few hours.

Introduction

For decades it was believed that H_2S had only negative health effects because it is a highly poisonous gas that can kill at lower concentrations than carbon monoxide (CO).[37] Yet, recent work has shown that H_2S also has many potentially important, beneficial roles *in vivo* and it is widely recognized as the third gasotransmitter known in medicine – the other two gasotransmitters are CO

and NO.[1-7,16] Gasotransmitters are important gases because they have the ability to move across biological membranes, control biological pathways and functions, have short half-lives in the body, and are synthesized by enzymes.[38,39] The beneficial biological effects attributed to H_2S are proposed to be due to at least three different mechanisms. First, H_2S is a reducing agent and neutralizes reaction oxygen species (ROS) that cause cellular damage.[40-44] Second, H_2S can mediate the activation of adenosine triphosphate (ATP)-sensitive potassium channels (K_{ATP})[45-47] These channels play a pivotal role in regulating biological functions including heart activity, smooth muscle tone, insulin secretion, and neurotransmitter disease.[13,14] Third, H_2S can regulate the concentration of NO in cardiac tissue and affect the signaling pathways of both gasotransmitters.[48-51] H_2S is emerging as a key molecule in medicine that has potential to affect and treat a wide variety of diseases.

One of the challenges in the field of medicinal applications of H_2S is that its concentration must be accurately controlled at nM to μM concentrations.[51-53] H_2S is produced *in vivo* by at least four different enzymes and its concentration *in vivo* is generally regarded as being less than 1 μM.[3,9,52] Its concentration must be so low because H_2S causes pulmonary edema and olfactory paralysis at even modest concentrations of tens of μM; at concentrations >100 μM death may occur.[3,54] Yet, the body produces H_2S and maintains its concentration at less than 1 μM.[55] Modest, therapeutic doses of H_2S at μM concentrations has been shown to have a positive effect in cells and tissues.[7] One of the unmet challenges in the field of H_2S in medicine is the challenge of delivering low, constant doses of H_2S at targeted tissue.[7] In prior work, NaSH has been used to deliver H_2S *in vivo*, but its use led to large spikes in concentration of H_2S.[20] To provide a slow release of H_2S *in vivo*, numerous small molecules were investigated that release H_2S by degradation (Figure 2.1).[19-23,56] These molecules

have been used to affect the concentration of H_2S over minutes to hours, but they are rapidly cleared from the body which necessitates repeated administration of these molecules every few hours. An important limitation in this field is that no method exists to deliver a steady, low dose of H_2S over hours to weeks at desired locations in the body. In this chapter we report the first synthesis of a polymer with a H_2S-releasing prodrug that can slowly release the prodrug – and H_2S – over days to weeks.

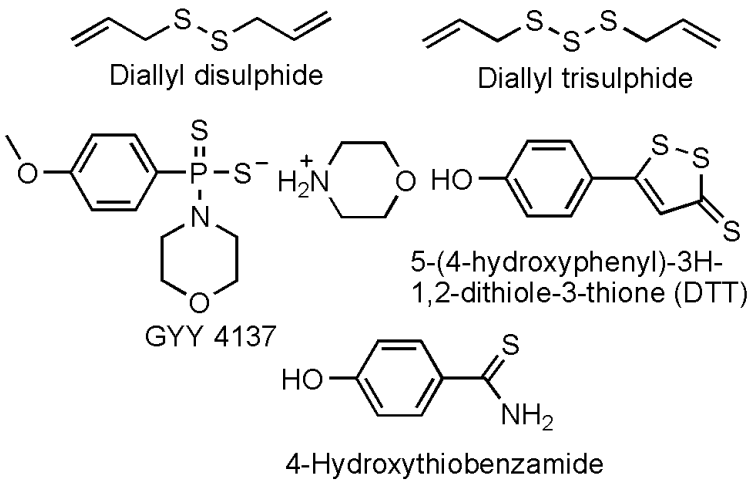

Figure 2.1. The five most common molecules used to release H_2S *in vivo*.

Biodegradable polymers have been used in medicine to deliver steady, low doses of drugs over days to weeks.[57,58] The drugs are typically encapsulated in nano- to micro-sized particles composed of a polymer that slowly degrades to release the drug.[57] Typically, polyesters or polyanhydrides are used due to their ability to degrade by hydrolysis without the need for enzymes, glutathione, or other molecules.[58] Poly(lactic acid) is one of the most studied polymers in this

field because of its ease of synthesis, ease of forming copolymers with glycolic acid to tune its degradation profile, and its approval by the FDA for use in medical devices.[57-59] The degradation of poly(lactic acid) produces lactic acid which is considered a safe molecule *in vivo*. Poly(lactic acid) and poly(lactic-*co*-glycolic acid) are used in numerous applications in medicine and are an attractive choice for the development of future applications because of their proven safety.[57,59]

In this chapter we report the design and synthesis of a polymer based on poly(lactic acid) that has 4-hydroxythiobenzamide bonded to the backbone of the polymer. The polymer was produced by the copolymerization of L-lactide and a lactide bonded to 4-hydroxythiobenzamide. The ratio of the two monomers provided control over the loading of the thiobenzamide and how much H_2S would be released from a particle fabricated from the copolymer. 4-Hydroxythiobenzamide was chosen because it has been shown to release H_2S *in vivo* and has been shown to have synergy with other drugs such as naproxen which is a non-steroidal anti-inflammatory drug (NSAID; Figure 2.2).[22] The synergy of therapeutic doses of H_2S with drugs such as aspirin, diclofenac, and sildenafil have shown that the simultaneous release of H_2S and a drug can result in a better therapeutic effect than the delivery of the drug or H_2S individually.[23,25,56] 4-Hydroxythiobenzamide has a phenol group that was used to attach to drugs through an ester bond that was rapidly cleaved *in vivo* to release a drug such as naproxen and 4-hydroxythiobenzamide. An important advantage of the polymers reported in this chapter are that in future work they will allow the noncovalent encapsulation of drugs within microparticles for the simultaneous release of a drug and 4-hydroxythiobenzamide.

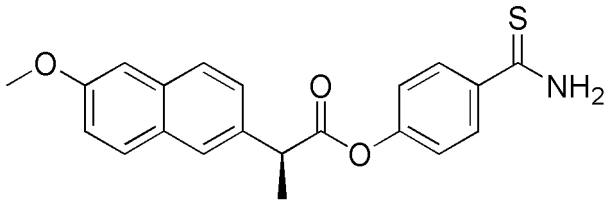

Figure 2.2. A prodrug of naproxen and 4-hydroxythiobenzamide. The ester bond is cleaved *in vivo* to release naproxen and the thiobenzamide that degrades to release H_2S.

Results and Discussion

Synthesis of a Functionalized Lactide Monomer

The convergent synthesis of a monomer containing 4-hydroxythiobenzamide took seven steps (Figure 2.3). Commercially available lactide was reacted with NBS followed by triethylamine to yield **2** in 51% yield. This sequence was first reported by Hillmyer et al. in 2008, and it proceeded as described in the literature.[60-62]

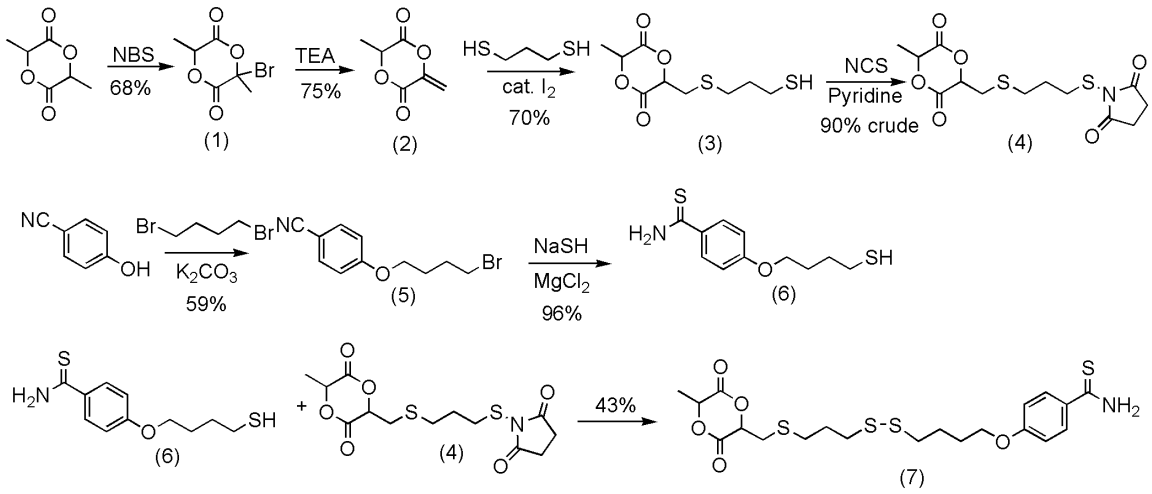

Figure 2.3**.** The convergent synthesis of molecule 7 is shown.

In prior work **2** was reacted with cyclopentadiene to yield a monomer that could be polymerized by the Grubbs catalyst and by ring opening of the lactide. Other reactions to functionalize **2** have not been reported, so the reaction of **2** with different nucleophiles was investigated. Nucleophilic addition reactions at the α,β-unsaturated ester of **2** were expected to be challenging due to the facile ring-opening of the lactide with nucleophiles. Several different nucleophiles were investigated to learn which would react with the α,β-unsaturated ester rather than ring open the lactide. Initial attempts with a secondary amine (methylbenzylamine) were unsuccessful and resulted in ring-opening of **2**. Similar results were obtained when **2** was reacted with propanethiol with catalytic triethylamine as a base. When propanethiol and **2** were reacted with sodium bicarbonate, sodium carbonate, or at 80 ^{o}C in the absence of base no, reaction was observed.

The reaction of propanethiol with **2** proceeded to 32% yield under click reaction conditions with azobisisobutyronitrile (AiBN) at 75^{o}C.[63] Attempts to optimize this reaction failed and lead to the formation of several products that were challenging to separate. The addition of propanethiol was successful when catalytic amounts of I_2 were added.[64] In a control experiment to investigate if the catalytic species was I^-, KI was added to **2** and propanethiol but no reaction was observed.

The reaction of molecule 2 with a 5 molar excess of 1,3-propanedithiol and a 5 mol % loading of I_2 to the formation of **3** in 70% yield. This reaction yielded two diastereomers as shown in Figure 2.4 in a 3:1 ratio. A NOESY experiment was conducted to investigate which diastereomer was formed in higher yield. A correlation between the two tertiary hydrogens on the ring was observed for the major diastereomer but not for the minor diastereomer. The

major diastereomer was therefore assigned as the cis-product as shown in Figure 2.4.

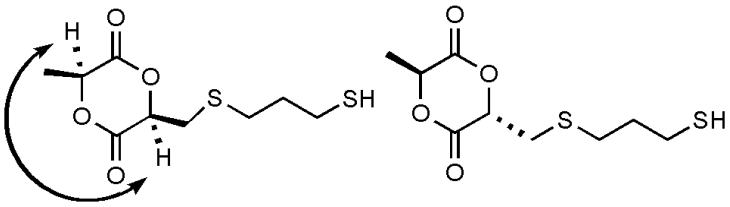

Figure 2.4. A NOESY correlation was observed between the two indicated H atoms in the major diastereomer.

To complete the synthesis of the monomer, an aromatic nitrile group was converted to a thioamide in the same step an alkyl bromide was converted to a thiol (**6**).[65] This reaction yielded a thiol that was reacted with **3** under a variety of conditions including catalytic I_2 and click conditions with AIBN. These reactions were unsuccessful, so the thiol on **3** was activated with *N*-chlorosuccinimide and then reacted with **6** to yield a lactide monomer bonded to a thiobenzamide. The overall yield over seven steps was 18%.

Copolymerization of L-Lactide and Molecule 7

Molecule **7** was copolymerized with lactide to yield polymers that had different amounts of thiobenzamide along the backbone (Figure 2.5). Many catalysts have been discovered and developed that will rapidly polymerize lactide, but this report focused on basic catalysts due to the presence of the mildly basic thioamide functional group that coordinates to Lewis acid catalysts.[66,67] DMAP was chosen based on its ready availability and prior work that demonstrated that it would rapidly polymerize lactide under mild reaction conditions.[68] Octadecanol was chosen as the initiator for these polymerizations

because the large number of methylenes in this molecule provided a method to estimate the molecular weight of the polymers using end group analysis from the ^{1}H NMR spectra.

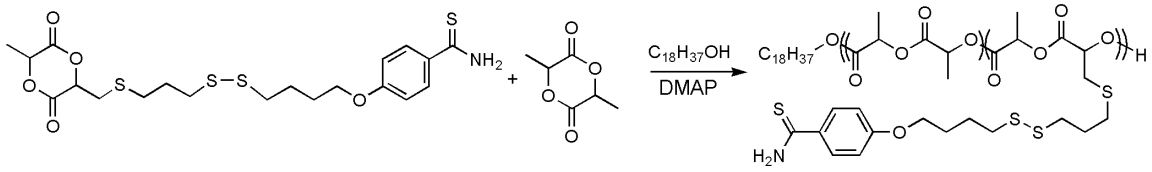

Figure 2.5. The copolymers of the two monomers led to polymers functionalized with a thiobenzamide.

The copolymerization of lactide and molecule 7 was first attempted in THF and CH_2Cl_2 for 48 h to investigate which solvent was best for the polymerization (entries 1 and 2 in Table 2.1). The polymerization in THF went to 50% conversion, but the polymerization in CH_2Cl_2 went to 98% conversion. The polydispersity index **(**PDI) for entry 2 was high, so the concentration of monomers was cut in half (entry 3 in Table 2.1). This polymerization took longer (96 h) to reach a high conversion, and the molecular weight measured by end group analysis using ^{1}H NMR spectroscopy disagreed with the molecular weight measured by Size-exclusion chromatography (SEC) using multi-angle laser light scattering and refractive index detectors that measure the absolute molecular weight. A likely explanation for this difference in molecular weight is that, at long reaction times of 96 h, cross-linking of the polymer became significant. One method to cross-link the polymer is through a disulfide metathesis reaction which is known to be catalyzed by light (Figure 2.6).[69] This reaction would form undesired cross-links between two polymers. The product of the disulfide metathesis was observed after 500 mg from entry 9 in Table 2.1 was dissolved in

CH_2Cl_2, exposed to light, and heated to 35 ºC for 1 week. Molecule 8 was observed by ^1H NMR spectroscopy and its presence was confirmed by high-resolution mass spectrometry. To minimize the cross-linking reaction, the concentration of monomer was increased to 2.75 M or 2.50 M to lower the time necessary for completion. The polymerizations were mostly completed within 24 h and a good agreement was observed between the molecular weight measured by end group analysis and SEC (entries 4 and 5 in Table 2.1). Furthermore, the ratio of lactide to molecule 7 was varied from 10/1 to 20/1 to produce polymers with varied loadings of thiobenzamide.

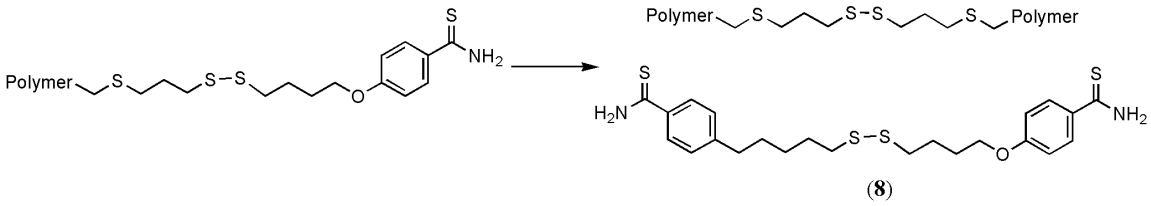

(**8**)

Figure 2.6. The disulfide metathesis reaction was shown to occur by the reaction of a polymer at 35 ºC for 1 week that yielded molecule 8.

Polymerizations to yield polymer with predicted molecular weights above 10,000 g mol^{-1} were limited by disagreement between the molecular weight measured by end group analysis and SEC. Polymerizations were completed to yield a polymer with a molecular weight close to 20,000 g mol^{-1}, but reaction times of 115 h yielded polymers that had been cross-linked but still had low PDIs (entries 7 and 8 in Table 2.1). When the polymerization time was decreased to 72 h, the conversion was still high and the agreement between molecular weights measured by end group analysis and SEC were much closer (entry 9 in Table 2.1).

Table 2.1. Data of the copolymerizations of lactide and molecule 7.

	Initial ratio[a]	Time (h)	solvent	Conc [b] (M)	M/I[c]	Calc Mw[d] (g mol^{-1})	Ratio[e]	conv[f]	Mn[g] (NMR)	Mn (SEC)	Yield	PDI
1	10/1	48	THF	2.75	55	9930	Na	50%	Na	Na	Na	na
2	10/1	48	CH_2Cl_2	2.75	55	9930	10/1	98%	8670	13300	85%	1.55
3	10/1	96	CH_2Cl_2	1.38	55	9930	10/1	96%	7050	22700	73%	1.19
4	10/1	24	CH_2Cl_2	2.75	55	9930	10/1	85%	8530	7850	54%	1.44
5	10/1	48	CH_2Cl_2	2.50	55	9930	9/1	95%	9200	11900	81%	1.25
6	20/1	48	CH_2Cl_2	2.75	63	10400	19/1	92%	9340	11000	75%	1.15
7	10/1	115	CH_2Cl_2	2.75	110	19600	11/1	95%	18700	88400	68%	1.24
8	20/1	115	CH_2Cl_2	3.15	126	20500	16/1	91%	16200	69100	82%	1.21
9	10/1	72	CH_2Cl_2	2.75	110	19600	9/1	91%	14600	22700	80%	1.30

Note: [a]Lactide to molecule 7 ratio in the polymerizations. [b]Concentration of the monomers. [c]Ratio of the sum of the monomers to initiator. [d]Calculated molecular weight based on the ratio of monomers to initiator. [e]Observed ratio of lactide to molecule 7 in the copolymer as shown by ^{1}H NMR spectroscopy. [f]Conversion of the polymerization. [g]The Mn was calculated from by end group analysis using ^{1}H NMR spectroscopy. [h]The temperature of polymerization was 40 ^{o}C for these experiments, it was 35 ^{o}C for all other polymerizations.

Release of Thiobenzamide from Microparticles

Entry 5 from Table 2.1 was used to make two sets of microparticles with radii of 12 and 0.53 μm (Figure 2.7). These particles were readily characterized by scanning electron microscopy (SEM) to show they possessed smooth surfaces. The zeta potential for the small particles were measured to be -29.3 mV which is consistent with prior work with particles formed from poly(lactic acid) under these conditions.

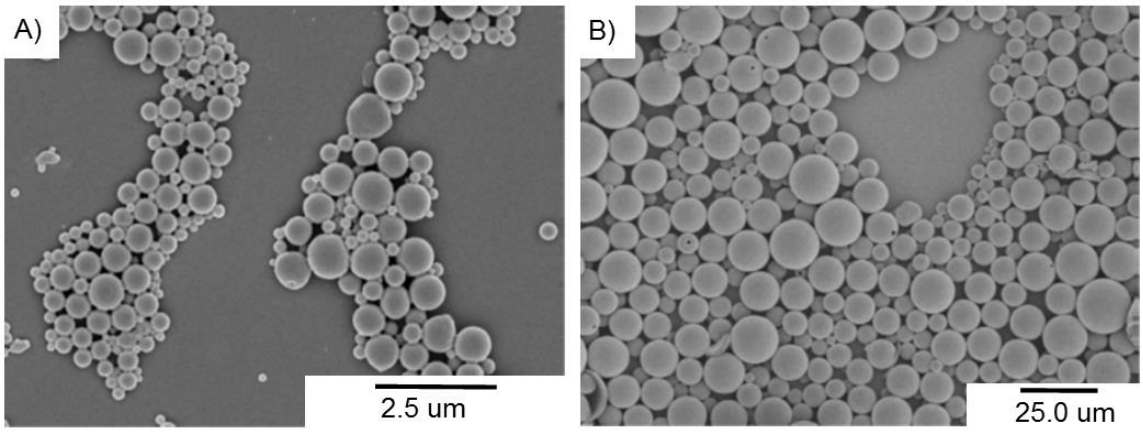

Figure 2.7. SEM micrographs show the a) 0.53 μm and b) 12 μm microparticles before hydrolysis.

The degradation of the small particles were studied at 37.6 ºC in buffered water at pH = 3.0 and 7.4 to investigate the release of thiobenzamide. After one day at pH 3.0 the microparticles released 4.1% of the thiobenzamide, but that value increased to 14.8% after one week. The particles degraded slowly only losing 7% of their weight after one week at pH 3. After one week at pH 7.4 the microparticles released, 7.5% of thiobenzamide which increased to 18.9% over 4 weeks as seen in Figure 2.8. The particles at pH 7.4 also degraded slowly – the particles lost only 9.7% of their weight over four weeks – which was expected based on degradation profiles of similar microparticles based on poly(lactic acid). It is important to note that the microparticles slowly degraded and released thiobenzamide which is well described in the literature as a molecule that releases H_2S *in vivo*.[7,21,22]

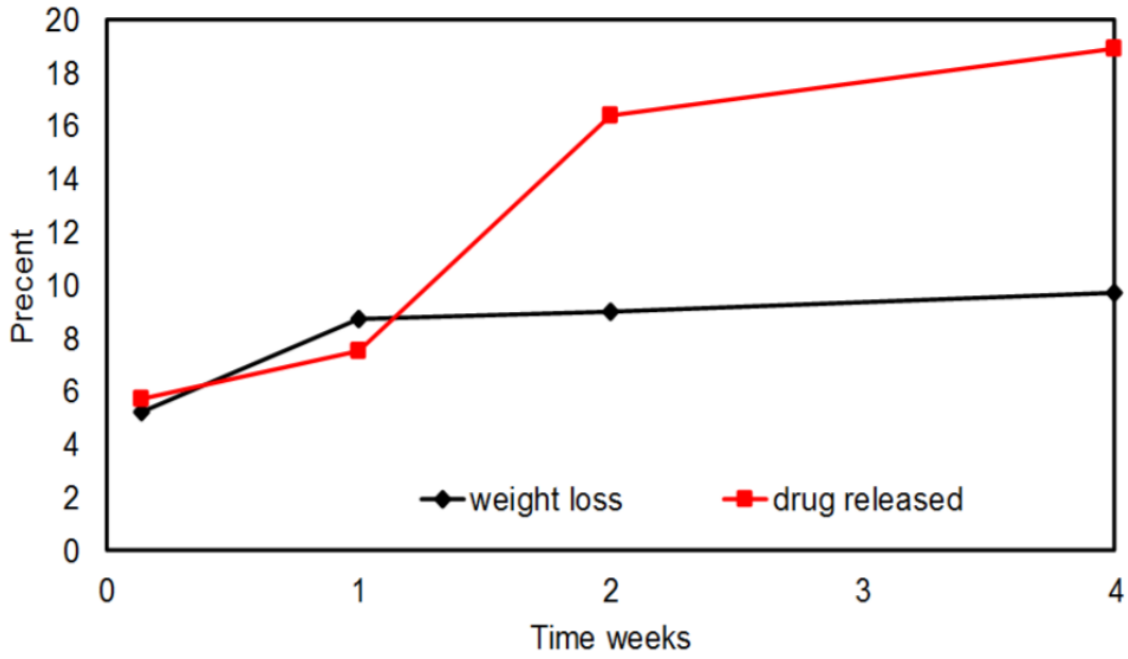

Figure 2.8. Graph of precent weight loss (black) and thiobenzamide released (red/gray) by the small particles at pH 7.4 over 4 weeks

Conclusions

This chapter describes the first method to achieve the long term release of H_2S. This is a critically important advance in the field of medicinal H_2S because prior methods only allowed the release of H_2S over minutes to hours and the concentration of H_2S was ill-controlled. The particles composed of the polymers can be used to deliver specific loadings of H_2S to selected sites in the body. The degradation can be controlled by varying the composition of the polymer and whether glycolic acid is integrated into the backbone. In future work we will investigate how these parameters affect the release of H_2S. Furthermore, the polymers reported in this chapter had different loadings of the thiobenzamide and possessed molecular weights from 8,000 to 88,000 g mol^{-1} with low values for the

PDI. A wide range of polymers can be envisioned that will allow some control over the degradation profile and release of thiobenzamide from particles.

A new method to functionalize a lactide monomer was also demonstrated by the reaction of **2** with thiols and catalytic I_2. Lactide is an important monomer in medicine; yet, it is challenging to functionalize to attach to other functional groups. This chapter reports a new way to attach molecules to lactide that builds on prior work by Hillmyer et al. This reaction can be used to attach different thiols to lactide to synthesize a wide range of new monomers.

Experimental

Materials. All chemicals and solvents were purchased from Aldrich or Acros at their highest purity. L-Lactide was purified by three crystallizations from EtOAc. The CH_2Cl_2 used for the polymerizations was dried under N_2 using 3 A molecular sieves. All other chemicals and solvents were used as received.

Characterization. ^{1}H NMR and ^{13}C NMR spectra were acquired at 300 MHz and 75 MHz, respectively, using a Bruker Fourier 300 MHz spectrometer and referenced either to TMS for $CDCl_3$ (δ=0.0) or to DMSO-d_6 (δ=2.5). The high resolution mass spectrometer used was a waters Q-Tof Premier. SEC was run using THF (1.00 mL min^{-1}) as the mobile phase. A Waters 515 pump and two Waters Styragel HR3 THF columns were used in series. A Wyatt DAWN Heleos-II 18 angle laser light scattering detector was used to measure light scattering and a Wyatt Optilab T-rEX was used to measure change in refractive index.

(3S,6S)-3-Methyl-[6-propylthiol sulfide]-1,4-dioxane-2,5-dione (3). (3S)-3-Methyl-6-methylene-1,4-dioxane-2,5-dione (**2**) (3.02 g, 21.3 mmol), was placed in 9 mL of CH_2Cl_2 and cooled to 0 °C. 1,3-Propanedithiol (11.5 g, 106 mmol) was added, followed by I_2 (0.271 g, 1.07 mmol) and reacted for 3h. The reaction was quenched by addition of 25 mL of saturated sodium thiosulfate. The

product was extracted with CH_2Cl_2 (3 x 50 mL) then the organic layer was washed with brine (3 x 150 mL) and evaporated. The product was purified by column chromatography using 7:3 (v:v) hexane:EtOAc. Two diastereomers were obtained with a combined yield of 3.74 g (70% yield). Two diastereomers were separated for characterization. ^{1}H NMR (300 MHz, $CDCl_3$) (major diastereomer): δ 5.15 (dd, 1 H, *J* = 6.0 Hz, 4.1 Hz), 5.07 (q, 1 H, *J* = 6.7 Hz), 3.20 (dd, 1 H, *J* = 14.9 Hz, 4.1 Hz), 3.09 (dd, 1 H, *J* = 14.9 Hz, 6.0 Hz), 2.82 (t, 2 H, *J* = 7.1 Hz), 2.65 (dt, 2 H, *J* = 8.0 Hz, 7.0 Hz), 1.91 (quin, 2 H, *J* = 7.0 Hz), 1.70 (d, 3 H, *J* = 6.7 Hz), 1.39 (t, 1 H, *J* = 8.0 Hz). ^{13}C NMR (75 MHz, $CDCl_3$) (major diastereomer): δ 166.44, 165.61, 76.87, 72.58, 33.15, 32.10, 32.00, 23.19, 16.12. HRMS-EI (m/z) (major diastereomer): $[M]^+$ calc for $C_9H_{14}O_4S_2$ 250.0334 ; found, 250.0320. ^{1}H NMR (300 MHz, $CDCl_3$) (minor diastereomer): δ 5.37 (q, 1 H, *J* = 7.2 Hz), 5.29 (t, 1 H, *J* = 4.4 Hz), 3.25 (dd, 1 H, *J* = 15 Hz, 4.4 Hz), 3.14 (dd, 1 H, *J* = 15 Hz, 4.3 Hz), 2.79 (dd, 1 H, *J* = 6.6 Hz, 1.4 Hz), 2.79 (dd, 1 H, *J* = 7.3 Hz, 0.9 Hz), 2.62 (dt, 2 H, *J* = 8.0 Hz, 7.0 Hz), 1.89 (quin, 2 H, *J* = 7.0 Hz), 1.73 (d, 3 H, *J* = 7.1 Hz), 1.38 (t, 1 H, *J* = 8.1 Hz). ^{13}C NMR (75 MHz, $CDCl_3$) (minor diastereomer): δ 165.53, 164.76, 77.16, 73.26, 33.09, 34.90, 32.05, 23.10, 18.32. HRMS-EI (m/z) (minor diastereomer): $[M]^+$ calc for $C_9H_{14}O_4S_2$ 250.0334 ; found, 250.0318.

(3S,6S)-3-Methyl-[(6-proplythio)-2,5-pyrrolidinedione sulfide]-1,4-dioxane-2,5-dione (4): *N*-Chlorosuccinimide (1.92 g, 14.4 mmol) and pyridine (1.34 g, 17.0 mmol) were dissolved in 30 mL of CH_2Cl_2 and cooled 0 °C. (3S,6S)-3-Methyl-[6-proplythiol sulfide]-1,4-dioxane-2,5-dione was dissolved in 12 mL CH_2Cl_2 and added to the reaction dropwise over 30 min and allowed to react at 0 °C for 2.5 h. The organics were then washed with brine (3 x 50 mL) and dried with $MgSO_4$. The solvent was removed under vacuum to give a colorless oil that

was used without purification (4.08 g, 90% crude yield). ^{1}H NMR (300 MHz, $CDCl_3$) should a shift in succinimide to δ 2.86 indicating the formation of product.

4-(4-bromobutoxy)-benzonitrile (5). 4-Nitrophenol (4.76 g, 40 mmol) in 15 mL of DMF was added dropwise to 1,4-dibromobutane (17.27 g, 80 mmol) and K_2CO_3 (8.39 g, 60 mmol) dissolved in 40 mL DMF. After heating at 70 °C for 2.5 h, the reaction was cooled to room temperature and 200 mL of CH_2Cl_2 was added. The organic layer was washed with brine (4 x 200 mL) and dried over $MgSO_4$. The solvent was removed under vacuum, and the product was purified with silica gel column chromatography using 17:3 (v:v) hexane:EtOAc to yield a white solid (5.96 g, yield 59%). ^{1}H NMR (300 MHz, $CDCl_3$) δ 7.57 (d, 2H, *J* = 9.0 Hz), 6.93 (d, 2H, *J* = 9.0 Hz), 4.04 (t, 2H, *J* = 5.7 Hz), 3.48 (t, 2H, *J* = 6.3 Hz), 2.11-1.92 (m, 4H). ^{13}C NMR (75 MHz, $CDCl_3$) δ 161.68, 133.87, 119.06, 115.00, 103.87, 67.12, 32.99, 29.10, 27.48. HRMS-EI (m/z): $[M]^+$ calc for $C_{11}H_{12}NOBr$, 253.0102; found, 253.0106.

4-(4-butylthiol)-benzothiolamide (6). A solution of 4-(4-bromobutoxy)-benzonitrile (5.72 g, 22.5 mmol) in 12 mL of DMF was added to a slurry of sodium hydrosulfide hydrate (12.42 g, 135 mmol) and magnesium chloride hexahydrate (5.49 g, 27 mmol) in 30 mL DMF. The reaction was stirred at room temperature for 5 h. The product was precipitated into 80 mL of water and then filtered. The solid was taken up with 160 mL of 1 M HCl and stirred for 20 min then filtered. The solid was dried under vacuum to yield a yellow solid (5.21 g, yield 96%). The product contained 15% disulfide that was removed after the next step. ^{1}H NMR (300 MHz, DMSO-d_6): δ 9.64 (s, 1H), 9.32 (s, 1H), 7.94 (d, 2H, *J* = 8.9 Hz), 6.94 (d, 2H, *J* = 8.9 Hz), 4.03 (t, 2H, *J* = 6.2 Hz), 2.55 (t, 2H, *J* = 7.2 Hz), 2.31 (t, 1H, *J* = 7.7 Hz), 1.85-1.63 (m, 4H), disulfide peak (CH_2SSCH_2) 2.78 (t, *J* = 6.3). ^{13}C NMR (75 MHz, DMSO-d_6) δ 198.68, 161.44, 131.16, 129.54, 113.42,

67.41, 29.96, 27.38, 23.61, disulfide δ 37.34, 25.18. HRMS-ES+ (m/z): $[M+Na]^+$ calc for $C_{11}H_{16}S_2NO$, 242.0673; found, 242.0673.

Molecule 7. (3S,6S)-3-Methyl-[(6-proplythio)-2,5-pyrrolidinedione sulfide]-1,4-dioxane-2,5-dione (4.01 g 11.5 mmol) and 4-(4-butylthiol)-benzothiolamide (2.79 g, 11.5 mmol) were dissolved in 20 mL of dry THF and stirred at room temperature for 5 h. The solvent was removed under vacuum to yield an orange oil. The oil was dissolved in 50 mL of CH_2Cl_2 and cooled to precipitate the disulfide impurity from the synthesis of compound 6. The CH_2Cl_2 solution was then washed with brine (3 x 100 mL) to remove the succinimide. The solvent was removed under vacuum, and the product was then purified with silica gel column chromatography using 9:11 (v:v) hexane:EtOAc to yield a yellow solid (2.44 g, yield 43%) with a diastereomeric ratio of 4:1. ^{1}H NMR (300 MHz, DMSO-d_6) (major diastereomer): δ 9.31 (s, 1H), 9.63 (s, 1H), 7.94 (dt, 2H, *J* = 8.9 Hz, 1.8 Hz), 6.94 (dt, 2H, *J* = 8.9 Hz, 2.1 Hz), 5.56 (dd, 1H, *J* = 4.1 Hz, 6.1 Hz), 5.45 (q, 1H, *J* = 6.7 Hz), 4.04 (t, 2H, *J* = 5.7 Hz), 3.12 (dd, 1H, *J* = 4.1 Hz, 15 Hz), 3.01 (dd, 1H, *J* = 6.1 Hz, 15 Hz), 2.78 (t, 4H, *J* = 7.2 Hz), 2.70 (t, 2H, *J* = 7.2 Hz), 1.90 (quin, 2H, *J* = 7.6 Hz), 1.81-1.79 (m, 4H), 1.47 (d, 3H, J = 6.7 Hz). ^{13}C NMR (75 MHz, DMSO-d_6) δ 198.63, 168.00, 166.89, 161.32, 131.26, 129.53, 113.54, 75.90, 72.30, 67.35, 37.44, 36.41, 31.04, 28.45, 27.34, 25.24, 15.31. HRMS-ES+ (m/z): $[M+Na]^+$ calc for $C_{20}H_{27}NO_5S_4Na$, 512.0670; found, 512.0683.

Copolymerization (entry 5 of Table 2.1). Molecule 7 (1.60 g, 3.27 mmol), lactide (4.71 g, 32.7 mmol), DMAP (0.319 g, 2.61 mmol), and octadecanol (0.177 g, 0.65 mmol) were added to a dry Schlenk flask. Dry CH_2Cl_2 (14.4 mL) was added and the solution was stirred at 35°C for 48 h. CH_2Cl_2 (100 mL) was added, and the solution was then washed with 0.5 M acetic acid solution (2 x 100 mL) then washed with brine (2 x 100 mL). The organic layer was dried with $MgSO_4$ and the solvent was removed under vacuum to yield an

orange oil. This oil was dissolved in CH_2Cl_2 (25 mL), precipitated with 100 mL of hexanes, and filtered. The solid was dissolved with CH_2Cl_2 (25 mL) and precipitated into hexanes for a second time. A yellow solid was isolated (5.28 g, 81% yield). ^{1}H NMR (300 MHz, $CDCl_3$) δ 7.90 (d, 10H, *J* = 9.6 Hz), 7.56 (s, 5H), 7.30 (s, 5H), 6.87 (d, 10H, *J* = 9.6), 5.16 (q, 100H, *J* = 7.6), 4.08-4.00 (m, 10H), 3.17-3.11 (m, 4H), 3.08-3.00 (m, 6H), 2.81-2.64 (m, 30), 2.23-1.84 (m, 30), 1.58 (d, 304H, *J* = 7.6), 1.30-1.23 (m, 32), 0.88 (t, 3H, *J* = 5.7). ^{13}C NMR (75 MHz, $CDCl_3$) δ 201.45, 175.44, 169.89, 167.69, 162.30, 134.29, 131.36, 129.48, 114.27, 72.68, 69.29, 67.91, 66.83, 38.70, 37.34, 32.22, 29.61, 28.07, 25.94, 22.93, 20.75, 16.92, 16.04, 14.37.

Formation of microparticles (0.53 μm in diameter). Entry 5 from Table 2.1 (200 mg) was dissolved in 1.5 mL of CH_2Cl_2. This solution was added to 30 mL of 1% poly(vinyl alcohol) in water and homogenized using an Ultra Turrax homogenizer at 9500 rpm min^{-1} for 30 s. The emulsion was stirred for 1.5 h to evaporate CH_2Cl_2. The particles were collected by centrifugation at 1000 rpm for 5 min, washed twice with nanopure water, dispersed in 5 mL of water, and lyophilized.

Formation of microparticles (12 μm in diameter). Entry 5 from Table 2.1 (200 mg) was dissolved in 1.5 mL of CH_2Cl_2. This solution was added to 30 mL of 1% poly(vinyl alcohol) in water and sonicated with a sonic dismembrator at 40% amplitude for 30 s. The emulsion was stirred for 1.5 h to evaporate the CH_2Cl_2. The particles were collected by centrifugation at 8500 rpm for 5 min, washed twice with nanopure water, dispersed in 5 mL of water, and lyophilized.

Degradation of particles. For degradation at pH 3, two sets of the small particles (150 mg) were dispersed in 30 mL of acetate buffer at pH 3.0 and incubated at 37 °C with 300 rpm shaking speed then stopped at 24h and 1 week. For degradation at pH 7.4, four sets of the small particles (150 mg) were

dispersed in 30 mL of PBS buffer at pH 7.4 and incubated at 37 °C with 300 rpm shaking speed then stopped at 24h, 1 week, 2 weeks and 4 weeks. After degradation the solution was centrifuged and 27 mL of the supernatant was removed. The particles were washed three times with 30 mL of nano-pure water, lyophilized, and weighed. The particles (about 50 mg) were washed with MeOH (3 x 10 mL) and the MeOH was filtered and dried under vacuum. The ^{1}H NMR spectrum was obtained using 1,4- dinitrobenzene as an internal standard to calculate the amount of thiobenzamide that was released.

CHAPTER 3

POLYDIMETHYLSILOXANE THIMBLES

Introduction

This chapter is a review of previous work that utilized a polydimethylsiloxane (PDMS) thimble for chemical site-isolation and cascade reactions. PDMS is a commercially available kit (Sylgard 184) that can be readily fabricated into thimbles with 100 micron thick walls. The differential flux of molecules through the PDMS depended on their solubility in PDMS and whether the molecule was a polymer. PDMS thimbles allowed for the site-isolation of reagents that reacted with each other such as water from $LiAlH_4$ or Grignard reagents; Grubbs catalyst from mCPBA, AD-mix, or $K_2Os(OH)_{6;}$ and polymer-bound acids from polymer-bound bases. The site-isolation of these reagents led to the development of a series of two-step, one-pot cascade reactions. PDMS thimbles were also able to site-isolate $PdCl_2$ catalyst from the organic products of reactions such as the Wacker-Tsuji oxidation and Pd-mediated homocoupling of aryl boronic acids, and was able to retain < 99.998% of the Pd catalyst. The site-isolation and the cascade reactions described in this chapter take advantage of the difference in flux based on the solubility the molecules in the. The PDMS thimbles have a large amount of potential as demonstrated in this chapter, but because PDMS is sold as a kit the properties of the polymer cannot be chemically altered easily to affect solubility of small molecules. Therefore, PDMS thimbles cannot be tuned to control what will and will not flux through them.

Polydimethylsiloxane

Polydimethylsiloxane also known as PDMS, dimethicone, polymerized siloxane, silicone, Sylgard 184, trimethylsiloxy terminated polydimethylsiloxane.

PDMS is a colorless free flowing liquid with a density of 0.98 g mL^{-1}. It is soluble in most chlorinated, hydrocarbon, or ethereal solvents, has limited solubility in DMF and DMSO, and is insoluble in MeOH, EtOH, glycerol, and water. PDMS thimbles are fabricated from commercially available Sylgard 184 – a two component prepolymer of PDMS. Typical impurities include residual Pt catalyst. This polymer has a high concentration of silica nanoparticles and the PDMS thimbles may be stored for over a year under ambient conditions.

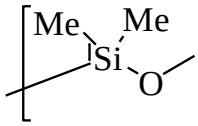

Figure 3.1. Polydimethylsiloxane

Preparation of PDMS Thimbles

The thimbles are readily fabricated from commercially available PDMS kits (Sylgard 184) from Dow Corning. The kit is a two-component mixture that is mixed in a 10:1 ratio to yield a viscous prepolymer of PDMS. A Pt catalyst found in one component adds a terminal [Si]-H bond across a [Si]-$CH=CH_2$ to yield cross-links in the polymer matrix of the form [Si]-CH_2CH_2-[Si]. The cross-linking chemistry is robust even when the two components are mixed at ratios distant from 10:1. Importantly, amines inhibit the cross-linking reaction through coordination to the Pt catalyst.

Thimbles were fabricated by first forming a monolayer of trichloro(1H, 1H, 2H, 2H-perfluoroctyl)silane on a glass vial with dimensions of several centimeters.[70] The vials were dipped into the PDMS mixture, cured in an oven at 65 ºC for 30 min, and then dipped into the PDMS mixture one more time before

curing for several hours at 65 ºC. Two coats of PDMS led to reproducible thicknesses for the PDMS walls of 100 microns. The thimbles were removed from the glass vials by swelling in hexanes which caused the PDMS to delaminate from the surface of the vials. Alternatively, metal rods were also used in the same fashion.[71]

Differential Flux of Reagents and Catalysts Through PDMS Thimbles

Flux of a molecule through a polymeric membrane depends on several factors, but two of the most important are the partition coefficient of a molecule from the solvent into the polymer and the rate of diffusion of a molecule in the polymer matrix. Simply, a molecule must be soluble in PDMS and possess a reasonable rate of diffusion within PDMS to flux through it. Numerous reviews cover these concepts and with mathematical rigor.[72-76]

Most organic molecules flux through PDMS thimbles with reasonable rates. Molecules with carboxylic acids, alcohols, amines, aromatic rings, nitro groups, esters, olefins, epoxides, and ketones readily flux through the walls of PDMS thimbles.[70,71,77-85] For instance, when the molecules shown in Figure 3.2 were dissolved in CH_2Cl_2 on the interior of PDMS thimbles with walls approximately 100 microns thick, they readily fluxed to CH_2Cl_2 on the exterior of the thimbles. The time it took for the ratio of the concentration for each molecule on the exterior to the interior of the thimble to reach 0.80 is shown. Clearly, even large molecules such as cholesterol can flux through PDMS walls at reasonable rates.

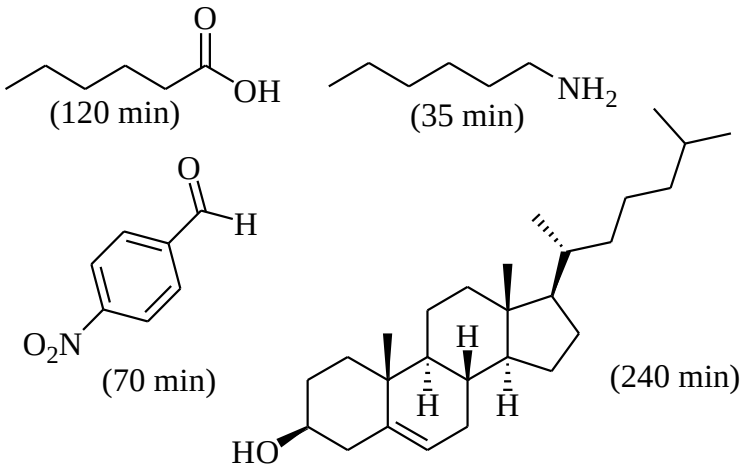

Figure 3.2. Hexanoic acid, 1-hexanamine, *p*-nitrobenzaldehyde, and cholesterol and the rate of flux through PDMS.

The flux was also dependent on the thickness of the walls of the thimbles, solvents, and temperature. Briefly, as the thickness of walls increased or the temperature decreased, the flux slowed. The solvent was a critical parameter and the flux increased with the ability of solvents to swell PDMS. To quantify how well solvents swelled PDMS, Whitesides et al. measured the lengths of PDMS rods before and after swelling in various solvents.[82] Apolar, aprotic solvents swelled PDMS well, but polar protic solvents were poor solvents for PDMS. For instance, PDMS rods were swollen in both CH_2Cl_2 and DMF and increased in length. The ratios of the lengths of the rods after swelling to their original, preswollen lengths were 1.22 for CH_2Cl_2 and 1.02 for DMF. When the flux of *p*-nitrobenzaldehyde through PDMS thimbles with walls approximately 100 microns thick were measured, the flux was much faster when CH_2Cl_2 was used as a solvent than when DMF was used.[79] Specifically, in experiments where *p*-nitrobenzaldehyde was initially added to the interior of the thimbles, the time it took for the ratio of its concentration on the exterior to the interior of the thimble

to reach 0.8 was approximately 70 min when CH_2Cl_2 was the solvent and 80 h when DMF was the solvent.

Molecules that possessed very low flux through the walls of PDMS thimbles included ionic liquids, *p*-toluenesulfonic acid, and polystyrene.[79,84] Others have shown that ionic liquids have no solubility within PDMS and our results support this. For instance, the ionic liquid shown in Figure 3.3 did not flux partition into PDMS.[86] In addition, *p*-toluenesulfonic acid did not flux through PDMS when DMF was used as the solvent. The negligible flux was probably due to its deprotonation and the fact that ionic molecules have little to no solubility in PDMS. Finally, it is well known that polymers do not flux through polymeric membranes. When polystyrene (Mw = 18,000 g mol^{-1}) was added to the interior of a thimble with CH_2Cl_2 on the interior and exterior, it did not flux through the walls of the thimble even after 3 d.[79]

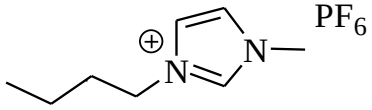

Figure 3.3. The Ionic liquid 1-Butyl-3-methylimidazolium hexafluorophosphate [BMIM][PF_6].

In summary, a wide variety of organic molecules with various functional groups flux through PDMS thimbles, but care should be taken to consider the solvent, thickness of the walls, temperature, and the presence of any ionic functional groups.

Site-Isolation of Water from $LiAlH_4$

Water was successfully added to the interior of a PDMS thimble and site-isolated from $LiAlH_4$ that was added to the exterior to complete a two-step, one pot reaction as shown in Figure 3.4.[70] In this reaction, 74 equivalents of water were added for every 1.25 equivalents of $LiAlH_4$ so control reactions where water and $LiAlH_4$ were not site-isolated by the walls of a PDMS thimble failed to yield the product.

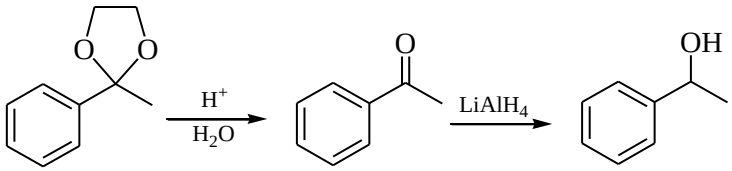

Figure 3.4. A two-step, one pot reaction using PDMS to site-isolate water from $LiAlH_4$.

Two methods were studied to demonstrate how to think about using PDMS thimbles. In the first method, all of the solvents and reagents were added and allowed to react as shown in Figure 3.5. The cyclic acetal, water, PTSA, and an organic solvent were added to the interior of a PDMS thimble and $LiAlH_4$ and an organic solvent were added to the exterior. This method was successful when hexanes was used as the solvent (quantitative conversions and 89% isolated yield), but significant amounts of the ketone were isolated when CH_2Cl_2, THF, or mixtures of hexanes with CH_2Cl_2 or THF were used as the organic solvents. The limitation in this method was that the THF and CH_2Cl_2 swelled the PDMS thimbles and allowed some water to flux through the walls of the thimble and quenched some of the $LiAlH_4$ before it had reacted with all of the ketone. When hexanes was used as the organic solvent on the interior and exterior of the

thimbles, the flux of water through the walls of the thimbles was lower relative to when THF or CH_2Cl_2 were used.

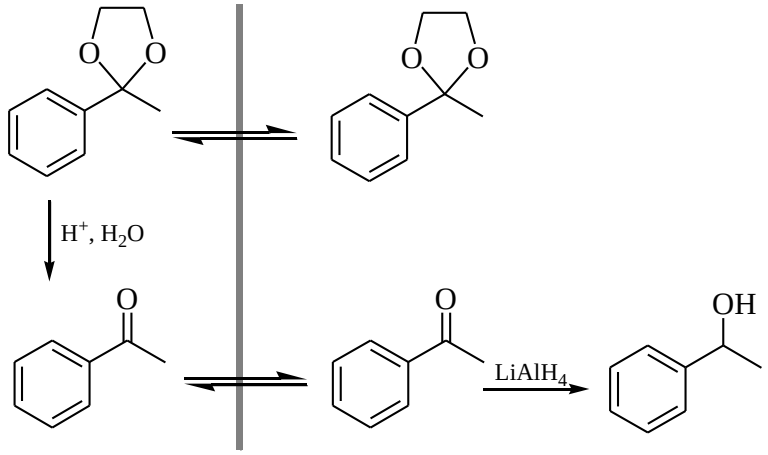

Figure 3.5. A two-step, one pot cascade reaction using PDMS to site-isolate water from $LiAlH_4$.

In a second method, the reaction on the interior of the thimble was allowed to go to completion with no solvent or $LiAlH_4$ on the exterior (Figure 3.6). Only after the reaction on the interior was complete was the organic solvent and $LiAlH_4$ added to the exterior of the thimble. These reactions proceeded to quantitative conversions and high yields for solvent mixtures of 1:3 CH_2Cl_2:hexanes, 1:3 THF:hexanes, and 1:1 THF:hexanes (*v*/*v*). These reactions were successful in solvent mixtures that failed for the method shown in Figure 3.5. The reason for this success was that the cyclic acetal was not allowed to flux through the walls of the thimbles until it had all been converted to ketone. The flux of the cyclic acetal to the exterior of the thimbles shown in Figure 3.5 slowed its conversion to the ketone (the cyclic acetal would flux to the exterior and had to flux back to the interior to yield the ketone) such that the flux of water to the

exterior to quench $LiAlH_4$ was competitive with the deprotection of the acetal. By converting all of the cyclic acetal to ketone as shown in Figure 3.6 prior to the addition of solvent and $LiAlH_4$ to the exterior of the thimble, the success of the reduction depended only on the fast flux through PDMS of the ketone as compared to the slower flux for water.[83,84]

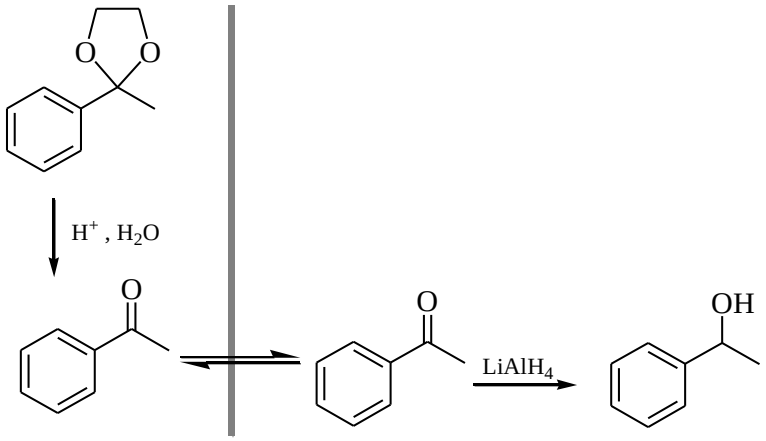

Figure 3.6. A two-step, one pot cascade reaction using PDMS to site-isolate water from $LiAlH_4$.

Site-Isolation of Water from Grignard Reagents

The same two-step, one pot cascade reaction was utilized for the reaction shown in Figure 3.7.[70] The acetal, water, an organic solvent (typically hexanes, diethyl ether, or a mixture of them), and PTSA were added to the interior of a PDMS thimble. When the first reaction was judged to be complete, an organic solvent and either Grignard reagent, butyl lithium, or an organocuprate were added to the exterior of the thimble. These reactions used 74 equivalents of water for every 5 to 8 equivalents of nucleophile and every one equivalent of cyclic acetal. Thus, the reactions failed without PDMS to site-isolate water from

the nucleophile. Reaction times for the first step ranged from 3.5 to 12 h and for the second step they ranged from 11 to 22 h. These reaction times were not optimized. Isolated yields of 77-93% were found.

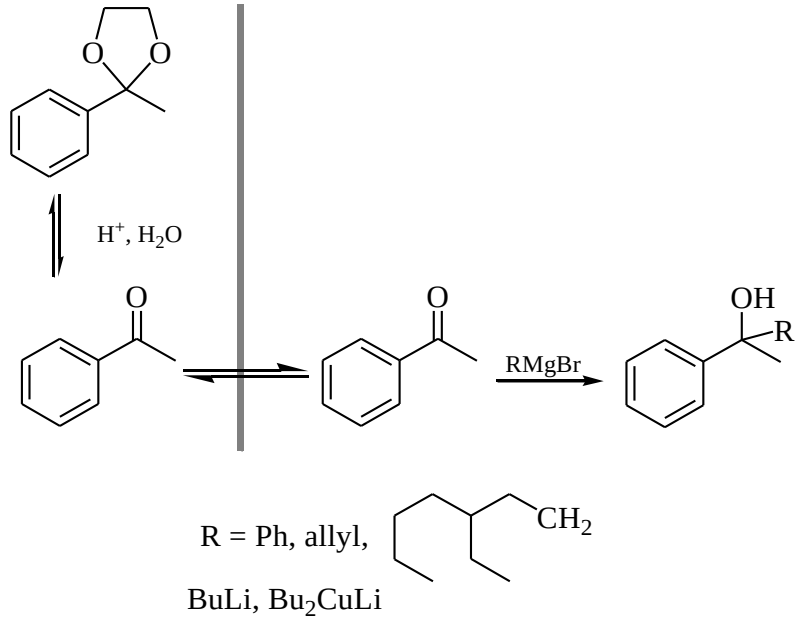

Figure 3.7. A two-step, one pot cascade reaction using PDMS to site-isolate the Grignard reagent from water.

The use of butyl lithium was problematic because it rapidly reacted with the walls of the PDMS thimbles such that holes formed and water leaked out to quench any remaining butyl lithium.

Site-Isolation of the Grubbs' Second Generation Catalyst from MCPBA

One concept that was critical for site-isolation of organometallic catalysts was that big molecules generally have slower flux through membranes than small molecules. This concept was critical for molecules such as the Grubbs'

catalysts, which possessed high molecular weights and cross-sectional areas (Figure 3.8). This discussion will address how to site-isolate organometallic and inorganic catalysts.

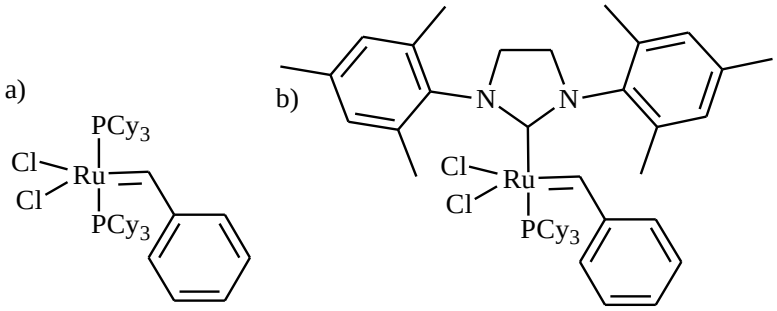

Figure 3.8. Grubbs' catalyst
a) First generation
b) Second generation

The Grubbs' second generation catalyst was site-isolated within PDMS thimbles because its flux was low due to its size and because it was insoluble in the solvent found on the exterior of the thimble.[71,81] Both factors were critically important to site-isolate the catalyst on the interior of the PDMS thimbles. When the catalyst was added to the interior of a PDMS thimble with CH_2Cl_2 on both the interior and exterior, the catalyst fluxed to the exterior within minutes. When the solvent on the interior and exterior of a thimble was changed to a 1:1 (v/v) mixture of CH_2Cl_2:1-butyl-3-methylimidazolium hexafluorophosphate [BMIM][PF_6], 14% of the ruthenium in the system was found on the exterior of the thimble after 16 h. The best site-isolation occurred when the solvent on the interior of the thimble was CH_2Cl_2:[BMIM][PF_6] and the solvent on the exterior was a 1:1 mixture of MeOH:H_2O. With these solvents only 0.4% of the ruthenium in the system was found on the exterior after 16 h. The reason for the success

was that the Grubbs' catalyst was not soluble in 1:1 MeOH:H_2O but it was soluble in the CH_2Cl_2:[BMIM][PF_6] solvent mixture on the interior of the thimble. Although the Grubbs' catalyst could flux through the thimble, it was insoluble in the solvent on the exterior of the thimble so it did not partition into the exterior. This method may be a general method to site-isolate catalysts using PDMS membranes.

This method was used to complete a series of ring closing and cross metathesis reactions (Figure 3.9). The Grubbs' second generation catalyst and CH_2Cl_2:[BMIM][PF_6] were added to the interior of a thimble and the starting material and MeOH:H_2O were added to the exterior. The starting materials fluxed to the interior of the thimble to react while the Grubbs' catalyst remained on the interior. Yields ranged from 69-93% with reaction times of 2.5 to 26 h.

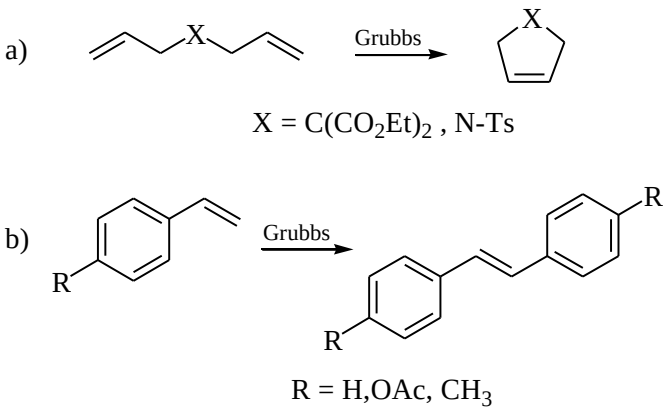

Figure 3.9. Metathesis reactions
a) Ring closing Metathesis
b) Cross Metathesis

The catalyst could be recycled for 5 cycles at quantitative conversions and with yields from 66-82% as shown in Figure 3.10. The catalyst was added to the interior of a thimble with CH_2Cl_2:[BMIM][PF_6] and the malonate. After the

reaction was complete, the product was extracted to the exterior of the thimble with MeOH. The MeOH on the exterior was removed from the reaction vessel and new malonate was added to the interior of the thimble to react with the catalyst.

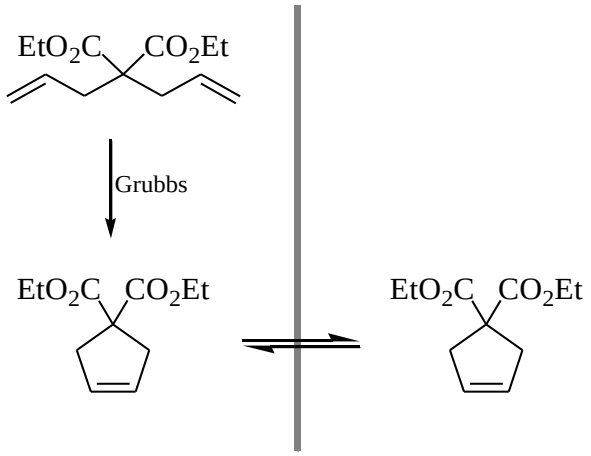

Figure 3.10. Ring closing metathesis reactions using PDMS to site-isolate product from Grubbs' catalyst.

The Grubbs' catalyst was successfully site-isolated from MCPBA using PDMS thimbles as shown in Figure 3.11. and Figure 3.12. In control reactions it was shown that at ratios of MCPBA to Grubbs' catalyst of 3,000:1, the Grubbs' catalyst catalytically decomposed MCPBA in a very rapid reaction such that the epoxidation of olefins proceeded to give low yields (<22%). The Grubbs' second generation catalyst was added to the interior of a thimble with CH_2Cl_2:[BMIM][PF_6] and a substrate. After the metathesis reaction was complete, MCPBA and MeOH:H_2O were added to the exterior to complete the epoxidation. Isolated yields of 67-83% were isolated for these substrates.

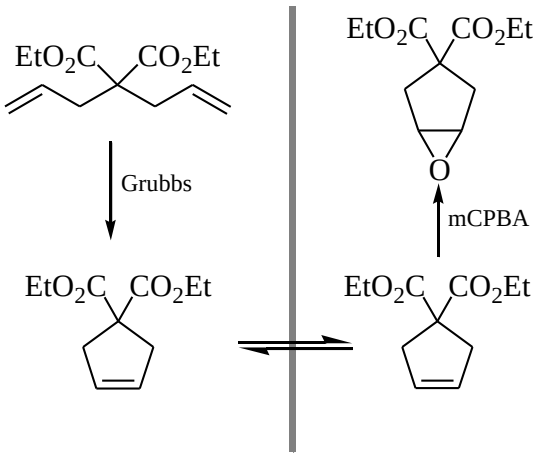

Figure 3.11. A two-step, one pot cascade reaction using PDMS to site-isolate Grubbs' catalyst from mCPBA.

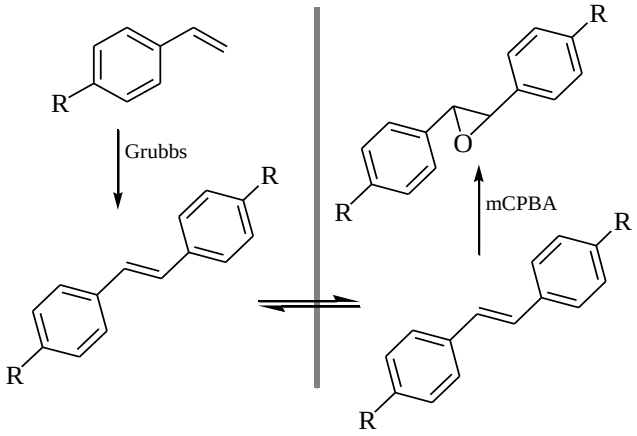

Figure 3.12. A two-step, one pot cascade reaction using PDMS to site-isolate Grubbs' catalyst from mCPBA.

The Grubbs' catalyst was recycled in a cascade sequence as shown in Figure 3.11. The Grubbs' catalyst was recycled as described before, but in these reactions the extracted product was epoxidized with MCPBA after removal from

the reaction vessel containing the PDMS thimble. The isolated yields of the product ranged from 60-86% through five cycles.

Site-Isolation of the Grubbs' Catalyst from the Sharpless Dihydroxylation Catalyst

The Grubbs' catalyst was site-isolated from AD-mix to complete cascade reactions as shown in Figure 3.13, 3.14, and 3.15.[77] The Grubbs' catalyst was added to the interior of a thimble with CH_2Cl_2:[BMIM][PF_6] and the metathesis reaction was run to completion. Next, the AD-mix was added to the exterior of a thimble with 1:1 (*v*/*v*) *t*-BuOH/H_2O or 1/2/3 (*v*/*v*/*v*) [BMIM][PF_6]/H_2O/acetone. The product of the metathesis reaction fluxed to the exterior and reacted to yield the diol.

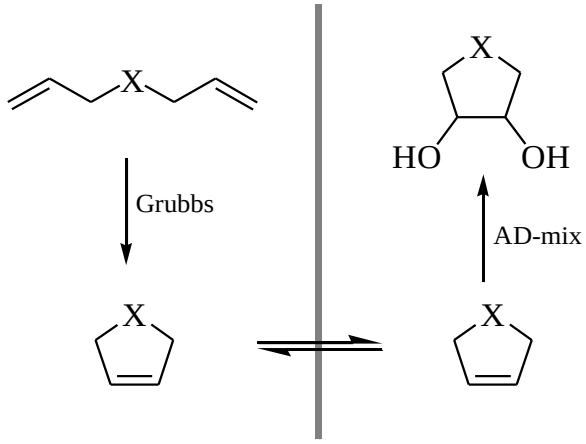

Figure 3.13. A two-step, one pot cascade reaction using PDMS to site-isolate Grubbs' catalyst from AD-mix.

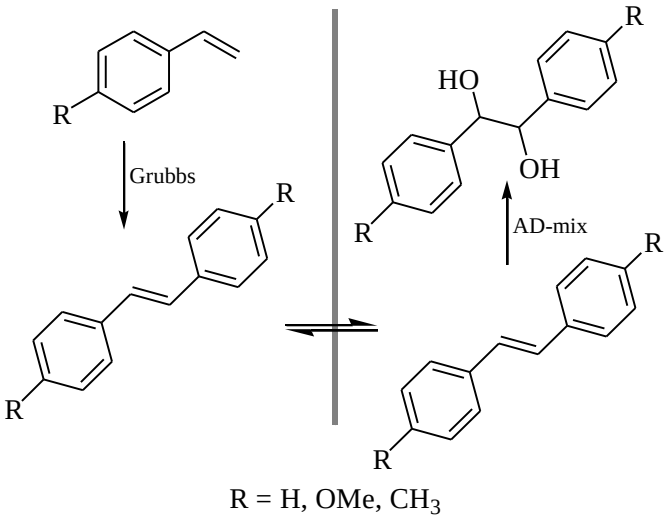

Figure 3.14. A two-step, one pot cascade reaction using PDMS to site-isolate Grubbs' catalyst from AD-mix.

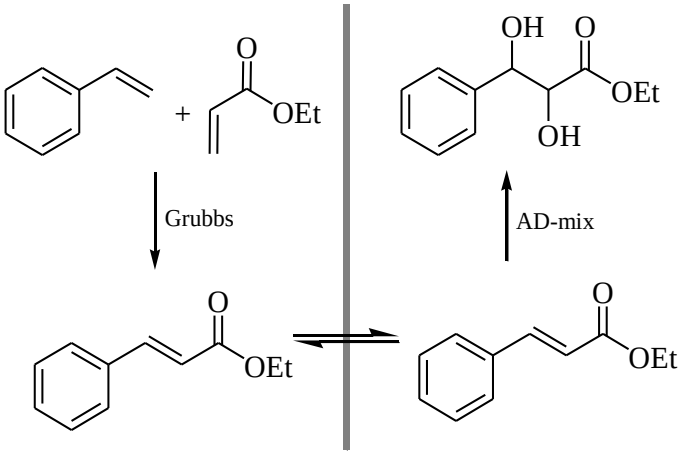

Figure 3.15. A two-step, one pot cascade reaction using PDMS to site-isolate Grubbs' catalyst from AD-mix.

The Grubbs' catalyst was site-isolated using the thimbles and solvents described here. Less than 1% fluxed to the exterior even after 24 h. In contrast, the Os [VIII] fluxed to the interior of the thimble but this had no apparent impact

on the yields and enantiomeric excesses. An achiral product was also isolated to demonstrate that the two-step process was successful for a cyclic substrate. The yields for the reactions ranged from 61-95% and the enantiomeric excesses were 84-98%. The enantiomeric excesses matched those reported by others for identical substrates in reactions completed in glass vessels.

This method was extended to substrates with intermediates that were challenging to isolate.[77] For instance, a metathesis-dihydroxylation cascade reaction was completed on a challenging substrate (Figure 3.16). The metathesis reaction of diallylamine yielded a molecule with an estimated boiling point of 55 °C, this molecule was not isolated but rather converted to the diol and isolated as a high boiling point product (80% isolated yield). It was not necessary to isolate the volatile intermediate in this sequence.

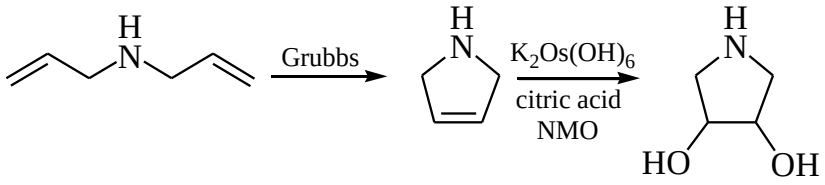

Figure 3.16. A two-step, one-pot cascade reaction using PDMS to site-isolate Grubbs' catalyst from $K_2Os(OH)_6$.

A second challenging metathesis-dihydroxylation cascade reaction was completed (Figure 3.17). Diallyl sulfide (boiling point: 138 °C) was reacted with the Grubbs' catalyst to yield a cyclic intermediate with an estimated boiling point of 90 °C. The intermediate had an unpleasant odor, but it was not isolated in this sequence. Rather, the formation of the diol and oxidation of the sulfur were

completed *in situ* to yield a product that was essentially odorless (79% isolated yield). Three reactions were completed in one pot with this substrate.

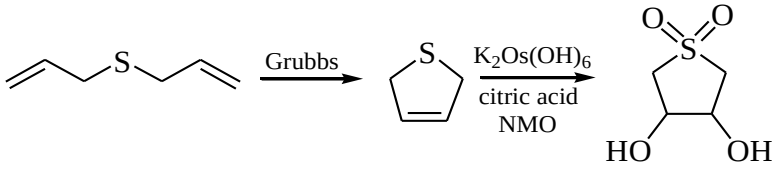

Figure 3.17. A two-step, one pot cascade reaction using PDMS to site-isolate Grubbs' catalyst from $K_2Os(OH)_6$.

Site-Isolation of Polymeric Catalysts

A common method to site-isolate catalysts from the products of a reaction is to attach the catalyst to a polymer that can be precipitated at the end of a reaction.[87-90] Catalysts attached to a polymer are generally not site-isolated from other catalysts attached to a different polymers such that only one catalyst can be added to a reaction mixture. The use of PDMS thimbles solves this problem.[79]

It is well known that polymers do not flux through polymeric membranes. In experiments with PDMS thimbles and CH_2Cl_2 as the solvent, the polymers shown in Figure 3.18. and Figure 3.19. did not flux through the membranes even after 3 d. No evidence of the polymers were found on the exterior of the thimbles which can be contrasted with the rapid flux of small molecules under identical conditions (Figure 3.2).

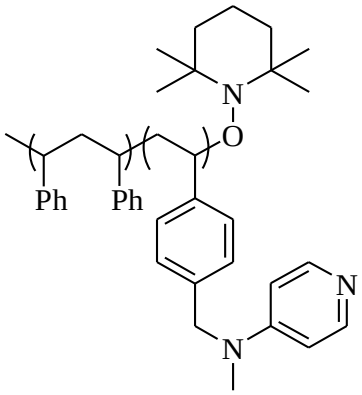

Figure 3.18. Polymer that does not flux through PDMS with DMAP bonded to the backbone.

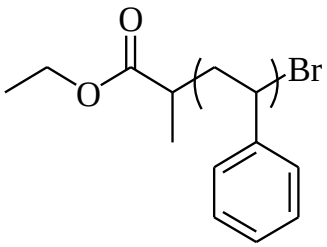

Figure 3.19. Polymer that does not flux through PDMS.

A series of cascade reactions with an acid catalyst on the interior of a PDMS thimble and a base catalyst on the exterior were completed (Figure 3.20). In these reactions the acetal was added to the interior of a thimble with an acid catalyst and methyl acrylate was added to the exterior with a basic catalyst. The solvent on the interior and exterior of a thimble were 7:1 (*v*/*v*) DMF:H_2O. The reactions were heated to 70 °C for 72 h and then product was isolated.

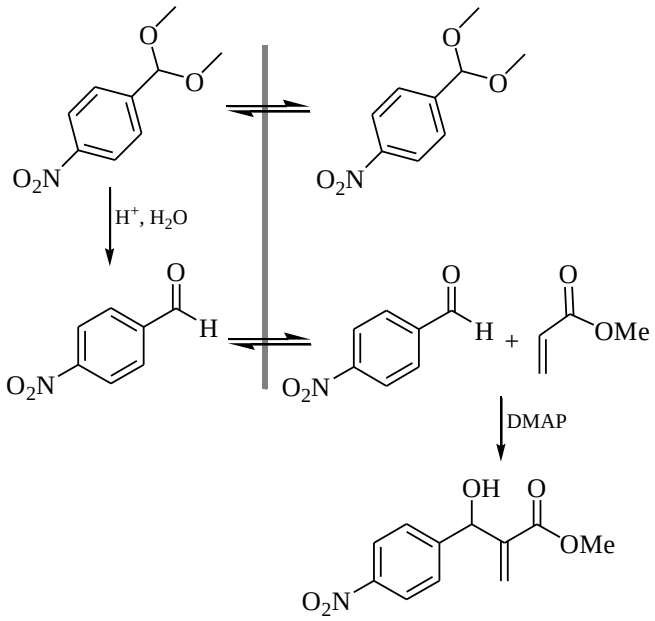

Figure 3.20. A two-step, one-pot cascade reaction using PDMS to site-isolate acid catalyst from base catalyst.

Striking differences in yields were observed in reactions run with or without PDMS thimbles. The acid catalyst was either PTSA or commercially available beads with PTSA bonded to the backbone (Figure 3.21). The basic catalyst was either DMAP, commercially available beads with DMAP bonded to the backbone (Figure 3.22), or a linear polymer (Figure 3.18). Six reactions were completed with either PTSA or the beads with PTSA and each of the three different bases. In reactions with PDMS thimbles to site-isolate the acid from the base, the isolated yields of the final product were 71-93%. The lowest yields were when DMAP was the basic catalyst. This result was probably due to the flux of DMAP through the thimbles that quenched some of the acid on the interior of the thimble.

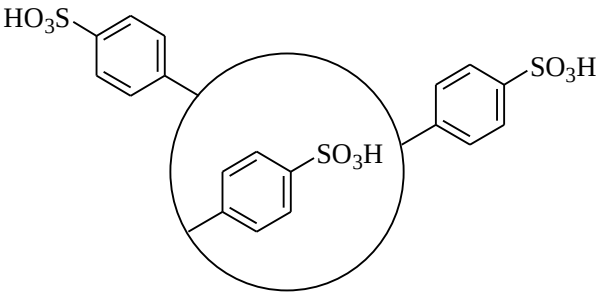

Figure 3.21. Polymer beads with PTSA bonded to the backbone.

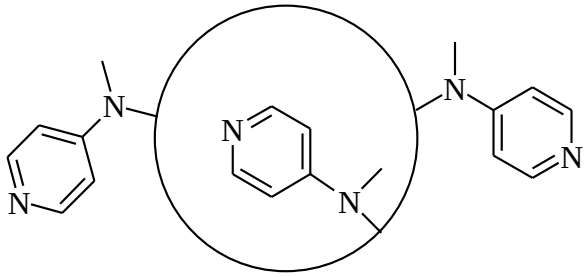

Figure 3.22. Polymer beads with DMAP bonded to the backbone.

In five of the six reactions without thimbles to site-isolate the acid and base catalysts, the isolated yields of the product ranged from 0-15%. Only in the reaction with polymeric beads with PTSA and beads with DMAP did the isolated yield reach 50%. In summary, the PDMS thimbles successfully site-isolated polymeric catalysts from one another and this approach should work for other polymeric catalysts.

Site-Isolation of $PdCl_2$

Due to the importance of Pd in organic synthesis, the site-isolation of $PdCl_2$ was studied.[78] The Wacker-Tsuji oxidation of olefins (Figure 3.23) and Pd-mediated homocoupling of aryl boronic acids (Figure 3.24) were completed on

the interior of PDMS thimbles. In each of these reactions the catalyst was $PdCl_2$ and a polar, protic solvent was used on the interior of the thimbles. The products were fluxed to the exterior of the thimbles by the addition of CH_2Cl_2 or hexanes to the exterior. Isolated yields were 56-93%.

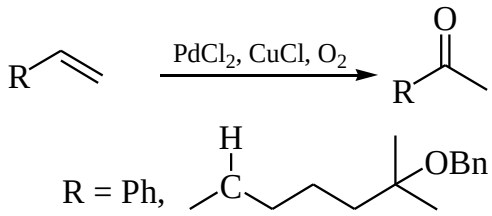

Figure 3.23. Wacker-Tsuji oxidation.

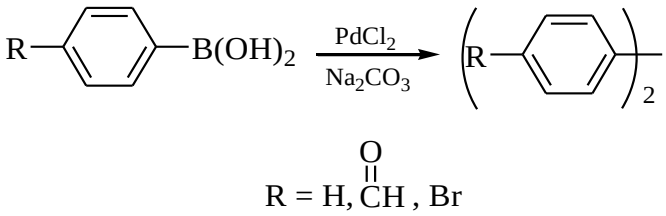

Figure 3.24. Pd-mediated homocoupling of aryl boronic acids.

In each of these reactions the Pd was site-isolated on the interior of the thimbles. To characterize the concentration of Pd in the products, the reactions were run to completion and the product was extracted to the exterior. The solvent on the exterior of the thimble was isolated and removed. The concentration of Pd in the product was found by ICP-MS. Between 0.225% and less than 0.002% of the Pd that was added to the interior of the thimble was found in the products on the exterior of the thimbles. In other words, >99.998%

and no less than 99.775% of the Pd remained on the interior of the thimbles even after the product was extracted to the exterior.

The reason for the low flux of $PdCl_2$ was that it was soluble only in polar, protic solvents. Its solubility in PDMS was negligible so it did not flux through the walls of the thimbles. When phosphines were added to the reaction mixture to coordinate to $PdCl_2$ and render it less polar, the phosphines and Pd readily fluxed through the walls of the PDMS thimbles. This method demonstrates that catalysts that do not partition into PDMS will remain site-isolated by it.

Conclusion

Small molecules, organometallic catalysts, inorganic catalysts, and polymeric catalysts were all successfully site-isolated at levels up to >99.998% using PDMS thimbles. When considering whether to site-isolate catalysts or reagents, the most important parameters to consider are the solubility and rates of diffusion within the swollen PDMS matrix and the solubility in the organic solvents on the interior and exterior of thimbles. However the solubility of small molecules in the swollen PDMS matrix cannot be easily altered. Although the applications that are discussed in this chapter are extremely useful, they are limited.

Polydicyclopentadiene (PDCPD) however, is prepared from the polymerization of dicycylopentadiene with Grubbs catalyst (Figure 3.25a) and can be readily functionalized through copolymerization as seen in Figure 3.25b. A variety of copolymers could prepared with a wide range of properties that would drastically effect the solubility of molecules in the thimble.

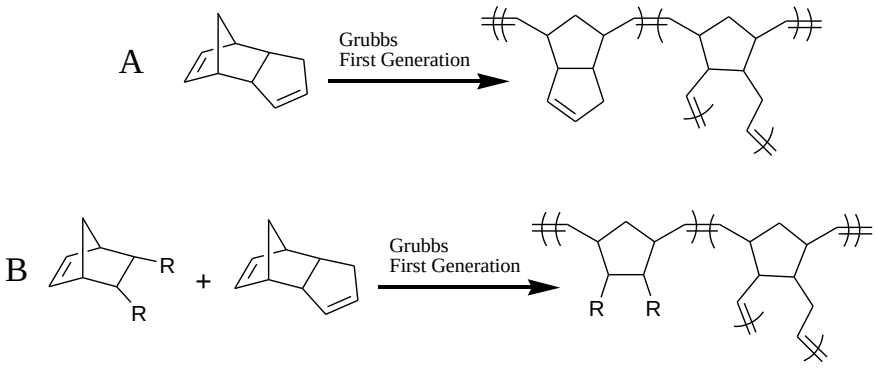

Figure 3.25. The synthesis of polydicyclopentadiene and polydicyclopentadiene copolymer with Grubbs catalyst.
a) The synthesis of polydicyclopentadiene
b) The synthesis of polydicyclopentadiene copolymer

In the initial testing of PDCPD for use as a thimble it was discovered that PDCPD could separate different molecules based on their minimum cross-sectional areas without any further modifications. The rate of flux through PDCPD was more dependent on the rate of permeation through the thimble rather than solubility in the thimble. PDCPD was also cast into a membrane rather than a thimble because membranes can be scaled up easily and are more suited for industrial applications. The development of PDCPD membranes is described in Chapter 4.

CHAPTER 4

SELECTIVE FLUX OF ORGANIC LIQUIDS AND SOLIDS USING NANOPOROUS MEMBRANES OF POLYDICYCLOPENTADIENE

Abstract

Membranes were fabricated from the ring opening metathesis polymerization of dicyclopentadiene with the Grubbs first generation catalyst, and the permeability of twenty-one molecules through them was studied. Both polar and apolar molecules with molecular weights from 101 to 583 g mol^{-1} permeated these membranes with values for flux of 10^{-5} to 10^{-6} mol cm^{-2} h^{-1}, but selected molecules did not permeate them and had flux 10^{4} to 10^{5} times slower. The difference in flux was large between molecules that permeated and those that did not permeate, but no trend was observed that correlated flux with molecular weight or hydrophobicity. Rather, molecules that did not permeate the membranes had large cross-sectional areas that led to low rates of diffusion within the highly cross-linked polydicyclopentadiene membranes. The degree of cross-linking within the polydicyclopentadiene membranes was measured using infrared spectroscopy and approximately 84% of the dicyclopentadiene monomer had reacted to form cross-links. These are the first organic solvent nanofiltration membranes that separate molecules with molecular weights from 100 to 600 g mol^{-1} based on cross-sectional areas.

Introduction

Membranes are among the most common and economically efficient methods to purify active pharmaceutical ingredients (API) in industry and provide a critical alternative to distillations, recrystallizations, and column chromatography. Distillations require that an API be stable to elevated

temperatures and require significant amounts of energy to complete. Recrystallizations often result in APIs with high purities, but not every molecule can be recrystallized and recrystallization conditions are often difficult to optimize and scale up to an appropriate level.[91,92] In addition, the formation of multiple crystalline isomorphs is poorly understood and results in APIs with different delivery characteristics in the body.[93-98] Column chromatography is often used in the early discovery and development of APIs due to its simplicity and success, but it is not widely used for large scale production of APIs due in part to the large volumes of solvents that are used which necessitate further purification. In contrast, the use of nanoporous membranes to purify APIs can be readily scaled up to purify large quantities of product, use little energy, and does not require large amounts of solvent.[99-103] The use of nanoporous membranes in industry is common in aqueous separations or to purify gases by pervaporation, but nanoporous membranes are used less commonly with organic solvents. A breakthrough was realized in 1990 when nanoporous membranes based on “organic solvent nanofiltration” (OSN) membranes were used in an ExxonMobil refinery to separate oil from dewaxing solvents.[104] The next generation of OSN membranes based on cross-linked polyaniline, polyimides, and other polymers and sold as StarMem, Duramem, and PuraMem have been developed that function in a wide range of organic solvents and separate organic molecules dissolved in organic solvents.[99,101-103,105-108]

All OSN membranes report values for the “molecular weight cutoff” (MWCO) that correspond to the molecular weight where molecules transition from having high to low values of permeation.[107,108] Simply put, molecules below the MWCO permeate the membranes, but molecules above the MWCO have significantly reduced permeation and are retained. The use of membranes that feature a MWCO has limitations for the separation of catalysts from APIs

because the ligands on a catalyst often have molecular weights that are similar to that of the product. Thus, ligands such as PPh_3 (MW: 262 g mol^{-1}), PCy_3 (MW: 280 g mol^{-1}), and binol (MW: 286 g mol^{-1}) can be very challenging to separate from APIs with similar molecular weights or impossible to separate if an API has a higher molecular weight. In this chapter we report the first nanoporous membranes composed of polydicyclopentadiene (PDCPD) that separate many common ligands from metals from other molecules that possess molecular weights lower and higher than those of the ligands (Figure 4.1a). These ligands include phosphines, trisubstituted amines, binol, and salen. The separation is due to the large cross-sectional area of ligands which hinders their diffusion through heavily cross-linked PDCPD. In contrast to the ligands which do not permeate these membranes at any level, molecules with low to high molecular weights permeate them if their cross-sectional areas are below a critical threshold. The significance of this work is that PDCPD membranes retain key molecules that are common ligands for metals while allowing molecules with molecular weights over three times as high to permeate. No OSN membranes have this property for molecules with molecular weights of 100-600 g mol^{-1}.

The state-of-the-art membranes to separate catalysts from the products of reactions are based on highly cross-linked organic polymers that function in a range of organic solvents. For instance, in the reaction shown in Figure 4.1b the RuBINAP catalyst (molecular weight 795 g mol^{-1}) was retained by OSN membranes at levels of approximately 98% for multiple cycles and was active for long periods of time.[109] The product was allowed to permeate the membranes and was isolated on the side of the membrane opposite to the catalyst. Part of the success of this project was the high molecular weight of the catalyst compared to the product (molecular weight 160 g mol^{-1}) which allowed the

catalyst to have a molecular weight significantly higher than the MWCO of the membrane (220 g mol^{-1}).

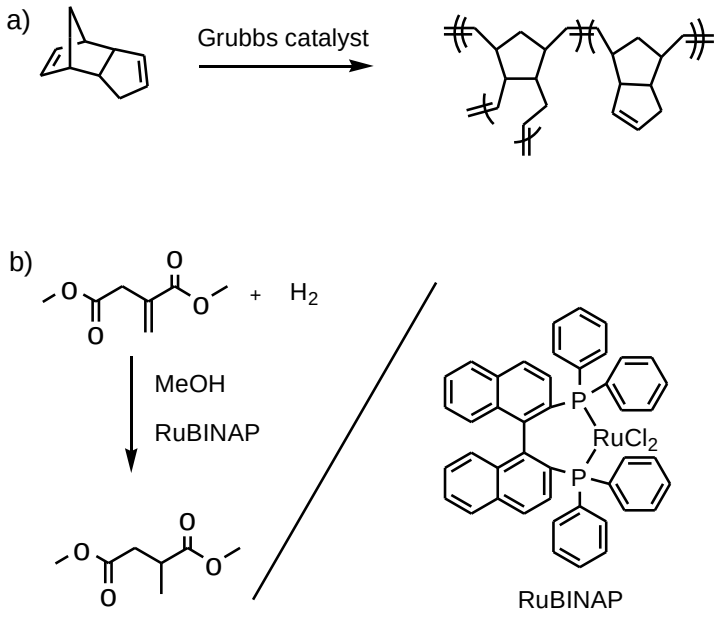

Figure 4.1. Polydicyclopentadiene and other OSN membrane.
a) Polydicyclopentadiene was synthesized by polymerizing dicyclopentadiene with the Grubbs first generation catalyst at monomer to catalyst loadings of 5,000:1.
b) Despite the large difference in molecular weight between RuBINAP and the product of the reaction, RuBINAP was only site-isolated at 98% using an OSN membrane.

In other work, the flux of trialkylamines (i.e. NR_3 where R is methyl, ethyl, propyl, etc) through commercially available OSN membranes (StarMem™ membranes) were studied.[105] This study described perplexing results because even though the molecular weight cutoff was 220 g mol^{-1}, only 19% of tridodecylamine (molecular weight 522 g mol^{-1}) was retained (81% permeated the membrane). Also, when the system was studied using cross-flow, the rejection

rate for all of the trialkylamines was much poorer than expected. The authors concluded that the use of a molecular weight cutoff for trialkylamines and the StarMem membranes was not useful and gave misleading predictions.[105]

OSN membranes have an important role in the chemical industry, but they have two limitations that hinder applications in many commercial syntheses of small molecules.[101-103,106,107,110] First, to be effective there must be a large difference between the molecular weight of the catalyst and the organic product. The molecular weights of many common ligands range from a couple to several hundred grams per mole and would not provide enough difference in molecular weight to separate them from products with similar or higher molecular weights. Second, the MWCO of a membrane is defined as the molecular weight at which 90 to 98% of the solute is rejected; thus, significant amounts of a molecule may pass through these membranes even if the molecular weight is larger than the cutoff.

Other membranes composed of nanopores etched in polycarbonate, zeolites, and metal-organic frameworks have been fabricated by others that can separate organic molecules. Zeolites are well known for distinguishing molecules based on size, but they are not used as membranes for molecules with the dimensions described in this proposal. Nanopores etched in polycarbonates have found some success, but the molecular size cutoffs are typically not sharp and the membranes suffer from low flux, fouling, and degradation with time.[111,112] Metal-organic frameworks have been developed that use porphyrins to define pores, but all of these examples require either water as the solvent or only separate gasses.[113-120] Although promising, none of these other approaches have the selectivities and properties of PDCPD membranes as described in this report.

In this chapter we report the first use of PDCPD as membranes and the very low flux of common organic ligands through these membranes. PDCPD synthesized from the polymerization of commercially available dicyclopentadiene and the Grubbs catalyst is a relatively new material.[121-125] This polymer is heavily cross-linked and forms a solid, hard material that, when synthesized by other catalysts, is used in the fabrication of the hoods of semitrucks and snowmobiles. This chapter reports that although it is a hard polymer, it will readily swell in organic solvents and allow molecules to permeate through it. This is the first reported use of PDCPD as a membrane for liquid separations. We will describe how molecules with a variety of polar functional groups and differing molecular weights permeate PDCPD membranes while other molecules do not permeate.

The difference in permeation is based on cross-sectional area of each molecule.[72-76,83,84,126-129] Molecules that have cross-sectional areas larger than a critical value do not permeate the membranes while those below the critical value do permeate them. Both polar and apolar molecules permeate if their cross-sectional area is below the critical value. This criterion for separation is based on the highly cross-linked matrix of PDCPD that results in a set of pores that allow the polymer to have unique properties for molecules with molecular weights between 100-600 g mol^{-1}. These are the first membranes to separate organic molecules with these molecular weights based on the large cross-sectional areas of many common ligands for metals. This chapter will describe the permeation of over 20 different molecules, their chemical and physical properties, and the degree of cross-linking within PDCPD.

Results and Discussion

Fabrication of PDCPD Membranes and the Apparatus to Measure Permeation

Membranes composed of PDCPD were readily fabricated by the polymerization of commercially available dicyclopentadiene using the Grubbs first generation catalyst at molar ratios of >4,000:1 dicyclopentadiene:Grubbs catalyst (Figure 4.1a). The Grubbs catalyst was added to dicyclopentadiene, mixed thoroughly, and placed between two glass slides separated by approximately 100 microns. These membranes were robust and could be manipulated by hand.

In the experiments described in this report, the membranes were placed in an apparatus between two reservoirs of solvent (Figure 4.2). The membranes were kept in place using O-rings on either side and held in place using a clamp. The solvent on either side of the membrane was agitated using stir bars and a magnetic stir plate to eliminate any boundary effects that might influence these experiments. In most experiments the permeation of a molecule through the membrane was studied by adding it to solvent on only one side of the membrane. This was called the “upstream” side of the membrane. Many molecules permeated through the membranes and were also found in the solvent “downstream” of the membrane.

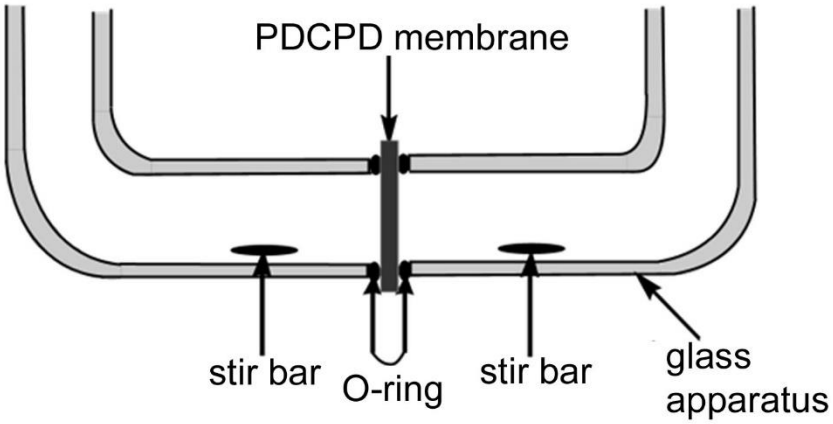

Figure 4.2. A cross-sectional schematic of the apparatus used to measure permeation through PDCPD membranes.

Permeation of Co(salen) using Membranes Composed of PDCPD or polydimethylsiloxane

Preliminary work indicated that membranes composed of PDCPD would not allow molecules above a critical cross-sectional area to permeate. To investigate the composition of PDCPD membranes that would retain selected molecules based on their cross-sectional area, the permeation of Co(salen) was studied due to its large cross-sectional area of 1.15 nm^2. To contrast the results with PDCPD membranes, the permeation of Co(salen) and hexadecane through membranes composed of polydimethylsiloxane (PDMS) were also studied. PDMS was chosen based on our prior work to site-isolate water, Grignard reagents, butyl lithium, $PdCl_2$, and other catalysts and reagents.[70,71,77-80] In this prior work, PDMS successfully retained a wide variety of reagents and catalysts based on their low solubility in hydrophobic PDMS.

A membrane composed of PDMS was fabricated with a thickness of 450 microns and equilibrated with CH_2Cl_2 on both sides of the membrane. Co(salen)

and hexadecane were added upstream of the membrane and the concentration of Co(salen) and hexadecane upstream (S_u) and downstream (S_d) of the membrane were measured at 2, 4, and 6 h (Table 4.1). In prior work little evidence was observed for the ability of PDMS membranes to distinguish molecules based on their cross-sectional areas, and in experiments with Co(salen) and hexadecane, both molecules permeated the membranes at similar rates.

Table 4.1. Permeation of Co(salen) and hexadecane using PDMS membranes and CH_2Cl_2 as the solvent.

Molecule	S_d/S_u at 2 h	S_d/S_u at 4 h	S_d/S_u at 6 h
Co(salen)	0.03	0.07	0.13
hexadecane	0.17	0.52	0.61

PDCPD membranes were fabricated with different loadings of dicyclopentadiene:Grubbs catalyst as shown in Table 4.2 to determine the ratio that led to retention of Co(salen). In all of these experiments the concentration of Co(salen) was studied by UV-VIS spectroscopy rather than ^{1}H NMR spectroscopy because the UV-VIS spectrometer allowed lower concentrations of Co(salen) to be measured and because Co(salen) was paramagnetic. At high loadings of 50,000:1 dicyclopentadiene:Grubbs catalyst the polymerization was incomplete and the polymer membrane was tacky and not robust. At loadings of dicyclopentadiene:Grubbs catalyst below 4,000:1 the polymerization was too rapid and the solution hardened before it could be cast into a thin film.

PDCPD membranes synthesized with molar ratios of 4,000 to 20,000 dicyclopentadiene to one Grubbs catalyst resulted in controlled polymerizations

and well-defined membranes. These membranes were used to study whether Co(salen) permeated them using CH_2Cl_2 as the solvent. In each of these experiments Co(salen) was not detected by UV-VIS spectroscopy downstream of the membrane at 24 or 48 h (Table 4.2). To provide further evidence for the retention of Co(salen), the concentration of Co downstream and upstream of the membranes were measured by ICP-OES at 48 h for entries 4 and 5. In these experiments, <0.5% of the Co was found downstream of the membrane which demonstrated that it did not permeate.

In entries 2-5 in Table 4.2 less than 30% of the Co(salen) permeated into the PDCPD matrix after 48 h, the remainder was found in the solvent upstream of the membrane. Thus, the Co(salen) was soluble in the PDCPD membrane and readily partitioned into it, so its slow permeation through the membrane was due to a very low rate of diffusion in the PDCPD matrix. In a later section it will be shown that molecules can be extracted from the PDCPD membrane and do not remain “trapped” in the PDCPD matrix.

These membranes were futher studied for the effect of ethyl vinyl ether on the permeation of Co(salen). When dicyclopentadiene is polymerized with the Grubbs catalyst, the strained bicylic olefin reacts rapidly to yield a polymer and the other olefin reacts at a slower rate to yield cross-links in the PDCPD matrix.[122,124,125,130-133] We hypothesized that the membranes underwent further cross-linking when swollen in organic solvent prior to being used as membranes because they were fabricated in the absence of solvent and initially yielded hard, solid materials that hindered the diffusion of the Grubbs catalyst. To investigate whether the Grubbs catalyst reacted when the membranes were swollen in organic solvents, they were swollen in CH_2Cl_2 with ethyl vinyl ether to terminate the Grubbs catalyst. If the Grubbs catalyst was inactive when the membranes were swollen in CH_2Cl_2, membranes treated with ethyl vinyl ether would have

similar properties for the permeation of Co(salen) as those not exposed to ethyl vinyl ether. If the Grubbs catalyst was dormant in the solid PDCPD and further cross-linked PDCPD when swollen in CH_2Cl_2, the addition of ethyl vinyl ether would stop any further cross-linking and affect the permeation of Co(salen). When these membranes were studied for their ability to resist the permeation of Co(salen), all of them allowed Co(salen) to permeate (entries 6-8 in Table 4.2). In a control experiment to study whether the addition of ethyl vinyl ether resulted in different permeation rates due to a change in solvent polarity, THF was added to CH_2Cl_2 rather than ethyl vinyl ether (entry 9 in Table 4.2). In this experiment Co(salen) did not permeate the membrane which demonstrated that the effect of ethyl vinyl ether could not be explained by a change in solvent polarity.

Table 4.2. Permeation of Co(salen) using PDCPD membranes fabricated with different catalyst loadings.

Entry	Dicyclopentadiene :Grubbs catalyst	Ethyl vinyl ether	[a]Thickness (μm)	[b]S_d/S_u at 24 h	[b]S_d/S_u at 48 h
1	[c]50000/1	[d]none	Na	Na	Na
2	20000/1	none	110	≤0.004[e]	≤0.005[e]
3	10000/1	none	110	≤0.005[e]	≤0.006[e]
4	5000/1	none	110	≤0.006[e]	≤0.007[e]
5	4000/1	none	100	≤0.005[e]	≤0.007[e]
6	10000/1	[f]10 mL	120	0.49	0.35
7	5000/1	[f]10 mL	88	0.05	0.06
8	4000/1	[f]10 mL	110	0.04	0.08
9	5000/1	[g]none	98	≤0.006[e]	≤0.009[e]

Note: [a]The thickness of the membrane. [b]The ratio of the downstream (S_d) concentration of Co(salen) to the upstream (S_u) concentration. [c]Incomplete polymerization after 47 h at 50 °C. [d]No ethyl vinyl ether was added to the solvent on either side of the membrane. [e]No Co(salen) was detected in the solvent downstream of the membrane. [f]Ethyl vinyl ether was added to the solvent on each side of the membrane. [g]THF was added to the solvent on either side of the membrane in the same concentration as ethyl vinyl ether from entries 6-8.

These experiments provided evidence that the cross-linking of the PDCPD matrix is incomplete when a solid polymer matrix is formed and the membranes must be swollen in organic solvents to have the desired properties to retain Co(salen). In the next section of this report, the density of cross-links in PDCPD before and after swelling in CH_2Cl_2 will be reported that provide further evidence that the Grubbs catalyst is dormant in PDCPD and reacts to form more cross-links when the polymer is swollen in organic solvents.

Measurement of Density of Cross-Links in PDCPD

The density of cross-links in PDCP was measured using IR spectroscopy. It important to understand that when dicyclopentadiene is polymerized it yields a hard, solid material that lacks well-defined, empty pores such as those found for zeolites or other nanoporous membranes. PDCPD was studied by scanning electron microscopy to reveal a flat, featureless surface. The surface of PDCPD was investigated by x-ray photoelectron spectroscopy and grazing angle total reflection-infrared (GATR-IR) spectroscopy in prior work.[134] The surface of PDCPD had little surface oxidation and its GATR-IR spectrum did not possess any unexplained peaks. Typical methods to characterize the distribution of empty pores were not attempted because of the lack of empty pores within PDCPD.

The most important characteristic of PDCPD is the density of cross-links within the matrix that occur when the five membered ring in the monomer reacts with another polymer chain. The degree of cross-linking of PDCPD was measured using IR spectroscopy by investigating the peak at 704 cm^{-1} that was assigned to the cis oops bending of the unreacted olefin in PDCPD (Figure 4.3). Opening of this ring by the Grubbs catalyst led to cross-links in PDCPD; thus, measurement of the concentration of the unreacted cyclic olefin in a PDCPD matrix gave an approximate concentration of cross-links. The peak at 704 cm^{-1}

was assigned to the cis oops of the unreacted olefin based on literature precedent for peaks in this area.[135] Olefins that reacted with the Grubbs catalyst were no longer part of medium sized rings and their values for the oops peak appeared at higher wavenumbers based on analogy to linear molecules. For instance, the oops peak for cis-3 heptene was at 714 cm^{-1} and for cyclopentene it was at 697 cm^{-1}. Trans oops peak typically have values above 720 cm^{-1}. Thus, the peak at 704 cm^{-1} was used to find the concentration of uncross-linked monomer in PDCPD.

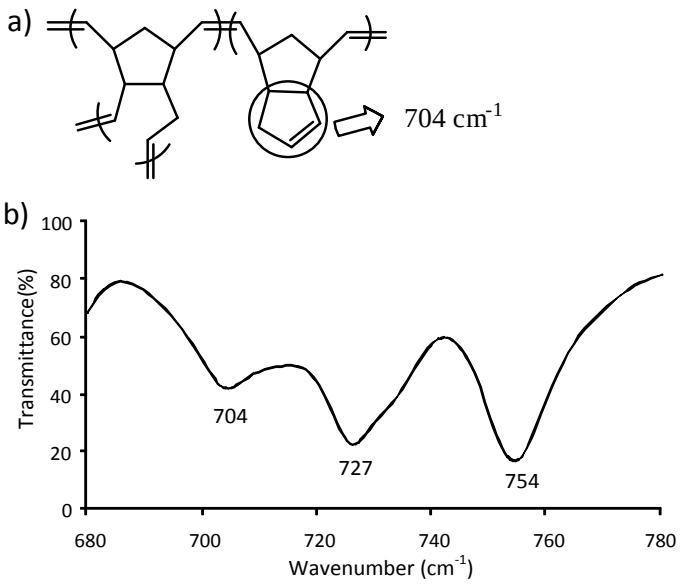

Figure 4.3. The IR spectrum of PDCPD
a) The unreacted five membered ring that is responsible for the peak at 704 cm^{-1}.
b) The IR spectrum of PDCPD in the region of interest.

A calibration curve for the cis oops peak was obtained by measuring the intensity of the peak for dicyclopentadiene dissolved in dioxane. Dioxane was chosen due to its low dielectric constant and absence of peaks in the area of

interest. Briefly, an IR flow cell with 100 micron spacings between the plates was filled with solutions of dicyclopentadiene in dioxane. The IR spectra were obtained for different concentrations and a calibration curve was measured.

Eleven PDCPD membranes were fabricated with molar ratios of dicyclopentadiene to Grubbs catalyst of 5,000:1 and their IR spectra were measured. Next, the membranes were swelled in CH_2Cl_2 for an hour, dried under N_2, and the solvent was completely removed by placing the membranes under vacuum for 12 h. The IR spectra were again measured for the membranes. The average density of unreacted cyclic olefin as shown by the peak at 704 cm^{-1} was only 47% (±19%) before swelling in CH_2Cl_2. Thus, approximately 53% (±19%) of the cyclic olefins had reacted to form cross-links. From the prior experiments with Co(salen) and PDCPD membranes that had been exposed to ethyl vinyl ether (Table 4.2), it was known that the Grubbs catalyst was reactive and would further cross-link the membranes when swollen in organic solvent. This conclusion was supported by the IR spectrum of the membranes after swelling in CH_2Cl_2 which showed that approximately 84% (±12%) of the cyclic olefins had reacted. Clearly, the Grubbs catalyst was able to react further when the hard, solid PDCPD membranes were swollen in CH_2Cl_2 for an hour. This result is understandable because of the stability of the Grubbs catalyst in air (particularly when it is embedded in a solid matrix), and the extent that the PDCPD membranes swell in CH_2Cl_2.

Flux of Organic Molecules Through PDCPD Membranes

PDCPD is significantly swollen by organic solvents (Table 4.3).[81,82,136] To quantify the ability of solvents to swell PDCPD a series of dry slabs of PDCPD were weighed, immersed in a solvent for 24 h, removed from the solvent, briefly

dried of any solvent on the exterior of the slab, and weighed. The data in Table 4.3 demonstrated that apolar solvents swelled PDCPD the best which was reasonable considering apolar structure of PDCPD. In addition, PDCPD adsorbed more than its weight in selected solvents.

Table 4.3: How solvents swell PDCPD

Solvent	Weight of swollen PDCPD/weight of PDCPD (g/g)
chloroform	3.38
dichloromethane	2.46
toluene	2.23
tetrahydrofuran	2.06
ethyl acetate	1.35
diethyl ether	1.34
hexanes	1.32
petroleum ether	1.27
dioxane	1.26
acetone	1.14
methanol	1.12

The flux of hexadecane through PDCPD membranes was quantified with CH_2Cl_2 and toluene as the solvents. The membranes were fabricated as before with a molar ratio of 5,000:1 dicyclopentadiene to Grubbs catalyst. The membranes were placed into the apparatus to measure flux and were equilibrated for 30 min with solvent on both sides. After this time period, 1 mmol of hexadecane was added to solvent on one side of the membrane (the upstream side) and aliquots upstream and downstream of the membranes were periodically removed to quantify the concentration of hexadecane. In Figure 4.4

the amount of hexadecane – measured in mmoles – downstream of the membranes as a function of time is shown. The values for the flux of hexadecane were calculated to be 1.02×10^{-5} mol cm^{-2} h^{-1} with CH_2Cl_2 as solvent and 6.53×10^{-6} mol cm^{-2} h^{-1} with toluene as solvent. Although these values are lower than those reported for other membranes, such as the OSN membranes used in the chemical industry, the PDCPD membranes were not optimized for their flux. The flux can be increased by using thinner membranes and by applying external pressure.

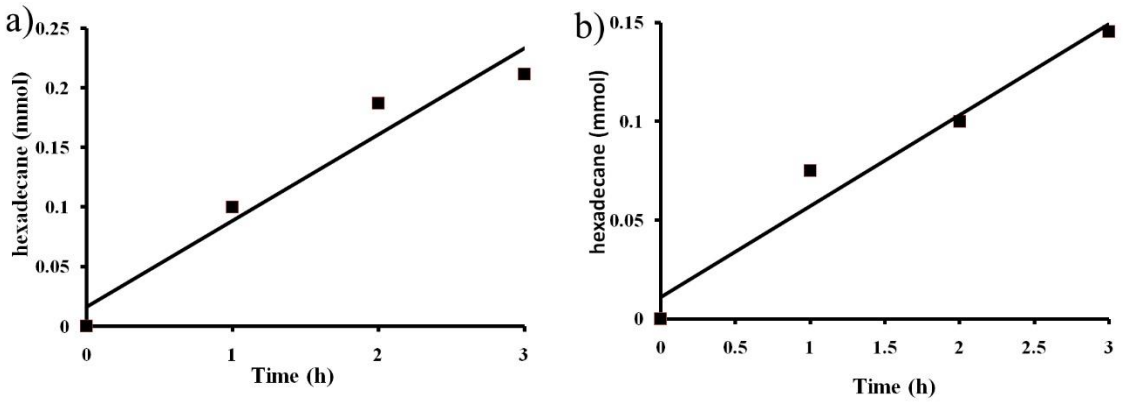

Figure 4.4. The amount of hexadecane in mmol that was downstream of a membrane as a function of time.
a) CH_2Cl_2 as solvent
b) Toluene as solvent

For comparison, the upper limit for the flux of Co(salen) in entry 4 of Table 4.2 with CH_2Cl_2 as the solvent was approximately 4×10^{-10} mol cm^{-2} h^{-1}. Thus, the difference for flux of hexadecane and Co(salen) was at least four to five orders of magnitude.

The ability of hexadecane, nitrobenzaldehyde, cholesterol, hexanoic acid, and 1,6-diaminohexane to permeate PDCPD membranes with CH_2Cl_2, toluene,

and THF as solvents was studied. In these experiments, each of the molecules and hexadecane were added to solvent on one side of the membrane and the concentrations upstream and downstream were found after 24 and 48 h (Table 4.4). Hexadecane was added as an internal control to ensure that each membrane had similar properties and that permeation was measured consistently. Each of these molecules had reasonable rates of permeation through the membranes and, except for cholesterol, the concentrations on either side of the membrane had mostly equilibrated at 48 h.

Table 4.4. Flux of five organic molecules through PDCPD membranes.

Molecule	Solvent	[a]Thickness (μm)	[b]S_d/S_u at 24 h	[b]S_d/S_u at 48 h
hexadecane	CH_2Cl_2	100	0.68	0.95
hexadecane	Toluene	110	0.82	0.86
hexadecane	THF	100	0.66	0.98
nitrobenzaldehyde	CH_2Cl_2	100	0.82	1.0
nitrobenzaldehyde	Toluene	110	0.96	0.98
nitrobenzaldehyde	THF	100	0.66	1.0
cholesterol	CH_2Cl_2	100	0.44	0.69
cholesterol	Toluene	110	0.54	0.58
cholesterol	THF	100	0.54	0.82
hexanoic acid	CH_2Cl_2	99	0.88	0.94
hexanoic acid	Toluene	110	0.55	0.82
hexanoic acid	THF	89	0.69	1.0
1,6-diaminohexane	CH_2Cl_2	80	0.81	0.93
1,6-diaminohexane	Toluene	98	0.95	0.97
1,6-diaminohexane	THF	120	1.0	1.0

Note: [a]The thickness of the PDCPD membrane that was prepared at a molar ratio of dicyclopentadiene:Grubbs catalyst of 5,000:1. [b]The ratio of the concentration downstream to the concentration upstream for each molecule.

The permeation of a molecule through a membrane is dependent on the rate of diffusion of that molecule within a membrane multiplied by its solubility in

the membrane according to the well-known equation P = DS.[72] Each of the five molecules shown in Table 4.4 permeated the membranes at appreciable rates which demonstrated that they were soluble and possessed reasonable rates of diffusion within the PDCPD matrix. What is notable is that both polar and apolar molecules permeated at similar rates through the hydrophobic, but swollen, PDCPD membranes.

The ability of 14 additional molecules to permeate PDCPD membranes fabricated from a dicyclopentadiene to Grubbs catalyst ratio of 5,000:1 were measured with CH_2Cl_2 as the solvent (Figure 4.5 and Table 4.5). Similar to other experiments, the molecule of interest and hexadecane were added to solvent upstream of the membranes. The internal control of adding hexadecane to each experiment ensured that the flux was similar for each membrane and that a lack of flux of a molecule through the membrane was not due to a faulty membrane, but rather it was due to an intrinsic property of the membrane.

Several conclusions can be drawn from the experiments in Table 4.5 and those presented earlier in this chapter. Whether a molecule will permeate PDCPD is clearly not dependent on molecular weight because the two molecules (MW: 528 and 583 g mol^{-1}) with highest molecular weights permeated the membranes, but tributylamine (MW: 185 g mol^{-1}) and triphenylphospine (MW: 262 g mol^{-1}) did not. Both hydrophobic and hydrophilic molecules permeated the membranes or failed to do so. For instance, apolar molecules such as hexadecane, cholesterol, and tripropylamine permeated the membranes, but tributylamine, triphenylphosphine, and tricyclohexylphosphine did not. Triphenylphosphine oxide was chosen because it is more polar than triphenylphosphine due to the presence of a polar P=O bond, but possessed a similar shape. Triphenylphosphine oxide did not permeate the membranes at any detectable amount. The presence of amine or phoshine groups was not a

distinguishing factor for whether a molecule would permeate the membrane because triphenylmethane also did not permeate it.

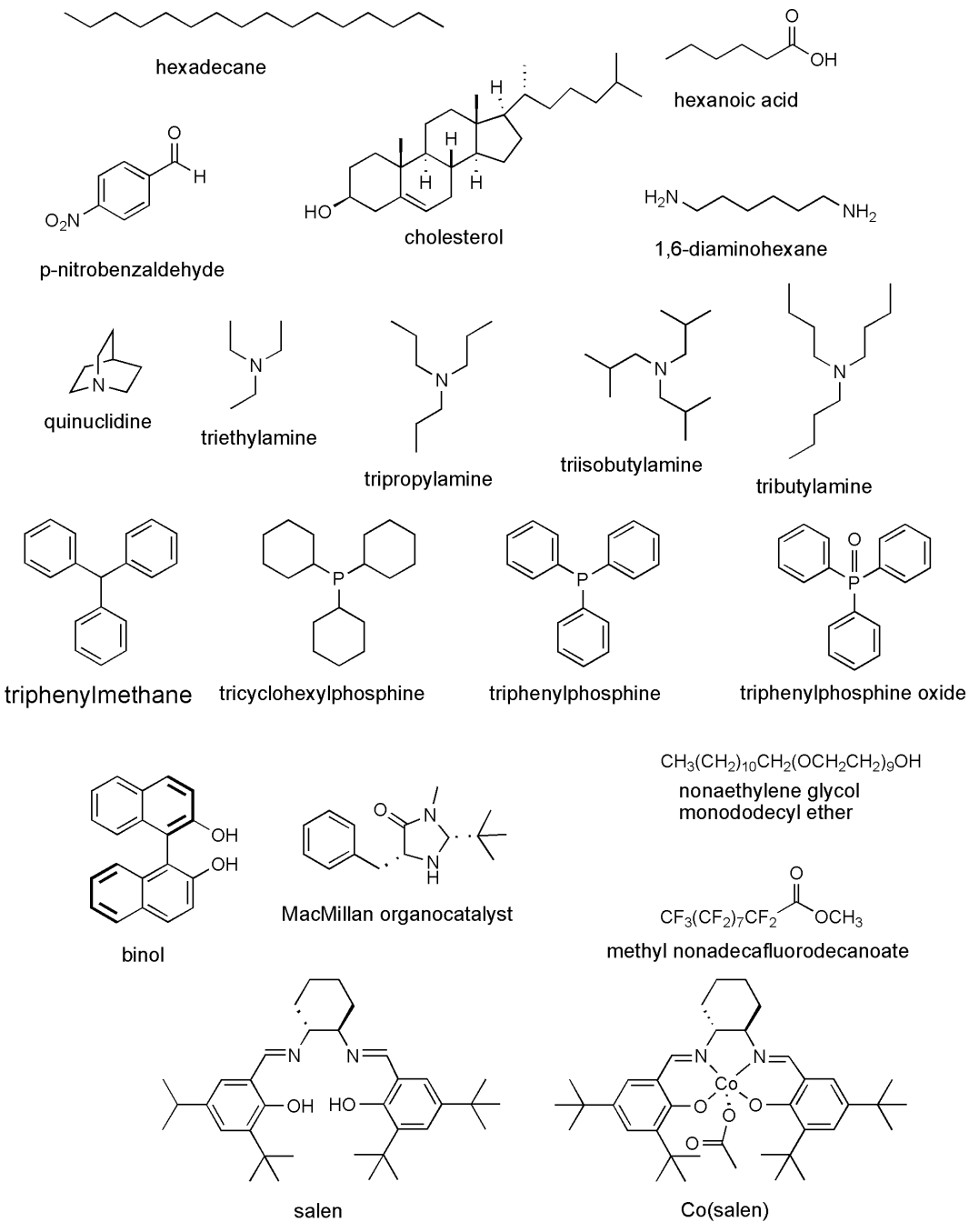

Figure 4.5. The molecules that were studied for their permeation through PDCPD membranes.

Table 4.5. Permeation of organic molecules using PDCPD membranes and CH_2Cl_2 as the solvent

Molecule	Molecular weight (g mol^{-1})	[a]Thickness (μm)	[b]S_d/S_u at 24h	[b]S_d/S_u at 48 h
quinuclidine	111	100	0.81	0.93
triethylamine	101	97	1.0	0.98
tripropylamine	143	100	0.67	0.87
tributlyamine	185	96	≤0.02[c]	≤0.03[c]
triisobutylamine	185	100	0.88	1.0
triphenylmethane	244	90	≤0.01[c]	≤0.01[c]
MacMillan organocatalyst	246	120	0.32	0.70
triphenylphosphine	262	100	≤0.02[c]	≤0.03[c]
triphenylphosphine oxide	278	84	≤0.02[c]	≤0.03[c]
[d]tricyclohexylphosphine	280	100	≤0.01[c]	≤0.02[c]
binol	286	96	≤0.01[c]	≤0.02[c]
salen	492	100	≤0.01[c]	≤0.01[c]
methyl nonadecafluorodecanoate	528	98	0.85	0.94
nonaethylene glycol monododecyl ether	583	130	0.04	0.33

Note: [a]The thickness of the membrane. [b]The ratio of the concentration of a molecule downstream to its concentration upstream. [c]The molecule was not observed downstream of the membrane. [d]Less than 10% of the tricyclohexylphosphine oxidized during these experiments.

Reason for the Retention of Selected Molecules by PDCPD Membranes

The flux of molecules through cross-linked polymeric membranes has been described theoretically by others through competing models.[72,75,76,84,127-129] A general description that is agreed upon is that the diffusion, D, of a molecule to move from point to point in a polymer matrix depends exponentially on energy of activation, E_a, according to the equation $D = D_o\exp(-E_a/RT)$. In a highly cross-linked polymer matrix, small molecules can diffuse with little or no rearrangement of the polymer and the value for E_a is small. Molecules with cross-sectional areas that are comparable or larger than the pores in a cross-linked polymer require substantial rearrangement of the polymer matrix that lead to high values for E_a

and low values for diffusion. Thus, the theoretical descriptions of flux and rates of diffusion make extensive use of cross-sectional areas to make predictions or to rationalize observed results. For instance, in a classic paper in 1982 by Berens and Hopfenberg the log of diffusion versus diameter and the square of diameter was plotted for 18 molecules that permeated polystyrene, polymethylmethacrylate, and polyvinyl chloride.[137] Neither plot was superior to the other due to scatter in the data, but it was clear that flux strongly depended on molecular diameter. In fact, the difference in flux for He (diameter = 0.258 nm) and neopentane (diameter 0.580 nm) was approximately ten orders of magnitude. Unfortunately, this difference in flux was not studied for molecules larger than hexanes because of the vanishingly slow values for diffusion. At the other end of the molecular weight spectrum, the separation of polymers from small molecules using porous polymeric membranes is well known and used in applications such as to dialyze proteins from small molecules.

Most prior membranes to separate organic molecules used molecular weight or hydrophobic/hydrophilic effects to distinguish between molecules. For instance, ionic liquids will not partition into PDMS (a hydrophobic polymer) so they have no measurable flux through membranes composed of PDMS.[86] Membranes that separate organic molecules possessing molecular weights from 100 to 600 g mol^{-1} use molecular weight as the criterion for separation rather than cross-sectional area for two reasons. First, molecular weight is straightforward and easy to define, but cross-sectional area is a more challenging concept to quantify. Second, some separations based on molecular weight are successful and required no allowances to be made for molecular size. Molecules below a MWCO permeate the membranes, but molecules above the MWCO do not permeate and no exceptions are needed for effects based on cross-sectional area. The use of molecular weight as the criterion for separation does not imply

any underlying importance to molecular weight in the mechanisms by which molecules are separated.

In Table 4.6 the molecular sizes of molecules that permeated or did not permeate PDCPD membranes are described. The surface area, molecular volume, critical dimension, and critical area were calculated by first minimizing the energy for each molecule using Spartan ’08 V1.2.0. Next, the surface area and molecular volume were calculated from space filling models as described in the experimental section. The critical area was defined as the smallest rectangular cross-sectional area of a molecule that must be met for it to pass through a pore. For instance, a penny would be viewed on its side such that its cross-sectional area is a thin rectangle and distinctly smaller than the cross-sectional area for a sphere with the same radius as a penny. This rectangular cross-sectional area was determined using Sparan ’08 V1.2.0 for each molecule as described in the experimental section. The critical dimension was the larger of the two distances used to find the critical area.

It is clear from Table 4.6 that the critical dimension and area both correlate to whether a molecule will permeate PDCPD. Molecules that permeated through PDCPD membranes had critical dimensions and areas of less than 0.80 nm and 0.38 nm^2, but molecules that did not flux through the membranes had critical dimensions and areas of at least 0.92 nm and 0.50 nm^2. Surprisingly, a difference in critical dimension or area significantly less than a factor of two had a substantial impact on the flux of molecules through PDCPD. The difference in permeation was striking. Molecules with no measurable flux through the membranes were not detected in the solvent downstream of the membrane and possessed values for flux 10^4 to 10^5 times slower than the molecules that did permeate the membranes.

Table 4.6. The chemical and physical sizes of molecules that did or did not permeate PDCPD membranes.

Molecule	Flux	Molecular weight (g mol^{-1})	Surface area (nm^2)	Molecular volume (nm^3)	Critical dimension (nm)	Critical area (nm^2)
triethylamine	Yes	101	1.64	0.138	0.67	0.18
quinuclidine	Yes	111	1.46	0.131	0.42	0.21
hexanoic acid	Yes	116	1.65	0.135	0.28	0.067
1,6-diaminohexane	Yes	116	1.80	0.146	0.28	0.067
tripropylamine	Yes	143	2.20	0.193	0.79	0.32
nitrobenzaldehyde	Yes	151	1.64	0.142	0.43	0.060
tributlyamine	No	185	2.86	0.249	0.92	0.50
triisobutylamine	Yes	185	2.82	0.248	0.80	0.38
hexadecane	Yes	226	3.52	0.307	0.28	0.067
triphenylmethane	No	244	2.92	0.285	0.95	0.51
MacMillan organocatalyst	Yes	246	2.96	0.279	0.62	0.36
triphenylphosphine	No	262	2.92	0.286	0.95	0.61
triphenylphosphine oxide	No	278	3.11	0.299	0.95	0.61
Tricyclohexyl phosphine	No	280	3.24	0.323	0.92	0.57
binol	No	286	2.99	0.298	0.72	0.51
cholesterol	Yes	387	4.49	0.454	0.55	0.28
salen	No	492	6.36	0.630	1.22	0.79
methyl nonadecafluoro decanoate	Yes	528	3.39	0.312	0.43	0.14
nonaethylene glycol monododecyl ether	Yes	583	7.37	0.640	0.28	0.067
Co(salen)	No	662	7.06	0.699	1.22	1.15

The difference in permeation of tripropylamine, triisobutylamine, and tributylamine illustrates the importance of cross-sectional area (Table 4.6). Triisobutylamine and tributylamine are constitutional isomers that possess the

same molecular weight and similar surface areas and volumes. The major difference between triisobutylamine and tributylamine are their cross-sectional areas, triisobutylamine (0.38 nm^2) has a similar cross-sectional area to tripropylamine (0.32 nm^2), but the cross-sectional area of tributylamine (0.50 nm^2) is larger. In flux experiments tripropylamine and triisobutylamine permeated the membranes but tributylamine did not permeate. These experiments demonstrate the selectivity of the membranes and the need to consider cross-sectional area as the important parameter for the flux of molecules.

Extraction of Nitrobenzaldehyde from Binol

The ability to efficiently extract a molecule through a PDCPD membrane while retaining a second molecule was studied using nitrobenzaldehyde and binol. It is important that a high yield of a molecule be obtained after permeation through a membrane, and it is also important that molecules that are retained by a membrane do not remain embedded with the PDCPD matrix. In some applications it will also be important that molecules that are retained be recycled and accessible after separations. These issues were initially addressed by studying the extraction of nitrobenzaldehyde from binol.

In these experiments, a mixture of nitrobenzaldehyde (484 mg) and binol (264 mg) were added upstream of a membrane in CH_2Cl_2 and extracted downstream using CH_2Cl_2. After 24 h, the solvent downstream was removed from the apparatus and fresh CH_2Cl_2 was added downstream. After an additional 24 h, the solvent downstream was removed and the extracted yield of nitrobenzaldehyde through two cycles calculated to be 90% with no detectable level of binol contamination by 1H NMR. The solvent upstream was also removed from the apparatus and the amount of binol in solution was only 17% of the original amount of binol added to the apparatus. The remainder of the binol

was in the PDCPD matrix and had to be extracted. A fresh aliquot of CH_2Cl_2 was added on the upstream side of the membrane and allowed to sit for 24 h. The CH_2Cl_2 was removed from the apparatus to yield an additional 39% of the original amount of binol. The membrane was cut into pieces and immersed in CH_2Cl_2 to further extract binol. After 24 h an additional 13% of the original amount of binol was isolated which yielded a total isolation of 69% of the original amount of binol. When this experiment was repeated the percent of nitrobenzaldehyde that was isolated downstream of the membrane was 87% and the amount of binol that was isolated was 72%.

These experiments demonstrated that high yields of clean nitrobenzaldehyde could be isolated from significant quantities of binol. Furthermore, most of the binol partitioned into the PDCPD membranes during these experiments, but it was readily extracted into fresh solvent where it was isolated and characterized. The partitioning of binol from solvent into the membranes was a reversible process that allowed much of the binol to be isolated at the end of these experiments.

Extraction of Cholesterol from Triphenylphosphine, Tricyclohexylphosphine, and Tributylamine using a PDCPD Membrane

To demonstrate the selective permeation of a high molecular weight compound from low molecular weight compounds based on their different cross-sectional areas, the extraction of cholesterol (3 mmol) from a mixture of triphenylphosphine (2 mmol), tricyclohexylphosphine (2 mmol), and tributylamine (3 mmol) was investigated. These four molecules were dissolved in 25 mL of CH_2Cl_2 and added to one side of a membrane and 23 mL of CH_2Cl_2 was added

downstream of the membrane. A 2 mL aliquot was immediately removed from the upstream side and characterized by ^{1}H NMR spectroscopy to show the initial mixture of molecules. After 48 h, aliquots were removed from both sides of the membrane and the contents were characterized by ^{1}H NMR spectroscopy.

The ^{1}H NMR spectra in Figure 4.6 clearly demonstrate that cholesterol was selectively extracted from the solvent mixture. The ^{1}H NMR spectra of the initial mixture of the four molecules, the organic compounds upstream of the membrane after 48 h, the organic compounds downstream of the membrane after 48 h, and a sample of pure cholesterol are all shown. Some oxidation of the PCy_3 occurred during the extraction, but the $OPCy_3$ was also retained by the membrane. The ^{1}H NMR spectrum of the organic product downstream of the membrane after 48 h matched the ^{1}H NMR spectrum of cholesterol and no evidence of PCy_3, $OPCy_3$, PPh_3, or NBu_3 were seen downstream of the membrane. This result was remarkable considering that the molecular weight of cholesterol (MW: 387 g mol^{-1}) is much higher than the other molecules (185-296 g mol^{-1}).

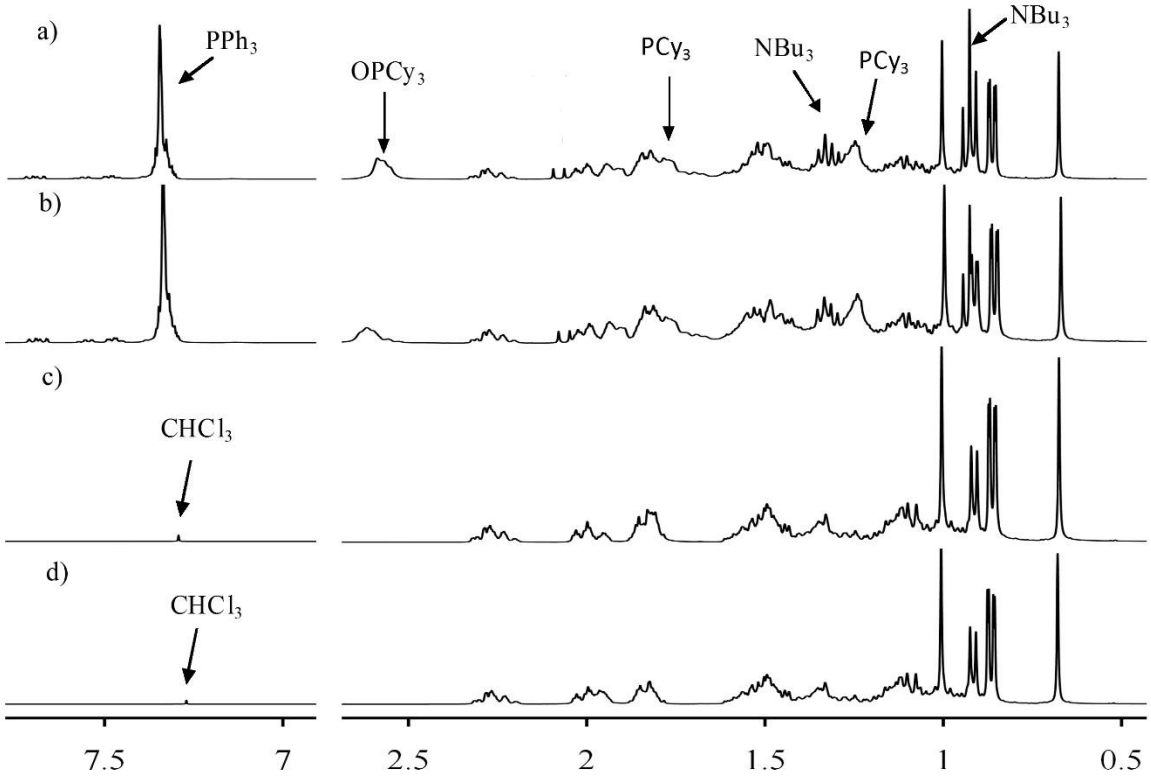

Figure 4.6. The ^{1}H NMR spectra of separation. The peaks for cholesterol at 3.52 and 5.35 ppm were observed in all four spectra but were omitted from this figure to emphasize the region from 0.5 to 2.7 ppm.
a) The initial mixture of cholesterol, $OPCy_3$, PCy_3, PPh_3, and NBu_3
b) The mixture of molecules upstream of the membrane after 48 h
c) The mixture of molecules downstream of the membrane after 48 h
d) Cholesterol

Recycling of PDCPD Membranes

The ability to recycle PDCPD membranes was studied using nitrobenzaldehyde and binol. In this experiment both nitrobenzaldehyde and binol were added upstream of a membrane and nitrobenzaldehyde was isolated downstream of the membrane. Nitrobenzaldehyde was extracted three times with fresh solvent over 72 h. After 72 h the binol that had permeated into the PDCPD matrix was extracted by the addition of fresh solvent upstream of the membrane. After the first cycle was complete, fresh nitrobenzaldehyde and binol were added

upstream of the membrane and the process was repeated with the same membrane.

A total of three cycles were completed and the extraction of nitrobenzaldehyde was high for each cycle. In the three cycles nitrobenzaldehyde was isolated in 99%, 79%, and 72% yield and the binol was isolated in 40%, 4%, and 82% yield. The fourth cycle was not finished because binol began to permeate the membrane. Notably, nitrobenzaldehyde was isolated as a clean product without any impurities from binol. The binol contained some nitrobenzaldehyde as an impurity and had to be extracted from the PDCPD membrane. This experiment demonstrates that the membranes can be recycled over several cycles, and future work will study how to optimize this process.

Conclusions

New technologies originate from new materials. Most past examples of membranes that separate organic molecules with molecular weights from 100-600 g mol^{-1} use the concept of a molecular weight cutoff that hinder the use of these membranes to separate catalysts from products of a reaction. Many catalysts and ligands for metals have modest molecular weights that place a real limitation on what molecules they can be separated from. The problem that PDCPD membranes solve is that they are the first membranes that separate molecules with molecular weights between 100 and 600 g mol^{-1} based on the concept of a cross-sectional area cutoff rather than a molecular weight cutoff. These membranes are significant because of the large number and importance of molecules within this range of molecular weights and the need to separate them in the chemical industry. For instance, many reactions require metal catalysts with ligands such as phosphines. It is important that the final product be clean of all but ppm levels of impurities of metal and phosphines so several

purification steps are often required to clean the product. PDCPD membranes offer a new solution to cleaning the products and recycling the catalysts.

The surprising aspect of PDCPD membranes is not that they separate molecules based on cross-sectional area because cross-sectional area is well known as a critical parameter that affects flux. Rather, it was surprising that these membranes were the first to have a critical importance of cross-sectional area for the flux of molecules within this range of molecular weights. In addition, the difference in permeation was very large; molecules that did not permeate the membranes were undetected in the solvent downstream of the membrane and possessed values for flux that were 10^4 to 10^5 times slower than molecules that permeated the membranes. The origins of the selectivity of these membranes lies in the size and distribution of pore sizes that result when the polymer is cross-linked, and these materials properties will be studied in more detail in future work. An understanding of what makes PDCPD so unique may allow the design of more membranes with similar separations but faster flux.

Experimental

Characterization and measurements. ^{1}H NMR spectra were acquired on a Bruker DPZ-300 NMR at 300 MHz or a Bruker DRX-400 NMR at 400 MHz using $CDCl_3$ as solvent and referenced to TMS. The concentration of Co(salen) was acquired on a Varian Cary 100 Scan UV-Visible spectrophotometer and Varian 720-ES ICP-OES (inductively coupled plasma-optical emission spectrometer). The thicknesses of the membranes were determined using a Micromaster microscope at the highest magnification. IR were acquired on a Bruker Tensor 27. A room temperature DTGS (deuterated triglycine sulfate) detector was used. All chemicals were purchased at their highest purity from Aldrich or Acros and used as received.

Calibration of UV-VIS spectrophotometer. Co^{II}(salen) (23 mg, 0.039 mmol) was dissolved in toluene (0.5 mL) prior to the addition acetic acid (0.01 mL, 0.18 mmol). The mixture was stirred at room temperature for 1 h to yield Co^{III}(salen) with an acetate counterion. Here Co^{III}(salen)OAc is referred to as Co(salen) for the rest of this report. Toluene and the excess acetic acid were removed under vacuum. The Co(salen) was dissolved in CH_2Cl_2 (10 mL) and stirred at room temperature for 24 h. The solvent was removed and Co(salen) was redissolved in CH_2Cl_2 (10 mL) to yield a 0.00386 M solution. This solution was diluted to make standard solutions to calibrate the instrument. The intensity of the peak at 410 nm in each of the spectra was measured and plotted against concentration to create a calibration curve.

Calibration of ICP-OES. Standards for Co were made by diluting a standard solution containing 9908 ppm of Co in 1-2 wt. % of HNO_3 with water. The concentrations of the standards were 0.248 ppm, 0.495 ppm 0.990 ppm, 1.99 ppm, 4.95 ppm, 7.93 ppm, 15.8 ppm, and 39.6 ppm. The standards were used to calibrate the ICP-OES before running the samples for Table 4.2. A 1 ppm solution of was Y used as an internal standard.

Optical spectroscopy. The thickness of a membrane was determined by cutting a section of a membrane and placing it under the microscope. The section of membrane was held vertically with tweezers and the edge was imaged at the highest magnification. An optical micrograph was taken and the thickness was measured.

Synthesis of PDCPD membranes at a 5,000:1 dicyclopentadiene:Grubbs catalyst ratio. A 20 mg/mL solution of Grubbs first generation catalyst was made using 1,2-dichloroethane. A sample of this solution (0.246 mL, 6.0×10^{-3} mmol of catalyst) was added to 4 mL of dicyclopentadiene heated to 40 °C to melt it. The melting point of dicyclopentadiene is 33 ^{o}C. This

solution was immediately placed between two glass slides with 100 µm thick paper as spacers along the edges. The sample was heated to 50 °C for 2 h and then removed from the glass slides.

Synthesis of PDMS membrane. These membranes were fabricated similar to methods described in prior work.[70,77,78] Sylgard 184 was mixed with a curing agent in a 10:1 ratio and degassed. The PDMS was poured over a flat glass slide while allowing any excess to flow over the side. The glass had been coated with a monolayer of trichloro(1H, 1H, 2H, 2H-perfluoroctyl)silane prior to its use. The PDMS was cured in a 65 °C oven for 24 h. The PDMS membrane was delaminated from the glass side by swelling in dichloromethane.

Permeation of Co(salen) through PDCPD membranes (Table 4.2). Co(salen) was synthesized with acetic acid and toluene as described before. A PDCPD membrane was added to the glass apparatus to study permeation. CH_2Cl_2 (25 mL) was added to the downstream side of the membrane. CH_2Cl_2 (25 mL) with Co(salen) (0.038 mmol) was added to the upstream side of the membrane. Both sides of the membrane were stirred continuously at room temperature. Aliquots (4 mL) were removed from both sides of the membrane at 24 and 48 h.

The concentration of Co(salen) was determined by UV-Vis spectroscopy or ICP-OES using the calibration curves that were determined as previously descibed. Samples for ICP-OES were prepared by first drying each aliquot and burning off all the organic materials with a Bunsen burner. The Co was dissolved in 1 mL of a 3:1 solution of concentrated HCl and concentrated HNO_3. The aliquot from upstream side of the membrane was diluted with 10 mL of water. The aliquot from the downstream side of the membrane was diluted with 5 mL of water. The samples were run through ICP-OES after it was calibrated on the same day as the measurements.

Permeation of Co(salen) through PDCPD membranes treated with ethyl vinyl ether (Table 4.2 entries 6-8). Co(salen) was synthesized with acetic acid and toluene as described earlier. CH_2Cl_2 (25 mL) and ethyl vinyl ether (5 mL, 52 mmol) were added to the downstream side of the membrane and CH_2Cl_2 (25 mL) and ethyl vinyl ether (5 mL, 52 mmol) with Co(salen) (0.038 mmol) were added to the upstream side of the membrane. Both sides of the membrane were stirred continuously at room temperature. At 24 and 48 h, aliquots (4 mL) of solvent were removed from both sides of the membrane. The aliquots were used to determine the concentration Co(salen) by UV-Vis spectroscopy as previously described.

Permeation of Co(salen) through a PDMS membrane (Table 4.1). Co(salen) was synthesized with acetic acid and toluene. A PDMS membrane was added to the apparatus to study permeation. CH_2Cl_2 (25 mL) was added to the downstream side of the membrane. CH_2Cl_2 (25 mL) with Co(salen) (0.038 mmol) were added to the upstream side of the membrane. Both sides of the membrane were stirred continuously at room temperature. At 2, 4, and 6 h aliquots (4 mL) were removed from both sides of the membrane. The aliquots were used to determine the concentration Co(salen) by UV-Vis spectroscopy as previously described.

Swelling of PDCPD by various solvents (Table 4.3). Commercially available dicyclopentadiene (24 mL, 0.177 mol) was heated in a glass vial at 35 °C for 10 minutes to melt it. The Grubbs catalyst (15 mg, 0.017 mmol) was mixed with CH_2Cl_2 (0.5 mL), added to the dicyclopentadiene, and thoroughly mixed. The solution was heated in a water bath at 50 °C for 1.5 h. The slab of PDCPD was removed from the vial and swelled in CH_2Cl_2 mixed with ethyl vinyl ether. The slab of PDCPD was cut into 12 small cubes. All the cubes were dried in air and then under vacuum.

The weights of cubes of PDCPD were measured. Each cube was placed in a glass vial with 10 mL of solvent to completely immerse the cube for 24 h. Next, the cubes were removed from the vials and briefly wiped with kimwipes to remove solvent from their surfaces. The weights of the swollen PDCPD cubes were measured. The swollen weight was divided by the dry weight of PDCPD to calculate how well each solvent swells PDCPD.

Permeation of organic molecules through PDCPD membranes with different solvents (Tables 4.4 and 4.5). A membrane – made with a monomer:catalyst loading of 5000:1 – was added to the apparatus to study permeation. CH_2Cl_2, toluene, or THF (25 mL) was added to the downstream side of the membrane and 25 mL of the same solvent was added to the upstream side of the membrane with 3 mmol of the substrate and 1 mmol hexadecane as an internal standard. Both sides of the membrane were stirred continuously at room temperature. At 24 and 48 h a 1 mL aliquot was removed from both sides. The aliquot was blow dry used to determine the concentration of the substrate and hexadecane by ^{1}H NMR spectroscopy using $CDCl_3$ as the solvint. The concentrations were found by the addition of known amounts of tetraethylene glycol to each aliquot and comparing the known concentration of tetraethylene glycol with the concentration of the molecule of interest.

Rate of flux of hexadecane through a 5000/1 PDCPD membrane. A membrane – made with a monomer:catalyst loading of 5000:1 – was added to the apparatus to study permeation. CH_2Cl_2 (20 mL) was added to the upstream and downstream sides of the membrane. The membrane was allowed to equilibrate for 30 min. CH_2Cl_2 (5 mL) was added to the downstream side of the membrane and CH_2Cl_2 (5 mL) was added to the upstream side of the membrane with hexadecane (1 mmol). Both sides of the membrane were stirred continuously at room temperature. At 1, 2, and 3 h a 1 mL aliquot was removed

from both sides. An ^{1}H NMR spectrum was taken of each aliquot using tetraethylene glycol as an internal standard as described previously.

Flux is the amount of material in moles that progress through a unit area of a membrane per unit time. The mmole of hexadecane on the downstream side as determined by ^{1}H NMR spectroscopy was plotted against time. The slope of the graph was divided by the area of the membrane (7.07 cm^2) resulting in the flux of hexadecane. The aliquots were obtained early when flux can be approximated as unidirectional.

Density of cross-links of PDCPD membranes. IR spectroscopy was used to determine the density of cross-links in PDCPD. Dicyclopentadiene (5%, 10%, 15% and 20% by volume solutions) in dioxane was used to find a calibration curve. The IR spectrum of each solution was measured using a cell with a fixed pathlength of 100 μm. The intensity of the peak at 704 cm^{-1} in each of the IR spectra was measured and plotted against concentration to yield the calibration curve.

A 20 mg/mL solution of the Grubbs first generation catalyst in 1,2-dichloroethane was made. Commercially available dicyclopentadiene (4 mL, 0.029 mmol) was heated to 40 ˚C. The catalyst solution (0.246 mL, 6.0 x 10^{-3} mmol of catalyst) was added to dicyclopentadiene. A sample of this solution was added to the top of a glass slide and was pressed by down by another glass slide. This set up was heated to 50 ˚C for 2 h. The glass slides were removed from the PDCPD membranes and the thicknesses were measured using an optical microscope as described previously.

Eleven PDCPD membranes were fabricated and the IR spectrum of each was obtained. The intensity of the peak at 704 cm^{-1} for each of the membranes was fitted to the calibration curve and the density of unreacted cyclic olefin in PDCPD was calculated. The membranes were immersed in methylene chloride

in glass vials for an hour. The dichloromethane was decanted off and any remaining solvent in the membrane was removed *in vacuo* for 12 h. The IR spectra were measured for all of the membranes. The intensity of the peak at 704 cm^{-1} for each of these membranes was fitted to the calibration curve and the density of unreacted cyclic olefin in PDCPD was calculated.

Isolation of cholesterol from tricyclohexylphosphine, triphenylphosphine, and tributylamine (Figure 4.6). A membrane – made with a monomer:catalyst loading of 5000:1 – was added to the apparatus to study permeation. CH_2Cl_2 (23 mL) was added to the downstream side of the membrane and CH_2Cl_2 (25 mL) was added to the upstream side of the membrane with cholesterol (3 mmol), tricyclohexylphosphine (2 mmol), triphenylphosphine (2 mmol), and tributylamine (3 mmol). The solutions on the downstream and upstream sides of the membranes were continuously stirred. A 2 mL aliquot was removed from the upstream side immediately after it was added to the apparatus. The solvent was removed and a ^1H NMR spectrum was obtained. At 48 h aliquots (5 mL) were removed from both sides of the membrane. The solvent was removed and ^1H NMR spectra were obtained.

Isolation of nitrobenzaldehyde from binol. A membrane – made with a monomer:catalyst loading of 5000:1 – was added to the apparatus to study permeation. CH_2Cl_2 (50 mL) was added to the downstream side of the membrane and CH_2Cl_2 (25 mL) was added to the upstream side of the membrane with binol (0.264 g) and nitrobenzaldehyde (0.484 g). The solvent on both sides of the membrane were stirred continuously at room temperature. At 24 h the solvent from the downstream side was removed and evaporated to recover nitrobenzaldehyde (0.249 g). The solvent was replaced with CH_2Cl_2 (50 mL). At 48 h the solvent was removed from the downstream side and evaporated recover nitrobenzaldehyde (0.186 g). Also at 48 h, the solvent from the upstream side

was removed and evaporated to recover nitrobenzaldehyde (50 mg) and binol (0.046 g). CH_2Cl_2 (25 mL) was added the upstream side and stirred for 24 h. The solvent was removed and evaporated to yield 0.103 g of binol. The membrane was removed from the apparatus, cut into pieces, and placed into a flask with CH_2Cl_2 (50 mL) for 24 h. The CH_2Cl_2 was evaporated to yield an additional 0.033 g of binol. The total recovery of nitrobenzaldehyde from solvent downstream of the membrane was 90% with <3% binol contamination. The total recovery of binol from solvent upstream of the membrane was 69%.

Recycling of a PDCPD membrane. A PDCPD membrane was added to the apparatus to study permeation. CH_2Cl_2 (50 mL) was added to the downstream side of the membrane and CH_2Cl_2 (15 mL) was added to the upstream side of the membrane with binol (0.286 g, 1 mmol) and nitrobenzaldehyde (0.151 g, 1 mmol). At 24 and 48 h the solvent from the downstream side was removed and evaporated to recover nitrobenzaldehyde. The solvent was replaced with fresh CH_2Cl_2 (50 mL). At 72 h the solvent on the upstream and downstream sides of the membrane were remove and evaporated to recover binol and nitrobenzaldehyde. Fresh CH_2Cl_2 (30 mL) was added upstream of the membrane to extract binol from the membrane. At 84 h solvent upstream of the membrane was removed and evaporated to recover binol. This completed cycle 1 and cycles 2 and 3 were completed with the same PDCPD membrane. In cycle 1 99% of the nitrobenzaldehyde and 40% of the binol were recovered, in cycle 2 79% of the nitrobenzaldehyde and 4% of the binol were recovered, and in cycle 3 72% of the nitrobenzaldehyde and 82% of the binol were recovered.

Measurement of the critical dimension and critical area. The software used for these measurements was Spartan `08 V1.2.0. Each molecule was drawn in the software using a ball and spoke representation and its energy was

minimized by finding the equilibrium geometry at ground state with a semi-empirical method using AM1 parameters. The surface area and molecular volume were calculated based on a space filling model. The space filling model chosen was a 3D molecular model with atoms represented by spheres whose radius is assumed to be the Van der Waals radius determined by the electron density cut-off at 0.002 electrons/$Å^3$.

Each molecule was analyzed to find the conformation with the lowest rectangular, cross-sectional area. The two dimensions of the rectangle were measured and the longer dimension was labeled the critical dimension and the area was labeled as the critical area.

CHAPTER 5

CONCLUSIONS AND RECOMMENDATIONS FOR FUTURE WORK

A Slow Release H_2S Delivery System

Conclusions

An H_2S delivery system that can release H_2S over the course of weeks to months instead of minutes to hours is an important development in the emerging field of medical H_2S. As described in chapter 2, an H_2S releasing prodrug based on thiobenzamide attached to a biodegradable poly(lactic acid) can release H_2S over weeks. The dose of H_2S can be varied by changing the composition of the polymer to have more or less thiobenzamide. This H_2S releasing polymer will assist in the continuing studies of the *in vivo* effect of H_2S and whether a low, steady dose of H_2S can have a beneficial and therapeutic effect for a multitude of diseases. This research has laid the ground work for future studies on the slow, steady release of H_2S.

This research also required the development of a new way to functionalize lactide. Poly(lactic acid) is widely used polymer for a variety of applications, especially medical applications, because of its biodegradability and biocompatibility. The functionalization of lactide could be used in other drug delivery systems or it could be used to change some of the properties of poly(lactic acid) such as solubility or rate of degradation. The functionalization of lactide may have numerous different applications to improve existing uses or develop new uses of poly(lactic acid).

Recommendation for Future Work

Three of the key areas that require further study to optimize a H_2S delivery system are the degradation of the microparticles, the detection of H_2S, and the integration of multiple H_2S releasing prodrugs. In my research the degradation of microparticles occurred at an exceptionally slow rate, even under acidic conditions. A slow degradation was desired for these microparticles, but the slow rate of degradation made it challenging to study the release of H_2S. A faster rate of degradation might be necessary to release a suitable amount of H_2S for detection and some medical applications. A possible solution would be to make a block copolymer with poly(ethylene glycol) which would allow water to enter the microparticles more easily and increase the rate of degradation.

The detection of H_2S has been particularly challenging at the low concentrations found in biological systems. Several H_2S detection systems have been developed (Chapter 1), but none are suitable to study the long, slow release of this or many other H_2S delivery systems. The field of medical H_2S delivery relies heavily on animal testing and measuring the effect of H_2S rather than the concentration of H_2S itself. Until a better detection system for H_2S is developed, animal testing might be the only way to get a good indication of the rate and duration of the H_2S from these microparticles.

Finally my H_2S delivery system lends itself to the exploration of other H_2S prodrugs. The synthesis of the H_2S releasing monomer will allow for the substitution of other known H_2S releasing prodrugs. Figure 5.1. shows the replacement of thiobenzamide with DTT (Figure 5.1a.) and allyl disulfide (Figure 5.1b.) which are both known to release H_2S and are described in Chapter 1. There is also room in the medical H_2S field for the development of new H_2S releasing prodrugs and a need to study the mechanism which these prodrugs release H_2S.

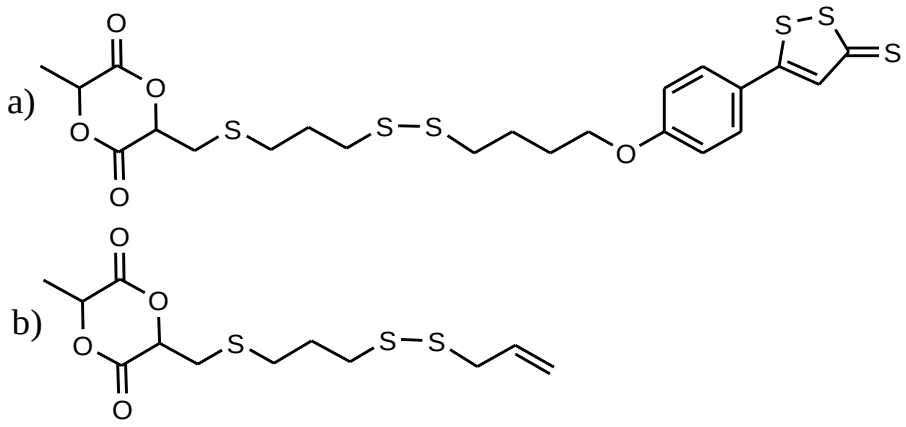

Figure 5.1. Other H_2S releasing monomer.
a) DTT prodrugs
b) Allyl disulfide prodrugs

Polydicyclopentadiene Membranes

Conclusions

PDCPD membranes are the first membranes that separate organic molecules with molecular weights from 100-600 g mol^{-1} and are described using the concept of a cross-sectional area cutoff rather than a molecular weight cutoff. This molecular weight range contains large number of important molecules used in the chemical industry including expensive catalysts and ligands. Also, there was a difference of 4 to 5 orders of magnitude in the flux between molecules that permeated the membrane and those that did not permeate. The difference in the cross-sectional area between molecules that permeate and do not permeate the membrane can be as low as 0.12 nm^2. This small difference in cross-sectional area demonstrates that the PDCPD membranes are extremely selective. The selectivity of these membrane can be seen in Figure 5.2, which shows little correlation between the retention of molecules and their molecular weights (Figure 5.2a). In contrast there is a strong correlation with the retention of

molecules versus their critical areas (Figure 5.2b). The cutoff for the critical area is between 0.4 nm^2 and 0.5 nm^2.

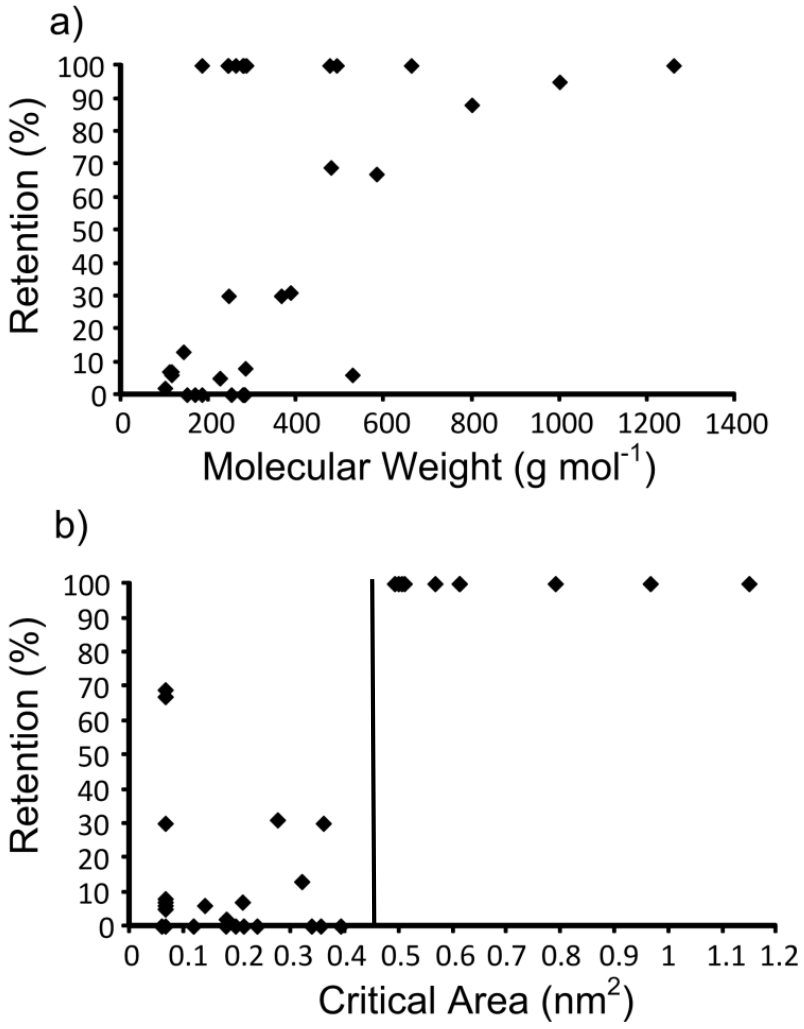

Figure 5.2. Plot comparing molecular weight to critical area.[138]
a) Plot of retention versus molecular weight.
b) Plot of retention versus smallest cross-sectional area (critical area).

This research was continued by Abhinaba Gupta who used PDCPD membranes to separate saturated and trans-fatty acid salts from cis-fatty acid salts.[138] Fatty acids come from a variety of different sources including vegetable

oil and marine oils and they are separated from glycerol as a mixture of saturated, monounsaturated, and polyunsaturated fatty acids. These fatty acids are hard to separate because they have similar molecular weights and physical properties. The difficulty and expense of this separation is a critical reason for challenge of using fatty acids as a starting material for industrial purposes. The separation of fatty acids was achieved by converting the fatty acids into salts by the addition of triisobutylamine which increased the cross-sectional area of selected cis-fatty acid salts so they were above the cross-sectional area cut-offs. The cross-sectional area of the saturated and trans fatty acid salts remained below the cross-sectional area cut-off and they fluxed through the membrane. The size of the amine can also be varied to separate a monounsaturated fatty acid salt from polyunsaturated fatty acid salts and different polyunsaturated fatty acid salts from each other. Gupta also was able to add pressure which increased the flux rate and used the membrane to separate Pd and phosphine ligands from the products of Pd catalyzed reactions.[139]

Recommendation for Future Work

The next step in the development of a PDCPD membrane is to increase the size of the membrane to do separations on an industrial scale. The fabrication method described in chapter 4 worked well to make membranes several inches in diameter, but the polymerization proceeded too fast for the polymer to be cast into a thin film to make a membrane a couple of feet in diameter. The polymerization of dicyclopentadiene (DCPD) with Grubbs catalyst is an exothermic reaction and when the polymerization is done at larger scale the excess heat that is created increases rate of the polymerization. The melting point DCPD is 32.5 ºC, this limits how much the reaction can be cooled. The

polymerization will need to be re-optimized for this larger scale with a lower catalyst loading and adding solvent to the DCPD to lower the melting point.

APPENDIX

EPOXIDATION OF THE SURFACE OF POLYDICYCLOPENTADIENE FOR THE SELF-ASSEMBLY OF ORGANIC MONOLAYERS

Prelude

This chapter discusses a project that was initially pursued by Mathew Perring and completed by me. Mathew Perring developed the method to epoxidize the surface of polydicyclopentadiene (PDCPD) and reacted the epoxidized surface with amines. He also characterized the surface by XPS and GATR-IR. I developed an application for the epoxidized PDCPD. The PDCPD membrane discussed in chapter 4 was epoxidized with MCPBA and reacted with poly(ethylene imine). The functionalized PDCPD membrane was then able to prevent the flux of $CuCl_2$ but small organic molecules were allowed to flux through it. The fabrication and functionalization of the membrane as well as the development and characterization of the site-isolation of $CuCl_2$ were my contributions to this project.

Abstract

Polydicyclopentadiene was reacted with *m*-chloroperoxybenzoic acid to yield a surface that was terminated with epoxides. The X-ray photoelectron spectrum (XPS) of the sample demonstrated that the top ten nm of the surface had been oxidized. The grazing angle attenuated total reflection-infrared spectrum of this surface was unchanged from that of native PDCPD which demonstrated that the oxidation was only on the surface and that the bulk PDCPD was unchanged. The PDCPD-epoxide surface was then reacted with two different amines that possessed F or Cl atoms to study the ring opening

reaction between surface epoxides and amines. This reaction was rapid and completed within an hour. The method of Tougaard was applied to the F and Cl peaks in the XPS to investigate their locations and whether the amines were uniformly distributed in the top ten nm or were localized at the surface. This analysis clearly described the amines as being present only on the surface. The PDCPD-epoxide surface was also reacted with poly(ethylene imine) to generate a surface that exposed numerous amines. The amines bonded to Cu, Au, and Pd such that these metals did not flux through PCPCD while the flux of 4-nitrobenzaldehyde was unaffected.

Introduction

Polydicyclopentadiene (PDCPD) is an important material that has found commercial applications due to its toughness, resistance to fracture, thermal stability, and ease of manufacturing via reaction injection molding.[122,124,125,132,140-147] For instance, this polymer is used for the hoods of semitrucks and the outer shell of snowmobiles. PDCPD is synthesized by the ring opening metathesis polymerization of dicyclopentadiene – a byproduct in naphtha crackers – and different catalysts. Until recently these catalysts were ill-defined products of a mixture of $SiCl_4$, $EtAlCl_2$, and a molybdenum precursor, but the discovery of the Grubbs catalysts made the manufacturing of PDCPD more robust.[148] Importantly, the Grubbs catalysts synthesize PDCPD with little to no unreacted dicyclopentadiene which possesses a strong, unpleasant odor that is undesired for the polymer.

PDCPD lacks heteroatoms such as oxygen or nitrogen that are used in other polymers to functionalize surfaces for the attachment of small molecules or polymers to form layered composites.[143,149-157] The molecular structure of PDCPD is mostly inert and does not promote the attachment of other molecules

or polymers. Rather than heteroatoms, a crucial molecular characteristic of this polymer is that is possesses a high density of one olefin for every five carbons (Figure A.1). Although olefins are only marginally reactive, they can be activated to yield other functional groups that can readily react with small molecules and other polymers to form strong, covalent bonds. In this chapter we report a method to convert the olefins in the top ten nanometers of PDCPD into epoxides and the reactions of these epoxides with small molecules and poly(ethylene imine).

We recently published a paper that described a method to assemble organic monolayers on PDCPD using two robust reactions.[121] First, the surface olefins were reacted with Br_2 for several seconds to fully brominate the surface (Figure A.1). The reaction between Br_2 and olefins was extremely rapid and completed in seconds, this reaction resulted in two new C-Br bonds for every olefin. Next, this substrate was reacted with amines to displace the Br and bond the amines to the surface. This method worked well and resulted in organic layers on PDCPD, but the reaction between Br_2 and PDCPD was too rapid to control. Nearly all of the olefins in the top 100-200 nm of the surface reacted with Br_2 within seconds. Longer reaction times led to a noticeable darkening of the PDCPD, the PDCPD becoming brittle, and a roughening of the surface. What was needed was a milder method to functionalize the surface of PDCPD such that the surface chemistry could be altered without affecting the physical properties of the polymer.

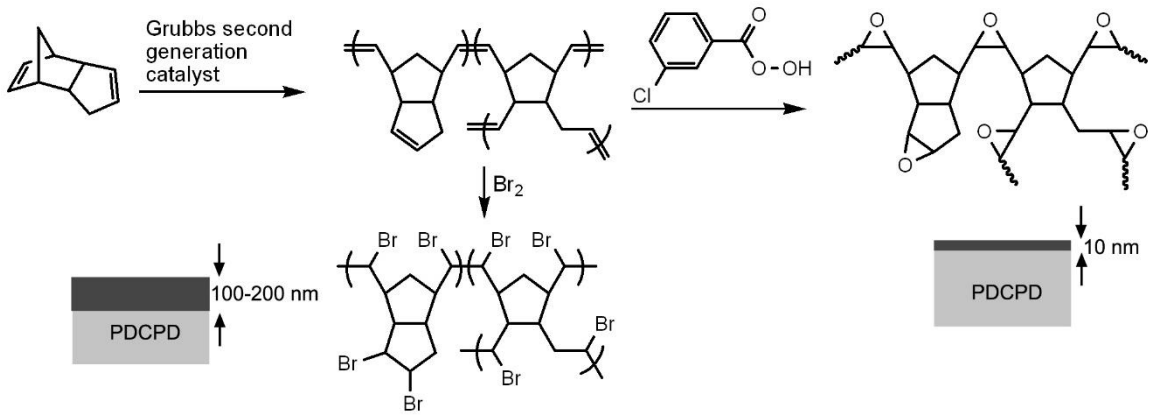

Figure A.1. The reaction of dicyclopentadiene with the Grubbs catalyst resulted in PDCPD. This material was exposed to Br_2 which led to a reaction with of most of the olefins in the top 100-200 nm of the surface. In contrast, MCPBA only reacted the olefins in the top ten nm of the surface.

We report such a method that uses *meta*-chloroperoxybenzoic acid (MCPBA) to epoxidize only the olefins in the top ten nanometers of PDCPD. These epoxides were then reacted with small molecules or a polymer to further functionalize the surface. MCPBA was chosen because it is an inexpensive reagent that readily reacts at room temperature with olefins to yield epoxides but would be expected to epoxidize only the surface of PDCPD.[158-162] Working with Br_2 was limiting because it has a high vapor pressure, small size, and reacted rapidly with olefins such that it reacted nearly all the olefins in the top 100-200 nm. In contrast, MCPBA is much larger than Br_2 and possesses a negligible vapor pressure such that its diffusion into PDCPD is significantly slowed. By reacting only the olefins near the surface, the physical properties of PDCPD would not be expected to be altered. Epoxides were advantageous because they are stable for long periods of time, but they are also highly reactive with a variety of nucleophiles such as those containing oxygen, amines, azides, or thiols. Reactions between epoxides and these nucleophiles are often high

yielding and can be used to introduce a variety of functional groups on the surface.

Results and Discussion

Reactions of *m*-Chloroperoxybenzoic Acid and PDCPD

PDPCD was synthesized according to a method published in prior work and reported in the experimental section.[121] This polymer yielded only the obvious peaks expected in the GATR-IR spectrum, and it had less than 0.9% atomic composition of oxygen by XPS (Figure A.2). The amount of oxygen in the XPS spectra varied slightly from sample to sample, but it was found to be less than 1% for most samples. The oxygen is most likely due to surface oxidation as expected for a polymer with a high density of olefins.

PDCPD was reacted with MCPBA to yield a surface with epoxides (Figure A.1). Although a variety of epoxidizing agents are known, MCPBA was chosen because it is small enough that reactions with surface olefins will not be limited by steric considerations, it is a homogeneous reagent, and its reaction with olefins are high yielding and result in few side products. In prior work in 1967, Meyersen and Wang reported the epoxidation of polycyclopentadiene using a peroxy acid. The reactions used a low molecular weight polycyclopentadiene that was soluble in organic solvents and the reactions went to high conversions. Although MCPBA reacts with olefins in solution over several hours, reactions with the surface of PDCPD were allowed to run for 24 h to ensure complete epoxidation of the surface.

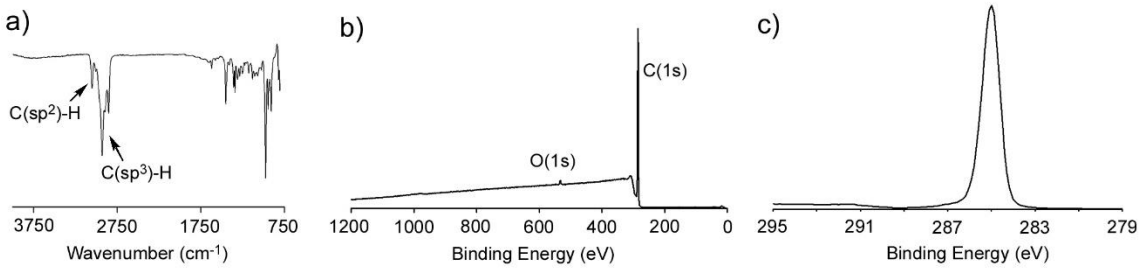

Figure A.2**.** Characterization the surface PDCPD.
a) The GATR-IR spectrum of PDCPD
b) Survey XPS spectra
c) High resolution of C(1s) XPS spectra of PDCPD

The PDCPD-epoxide surface was characterized by GATR-IR spectroscopy and XPS (Table A.1). Analysis of the XPS data yielded a surface composition of 85.2% C, 14.6% O, and 0.2% Cl. High resolution scans of the C(1s) region showed oxidized carbon at 284 eV that was consistent with ethers and epoxides and a small peak at 286.4 eV that was consistent with C=O (Figure A.3). The peak at 286.4 eV and the presence of some chlorine indicated that either some of the MCPBA (or *m*-chlorobenzoic acid that was produced after MCBPA reacted with olefins) became trapped in the PDCPD. Despite extensive washings with solvent, the Cl peak always remained at low levels in the XPS spectra.

Table A.1. Atomic composition of samples as determined by XPS.

		Atomic Composition (%)			
Sample	Time	C	O	Cl	F
PDCPD		99.1	0.9	0	0
PDCPD-epoxide		85.2	14.6	0.2	0
PDCPD-A	20 min	85.3	13.1	0.2	1.2
PDCPD-A	40 min	81.9	14.3	0.3	1.4
PDCPD-A	60 min	83.9	13.8	0.2	1.4
PDCPD-B	20 min	85.7	13.7	0.8	0
PDCPD-B	40 min	84.0	14.4	1.2	0
PDCPD-B	60 min	82.8	15.0	1.4	0
PDCPD-PEI[a]	60 min	80.8	13.7	0.6	0

Note: [a]The N(1s) integrated to 4.8%.

The GATR-IR spectrum of PDCPD-epoxide was identical to that of native PDCPD. In particular, the Csp^2-H peak at 3050 cm^{-1} did not decrease in intensity after reaction with MCPBA. This result is explained by the depth of analysis of GATR-IR spectroscopy. In this measurement, a polymer is placed into contact with the flat section of a Ge hemisphere through which IR light is passed. The IR spectrum is measured for the first 100 to 200 nm of the polymer that is in contact with the hemisphere. In our prior work using Br_2 to functionalize PDCPD, the Csp^2-H peak almost completely disappeared because the Br_2 reacted with most all of the olefins within the top 100 to 200 nm on the surface.[121] In this work, MCPBA does not readily penetrate the PDCPD so only the surface and near surface olefins were reacted. The lack of change in the GATR-IR spectrum demonstrated that the epoxidation only occurred near the surface rather than throughout the first 100-200 nm of the surface.

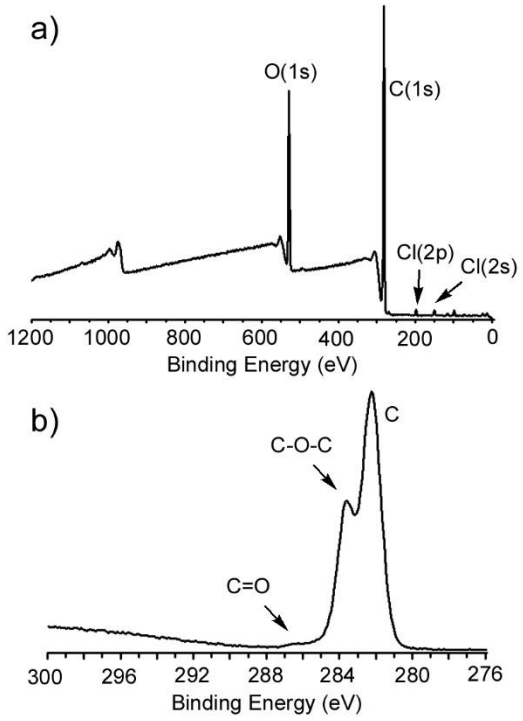

Figure A.3**.** Characterization the PDCPD-epoxide surface.
a) The survey XPS spectra
b) A high resolution spectra of the C(1s) region for PDCPD-epoxide

Reactions of Molecules Containing Amines with PDCPD-Epoxide

Homogeneous reactions between amines and epoxides proceed to high yields in short periods of time. In fact, reactions between molecules with two amines and molecules with two epoxides result in epoxy polymers that are produced in millions of tons per year.[163,164] This was a robust reaction that required no catalyst to proceed. In this work, PDCPD-epoxide was reacted with two different amines labeled A and B in Figure A.4. Molecule A was chosen

because it has fluorines that possess distinct XPS signals that can be uniquely assigned to that molecule.

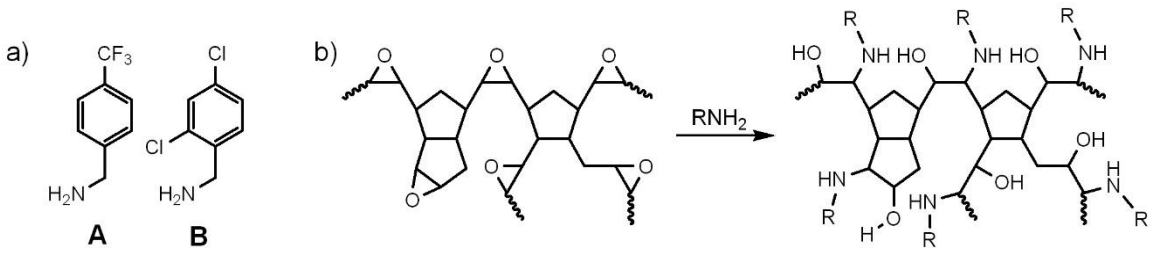

Figure A.4**.** The reaction between PDCPD-epoxide and amines.
a) Two amines that were reacted with PDCPD-epoxide are shown
b) The reaction between PDCPD-epoxide and amines resulted in amines covalently bonded to the surface. Each amine reacted with one epoxide to yield an alcohol and a covalent C-N bond.

Molecule A was reacted with PDCPD-epoxide for 20, 40, and 60 min and then studied by XPS. As shown in Table A.1, the intensity of the F(1s) peak increased from 0 to 20 min and then only slightly from 20 min to 40 min. After approximately 1 h the reaction was complete as judged by the intensity of the F(1s) peak in the XPS. It is notable that Cl was detected in all three samples at the same level found in PDCPD-epoxide which further indicated that MCPBA or *m*-chlorobenzoic acid could not be extracted from PDCPD. Although the sample was studied by GATR-IR spectroscopy, no evidence of reaction between the amine and epoxide was observed due to the surface localization of the reaction and the depth of penetration of this measurement.

The C(1s) and N(1s) regions in the XPS were of interest for this reaction (Figure A.5). Small amounts of N were observed in the XPS, but due to the low sensitivity of XPS for N(1s) this peak was too weak to accurately measure its concentration. In addition, the C(1s) region was similar to PDCPD-epoxide.

Although a peak for CF_3 in the C(1s) region could be expected at approximately 292.5 eV, this peak was too small to be detected.

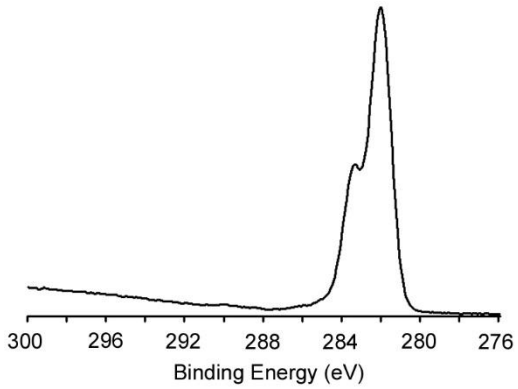

Figure A.5. The high resolution XPS spectrum of the C(1s) region for molecule A reacted with PDCPD-epoxide was similar to that measured for PDCPD-epoxide.

Reactions between molecule B and PDCPD-epoxide were complicated by the presence of Cl in the XPS of PDCPD-epoxide. Thus, the Cl(2p) peak in the XPS was assigned to molecule B after reacting with the surface and chlorine contamination from the epoxidation reaction. Despite these limitations to the analysis, the same general trend in reaction time was observed. The intensity of the Cl(2p) peak in the XPS rose in intensity initially but slowed after 40 min. This result indicated that the epoxidation was complete within an hour.

Surface Localization of CF_3 Group

It was important to determine if the amine reacted at the surface as expected or if it was also present in the subsurface. One method to determine the location of an element in XPS is to apply the results of Tougaard to determine if an element is on the surface, subsurface, or uniformly distributed throughout

the XPS detection depth.[165-168] In this method the inelastic background scattering for a peak is determined to find the location of that element. Simply, if the element is found on the surface the inelastic scattering will be minimal, but if the element is subsurface or uniformly distributed the inelastic scattering increases. This relationship is quantified by measuring the ratio of the peak area, Ap, and the background height, B, for a peak measured 30 eV below the peak. When Ap/B is >30 eV the element is only found on the surface, when Ap/B is 25 eV the element is uniformly distributed, and when Ap/B is <20 eV the element is localized beneath the surface. This method was applied to the F(1s) peak in samples measured after PDCPD-epoxide was exposed to molecule A for 20, 40, and 60 min (Figure A.6). The values for Ap/B decreased from 93 eV to 76 eV to 40 eV as time molecule A was exposed to PDCPD-epoxide increased from 20 min to 60 min. These results demonstrated that the CF_3 group was found on the surface and was not buried within PDCPD. Although the extent of surface localization was the greatest for the surface prepared for 20 min, even after 60 min the CF_3 group was still mostly localized at the surface.

This method was also applied to the Cl(2p) peak for the product of molecule B reacted with PDCPD-epoxide for 60 min. The value for Ap/B was 39 eV which supported the result that amines remained localized on the surface.

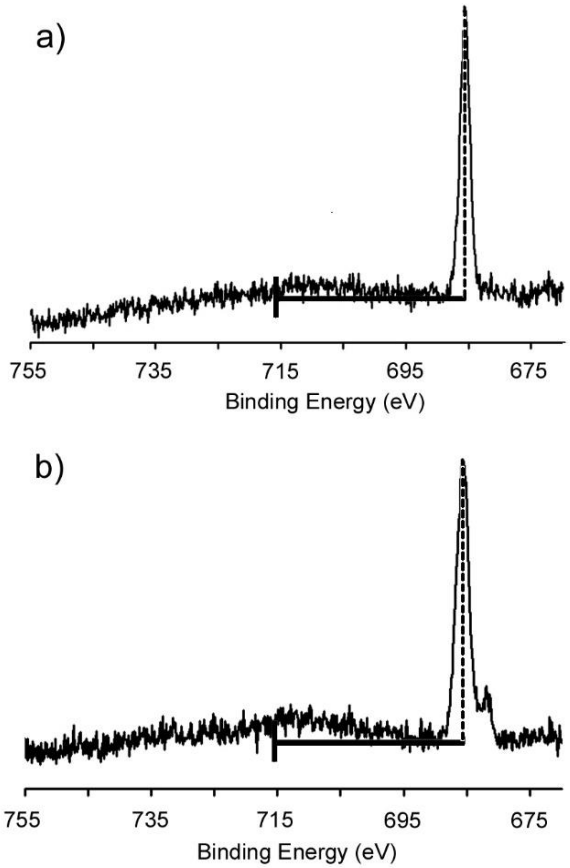

Figure A.6. The F(1s) peak after molecule A was exposed to PDCPD-epoxide. The lines are added to demonstrate how to apply the Tougaard method.
a) 20 min of exposure
b) 1 h of exposure

Reactions of PDCPD-Epoxide with Poly(Ethylene Imine)

Poly(ethylene imine) is a viscous polymer that is used in medicine for DNA delivery due to its high concentration of amines and ability to penetrate cell walls.[169,170] This polymer has two carbons for every amine and contains a mixture of primary, secondary, and tertiary amines (Figure A.7). PDCPD-epoxide was reacted with this polymer to create a polymer composite with many reactive surface amines for further functionalization.

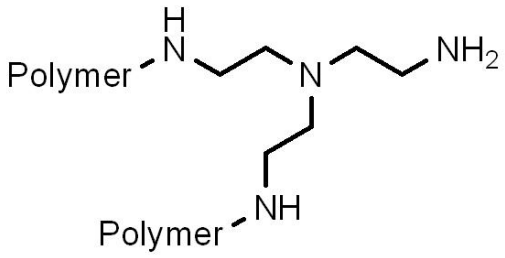

Figure A.7. PEI has primary, secondary, and tertiary amines.

PDCPD-epoxide was added to a solution of PEI in methanol for 1 h. The resulting polymer was washed with copious amounts of solvent to remove excess PEI and then it was studied by XPS and GATR-IR spectroscopy. The GATR-IR spectrum of the this polymer appeared identical to that of native PDCPD which indicated that only a thin layer of PEI was deposited on the surface.

The XPS of the sample had a N(1s) concentration of 4.8% which is consistent with the high concentration of amines in the polymer. If the PEI layer was thicker than the depth of measurement by XPS (approximately 10 nm), the ratio of the C to N peaks as measured by XPS would be approximately 2, but the measured ratio of C to N was 17. This result was consistent with only a thin layer of PEI on the surface.

Site-Isolation of $CuCl_2$ using Functional Membranes

Our group has an active research effort to site-isolate metal catalysts from the products of a reaction using thin, polymeric membranes.[70,71,77-79] In these systems a reaction was carried out in a solvent on one side of a membrane and, after the reaction was complete, the product fluxed through the membrane while the catalyst did not flux through it. Catalysts were successfully site-isolated on one side of a membrane and the products were on the other side. The catalysts were recycled and the products were isolated with minimal contamination from

the catalyst. The polymer membranes were composed of commercial polydimethylisiloxane (PDMS) purchased as a kit of Sylgard 184. Although successful for some catalysts, membranes composed of this polymer did not resist the flux of many metals. In more recent work, membranes composed of PDCPD were developed that have physical properties that can be rationally altered because their synthesis is well controlled and not subject to using a commercial "kit".[70]

It became necessary to functionalize PDCPD membranes because metals could flux through them. In control experiments where $CuCl_2$ was added to one side of a 117 micron thick membrane in a 1/1 mixture of CH_2Cl_2/CH_3OH, it fluxed through the membrane from the "interior" to the "exterior" (Figure A.8). In these experiments, both $CuCl_2$ and *p*-nitrobenzaldehyde were added to solvent on one side of a membrane and their concentrations were found by UV-VIS spectroscopy (for $CuCl_2$) and ^1H NMR spectroscopy (for *p*-nitrobenzaldehyde) after 24 h. The ratio of the concentration of $CuCl_2$ on the exterior to the interior ($[CuCl_2]_{ex}/[CuCl_2]_{int}$) was 0.50 and for the aldehyde ($[aldehyde]_{ex}/[aldehyde]_{int}$) was 0.67. These numbers demonstrated that both $CuCl_2$ and *p*-nitrobenzaldehyde fluxed through the membrane at similar rates.

These membranes were further functionalized with PEI to keep $CuCl_2$ from fluxing through them while still allowing organic molecules to pass through. It is well known that amines, such as those found in PEI, coordinate to Cu(II). This coordination would greatly slow their rate of diffusion through a layer of PEI and their overall flux through a hybrid membrane composed of PDCPD and PEI. Although the flux of $CuCl_2$ would be affected by PEI, it was believed that this layer would have little impact on the flux of neutral organic molecules such as *p*-nitrobenzaldehyde. In addition, it was critical to maintain the physical properties of PDCPD such that the flux of molecules through PDCPD before and after

reactions on its surface did not differ. This was important because it was necessary to flux organic molecules through PDCPD and their flux needed to be high and not hindered by reactions on PDCPD.

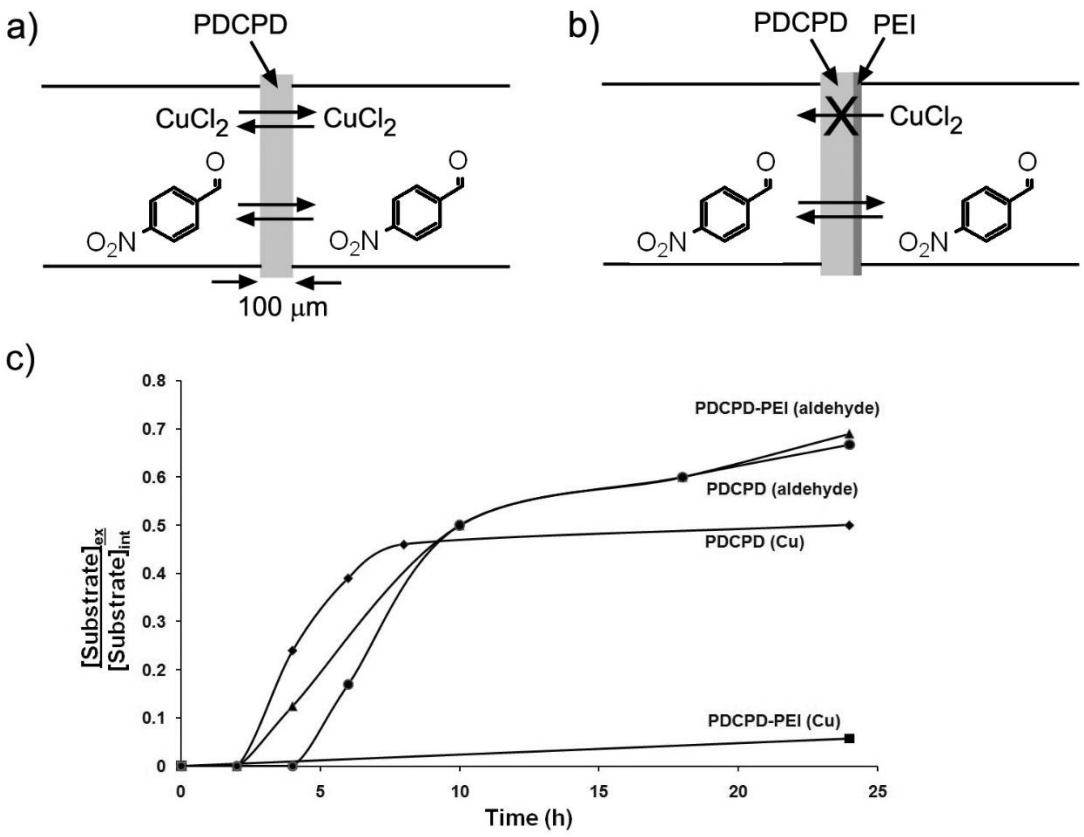

Figure A.8. The separation of $CuCl_2$ from *p*-nitrobenzaldehyde
a) $CuCl_2$ and *p*-nitrobenzaldehyde were added to one side of a PDCPD membrane (diameter of 2.5 cm and thicknesses of 100 microns) and both readily fluxed through to the other side.
b) When a thin layer of PEI was attached to the PDCPD, the flux of $CuCl_2$ was dramatically lowered while *p*-nitrobenzaldehyde was able to flux through the membrane.
c) The ratio of the concentration of the substrate on the exterior divided by the concentration on the interior for *p*-nitrobenzaldehyde and $CuCl_2$ fluxing through a PDCPD or PDCPD-PEI membrane.

In initial experiments, PDCPD membranes with a very thin layer of PEI as described in the previous section had no effect on the flux of $CuCl_2$ or *p*-nitrobenzaldehyde. This result was expected based on the amount of $CuCl_2$ (25.2 mg) used in these experiments and the ratio of Cu to amine. If the layer of PEI was 3 nm thick – a reasonable estimate based on the XPS data in Table A.1 – the ratio of Cu to amine was approximately 5,000/1 and the PEI layer was too thin to coordinate all but a small fraction of the $CuCl_2$.

The thickness of the PEI layer was expanded in a subsequent reaction to improve the ratio of amine to $CuCl_2$. The PDCPD-PEI surface was treated with fresh PEI and 1,2,7,8-diepoxyoctane dissolved in methanol. The diepoxyoctane reacted with amines on the surface of PDCPD-PEI and amines in PEI dissolved in solution. These reactions added cross-links between PEI in solution and that on the surface and lead to more PEI being bonded to the surface. In these reactions, the molar ratio of the repeat unit of PEI (-$NHCH_2CH_2$-) to 1,2,7,8-diepoxyoctane was 10:1 so that most of the amines were unreacted and coordinated to Cu(II). The excess PEI and diepoxyoctane were removed after the reaction was complete and the thickness of the PEI layer was measured by optical microscopy. In two experiments the thickness of the PEI layer was expanded to approximately 26 and 50 microns which corresponded to ratios of Cu to amine of 0.6:1 and 0.3:1 in the flux experiments. The concentration of $CuCl_2$ on the exterior and interior were found after 24 h for both membranes. The membrane with a PEI thickness of 26 microns had a ratio of $[CuCl_2]_{ex}/[CuCl_2]_{int}$ equal to 0.058, and the membrane with a PEI thickness of 50 microns had a ratio of $[CuCl_2]_{ex}/[CuCl_2]_{int}$ equal to 0.029. These results demonstrated that the flux of $CuCl_2$ could be greatly slowed by the addition of a suitably thick layer of PEI to coordinate to the Cu(II). The flux of *p*-nitrobenzaldehyde was very similar to that of native PDCPD ($[aldehyde]_{ex}/[aldehyde]_{int} = 0.69$) such that organic molecules

were not affected by the PEI layer. This method was very promising because the reactions on PDCPD were only on its surface rather than its subsurface such that the physical properties of PDCPD were unchanged.

Conclusions

Because amines only react with surface epoxides their densities could be estimated from the intensity of the C and F peaks in the XPS. After one hour of reaction between molecule A and PDCPD-epoxide, the approximate density of molecule A on the surface was 0.67 molecules per nm^2.[121] This value can be compared to the density of a well-packed monolayer of $HSCH_2C_6H_5$ on Au (4.9 molecules per nm^2) and to the density of molecule A after reaction with a brominated surface of PDCPD (1.35 molecule per nm^2).[171] Clearly, the method reported in this chapter does not result in a well-packed, dense monolayer, but this result was anticipated. PDCPD has only two olefins per 10 carbons, so at least 60% of the surface is unreactive towards MCPBA. Furthermore, each epoxide will react with only one amine. This result was in contrast to prior work when PDCPD was reacted with Br_2 to yield reactive C-Br bonds. In that work each olefin yielded two amines bonded to the surface. The reactions employed in this work and prior work predict that the concentration of amine after reaction with the brominated surface would be twice the concentration of amine after reaction with the epoxidized surface. This is the result that was observed. The limitations for the density of functionalization of PDCPD appear to be limitations of working with this material rather than limitations of the reactions.

We reported a method to functionalize the surface of PDCPD with epoxides that were reactive with amines. Only the olefins on or near the surface were functionalized which will allow the physical properties of PDCPD to remain unchanged even as its surface chemistry is altered. This result is in contrast to

prior work where Br_2 reacted with all of the olefins in at least the top 100 to 200 nm of the surface. The importance of this work is that the use of MCPBA will allow for a variety of different molecules and other polymers to be covalently bonded to PDCPD under mild conditions. The increasing applications of PDCPD will necessitate the integration of methods to bond it to other surfaces and materials, this chapter reports one simple method that does not affect the physical properties of PDCPD.

Experimental

Materials. Poly(ethylene imine) with a M_n of 60,000 g mol^{-1} in a 50% by weight solution in water was purchased from Sigma-Aldrich. The Grubbs second generation catalyst, 4-(trifluoromethyl)benzylamine, dicyclopentadiene (Fluka), *m*-chloroperoxybenzoic acid, and 2,4-dichlorobenzylamine were purchased from Sigma-Aldrich or Fluka and used as received.

Synthesis of PDCPD. The synthesis of PDCPD was previously reported in full detail.[121] The synthesis will be briefly outlined here to emphasize how the polymer was synthesized. A molar ratio of 20,000:1 of Grubbs second generation catalyst to dicyclopentadiene was heated from 55 to 80 ^oC for 30 min under vacuum. The resulting polymer did not smell of unreacted dicyclopentadiene and was used in further experiments. It was stored in a freezer in the dark to prevent oxidation of the surface.

Synthesis of PDCPD-epoxide. MCPBA (1.0 g) was dissolved in 20 mL of diethyl ether at room temperature. A slab of PDCPD was immersed in this solution for 24 h with constant stirring and then rinsed with copious amounts of diethyl ether.

Reactions of PDCPD-epoxide with amines. Amines A or B from Figure A.4 were dissolved in diethyl ether at loadings of 0.2 g of amine per 10 mL of

solvent. PDCPD-epoxide was completely immersed in the solution with constant stirring for the period of time indicated in Table A.1. The samples were removed and washed with copious amounts of diethyl ether.

Reactions of PDCPD-epoxide with poly(ethylene imine). A solution of poly(ethylene imine) in methanol (0.15 g of polymer in 10 mL of solvent) was thoroughly mixed. A slab of PDCPD-epoxide was added to the solution for 1 h with constant stirring. The polymer was removed, washed with copious amounts of methanol and water, and then placed under vacuum to dry the polymer prior to analysis by XPS.

Synthesis of PDCPD with micrometer-thick layers of PEI. A 100 micron thick PDCPD slab was fabricated as before and placed into a glass apparatus to form a membrane between two compartments. One side of the membrane was epoxidized with MCPBA and then reacted with PEI according to the procedure described above. Next, PEI (0.16 g, 3.72 mmol of nitrogen) and 1,2,7,8-diepoxyoctane (0.053 g, 0.372 mmol) were added in 11.6 mL of methanol to one side of the membrane. After approximately 1 h the solvent and excess reagents were removed.

To study the flux of $CuCl_2$ (25.2 mg, 0.186 mmol) and *p*-nitrobenzaldehyde (151.1 mg, 1.0 mmol), both were added to 10 mL of a 1:1 (v/v) mixture of CH_2Cl_2/MeOH on the side of the membrane that had been functionalized. 50 mL of the same solvent mixture was added to the other side and after 24 h the concentration of $CuCl_2$ on both sides was found by UV-VIS spectrometry and the concentration of *p*-nitrobenzaldehyde was found by ^{1}H NMR spectroscopy. The membrane was removed, dried, and the thickness measured by optical microscopy.

Surface characterization. The XPS spectra were recorded on an Axis Ultra instrument using A1 Kα X-ray source at a 90^o take off angle. The samples

were degassed and dried of residual solvent overnight in the sample exchange chamber. The survey spectra were recorded at 1 eV intervals with a dwell time of 200 ms and high resolution spectra were recorded at 0.1 eV intervals with a dwell time of 1000 ms. Grazing angle attenuated total reflection-infrared (GATR-IR) spectra were recorded on a Bruker Tensor 27 instrument with a liquid nitrogen cooled MCT detector. GATR-IR spectra were taken at a resolution of 4 cm^{-1} for 1024 scans.

REFERENCES

1. Martelli, A.; Testai, L.; Marino, A.; C. Breschi, M.; Da Settimo, F.; Calderone, V. Hydrogen Sulphide: Biopharmacological Roles in the Cardiovascular System and Pharmaceutical Perspectives. *Current Medicinal Chemistry* **2012***, 19*, 3325.

2. Martelli, A.; Testai, L.; Breschi, M. C.; Blandizzi, C.; Virdis, A.; Taddei, S.; Calderone, V. Hydrogen Sulphide: Novel Opportunity for Drug Discovery. *Medicinal Research Reviews* **2012***, 32*, 1093.

3. Olson, K. R. The Therapeutic Potential of Hydrogen Sulfide: Separating Hype from Hope. *AJP - Regulatory Integrative and Comparative Physiology* **2011***, 301*, R297.

4. Kashfi, K.; Olson, K. R. Biology and Therapeutic Potential of Hydrogen Sulfide and Hydrogen Sulfide-Releasing Chimeras. *Biochemical Pharmacology* **2013***, 85*, 689-703.

5. Chen, C.; Xin, H.; Zhu, Y. Hydrogen Sulfide: Third Gaseous Transmitter, but with Great Pharmacological Potential. *Acta Pharmacologica Sinica* **2007***, 28*, 1709-1716.

6. Liu, Y. H.; Lu, M.; Hu, L. F.; Wong, P. T. H.; Webb, G. D.; Bian, J. S. Hydrogen Sulfide in the Mammalian Cardiovascular System. *Antioxidants & Redox Signaling* **2012***, 17*, 141.

7. Caliendo, G.; Cirino, G.; Santagada, V.; Wallace, J. L. Synthesis and Biological Effects of Hydrogen Sulfide (H_2S): Development of H_2S-Releasing Drugs as Pharmaceuticals. *Journal of Medicinal Chemistry* **2010***, 53*, 6275-6286.

8. Whitfield, N. L.; Kreimier, E. L.; Verdial, F. C.; Skovgaard, N.; Olson, K. R. A Reappraisal of H_2S/Sulfide Concentration in Vertebrate Blood and its Potential Significance in Ischemic Preconditioning and Vascular Signaling. *AJP - Regulatory Integrative and Comparative Physiology* **2008***, 294*, R1930.

9. Toombs, C. F.; Insko, M. A.; Wintner, E. A.; Deckwerth, T. L.; Usansky, H.; Jamil, K.; Goldstein, B.; Cooreman, M.; Szabo, C. Detection of Exhaled Hydrogen Sulphide Gas in Healthy Human Volunteers During Intravenous Administration of Sodium Sulphide. *British Journal of Clinical Pharmacology* **2010***, 69*, 626.

10. DeBruyn, W. J.; Swartz, E.; Hu, J. H.; Shorter, J. A.; Davidovits, P.; Worsnop, D. R.; Zahniser, M. S.; Kolb, C. E. Henry's Law Solubilities and Setchenow Coefficients for Biogenic Reduced Sulfur Species Obtained from Gas-Liquid Uptake Measurements. *Journal of Geophysical Research* **1995***, 100*, 7245.

11. Martelli, A.; Rapposelli, S.; Calderone, V. NO-Releasing Hybrids of Cardiovascular Drugs. *Current Medicinal Chemistry* **2006***, 13*, 606.

12. Kimura, Y.; Goto, Y. I.; Kimura, H. Hydrogen Sulfide Increases Glutathione Production and Suppresses Oxidative Stress in Mitochondria. *Anioxidants & Redox Signaling* **2010***, 12*, 1-13.

13. Ashcroft, S. J.; Ashcroft, F. M. Properties and Functions of ATP-Sensitive K-Channels. *Cellular signalling* **1990***, 2*, 197-214.

14. Nichols, C. G. K_{ATP} Channels as Molecular Sensors of Cellular Metabolism. *Nature* **2006***, 440*, 470-476.

15. Masi, A. D.; Ascenzi, P. H_2S: A "Double face" Molecule in Health and Disease. *Biofactors* **2013***, 39*, 186-196.

16. Wang, R. Physiological Implications of Hydrogen Sulfide: A Whiff Exploration That Blossomed. *Physiological Reviews* **2012***, 92*, 791-896.

17. Banerjee, S. K.; Maulik, S. K. Effect of Garlic on Cardiovascular Disorders: A Review. *Nutrition Journal* **2002***, 1*, 4.

18. Amagase, H. Clarifying the Real Boiactive Constituents of Garlic. *Journal of Nutrition* **2006***, 136*, 716S-725S.

19. Benavides, G. A.; Squadrito, G. L.; Mills, R. W.; Patel, H. D.; Isbell, T. S.; Patel, R. P.; Darley-Usmar, V. M.; Doeller, J. E.; Kraus, D. W. Hydrogen Sulfide Mediates the Vasoactivity of Garlic. *Proceedings of the National Academy of Sciences of the United States of America* **2007***, 104*, 17677-17982.

20. Li, L.; Whiteman, M.; Guan, Y. Y.; Neo, K. L.; Cheng, Y.; Lee, S. W.; Zhao, Y.; Baskar, R.; Tan, C. H.; Moore, P. K. Characterization of a Novel, Water-Soluble Hydrogen Sulfide–Releasing Molecule (GYY4137): New Insights Into the Biology of Hydrogen Sulfide. *Circulation* **2008***, 117*, 2351-2360.

21. Martelli, A.; Testai, L.; Citi, V.; Marino, A.; Pugliesi, I.; Barresi, E.; Nesi, G.; Rapposelli, S.; Taliani, S.; Da Settimo, F.; Breschi, M. C.; Calderone, V. Arylthioamides as H_2S Donors: l-Cysteine-Activated Releasing Properties and Vascular Effects *in Vitro* and *in Vivo*. *ACS Medicinal Chemistry Letters* **2013***, 4*, 904-908.

22. Wallace, J. L.; Caliendo, G.; Santagada, V.; Cirino, G. Markedly Reduced Toxicity of a Hydrogen Sulphide-Releasing Derivative of Naproxen (ATB-346). *British journal of pharmacology* **2010***, 159*, 1236-1246.

23. Sparatore, A.; Perrino, E.; Tazzari, V.; Giustarini, D.; Rossi, R.; Rossoni, G.; Erdman, K.; Schröder, H.; Soldato, P. D. Pharmacological Profile of a Novel H_2S-Releasing Aspirin. *Free Radical Biology and Medicine* **2009***, 46*, 586-592.

24. Kodela, R.; Chattopadhyay, M.; Kashfi, K. NOSH-Aspirin: A Novel Nitric Oxide–Hydrogen Sulfide-Releasing Hybrid: A New Class of Anti-inflammatory Pharmaceuticals. *ACS Medicinal Chemistry Letters* **2012***, 3*, 257-262.

25. Shukla, N.; Rossoni, G.; Hotston, M.; Sparatore, A.; Del Soldato, P.; Tazzari, V.; Persad, R.; Angelini, G. D.; Jeremy, J. Y. Effect of Hydrogen Sulphide-Donating Sildenafil (ACS6) on Erectile Function and Oxidative Stress in Rabbit Isolated Corpus Cavernosum and in Hypertensive Rats. *BJU International* **2009***, 103*, 1522-1529.

26. Muzaffar, S.; Jeremy, J. Y.; Sparatore, A.; Del Soldato, P.; Angelini, G. D.; Shukla, N. H_2S-Donating Sildenafil (ACS6) Inhibits Superoxide Formation and GP91PHOX Expression in Arterial Endothelial Cells: Role of Protein Kinases A and G. *British Journal of Pharmacology* **2008***, 155*, 984-994.

27. Shen, X.; Pattillo, C. B.; Pardue, S.; Bir, S. C.; Wang, R.; Kevil, C. G. Measurement of Plasma Hydrogen Sulfide *in vivo* and *in vitro*. *Free Radical Biology and Medicine* **2011***, 50*, 1021-1031.

28. Furne, J.; Saeed, A.; Levitt, M. D. Whole Tissue Hydrogen Sulfide Concentrations are Orders of Magnitude Lower then Presently Accepted Values. *American Journal of Physiology* **2008***, 295*, R1479-R1485.

29. Hartman, M. C.; Dconaab, M. M. A New, Highly Water-Soluble, Fluorescent Turn-on Chemodosimeter for Direct Measurement of Hydrogen Sulfide in Biological Fluids. *Analyst* **2012***, 137*, 4910-4912.

30. Xuan, W.; Pan, R.; Cao, Y.; Liub, K.; Wang, W. A Fluorescent Probe Capable of Detecting H_2S at Submicromolar Concentrations in Cells. *Chemical Communication* **2012***, 48*, 10669-10671.

31. Peng, H.; Cheng, Y.; Dai, C.; King, A. L.; Predmore, B. L.; Lefer, D. J.; Wang, B. A Fluorescent Probe for Fast and Quantitative Detection of Hydrogen Sulfide in Blood. *Angewandte Chemie* **2011***, 50*, 9672-9675.

32. Chen, B.; Li, W.; Lv, C.; Zhao, M.; Jin, H.; Jin, H.; Du, J.; Zhanga, L.; Tang, X. Fluorescent Probe for Highly Selective and Sensitive Detection of Hydrogen Sulfide in Living Cells and Cardiac Tissues. *Analyst* **2013***, 138*, 946-951.

33. Lippert, A. R.; New, E. J.; Chang, C. J. Reaction-Based Fluorescent Probes for Selective Imaging of Hydrogen Sulfide in Living Cells. *Journal of the American Chemical Society* **2011***, 133*, 10078-10080.

34. Xuan, W.; Sheng, C.; Cao, Y.; He, W.; Wang, W. Fluorescent Probes for the Detection of Hydrogen Sulfide in Biological Systems. *Angewandte Chemie* **2012***, 51*, 2282-2284.

35. Liu, C.; Pan, J.; Li, S.; Zhao, Y.; Wu, L. Y.; Berkman, C. E.; Whorton, A. R.; Xian, M. Capture and Visualization of Hydrogen Sulfide by a Fluorescent Probe. *Angewandte Chemie* **2011***, 50*, 10327-10329.

36. Montoya, L. A.; Pearce, T. F.; Hansen, R. J.; Zakharov, L. N.; Michael D. Pluth, M. D., Development of Selective Colorimetric Probes for Hydrogen Sulfide Based on Nucleophilic Aromatic Substitution. *Journal of Organic Chemistry* **2013***, 78*, 6550-6557.

37. Vandiver, M. S.; Snyder, S. H. Hydrogen Sulfide: A Gasotransmitter of Clinical Relevance. *Journal of Molecular Medicine* **2012***, 90*, 255-263.

38. Wang, R. Two's Company, Three's a Crowd: can H_2S be the Third Endogenous Gaseous Transmitter? *FASEB Journal* **2002***, 16*, 1792-1798.

39. Kasparek, M. S.; Linden, D. R.; Kreis, M. E.; Sarr, M. G. Gasotransmitters in the Gastrointestinal Tract. *Surgery* **2008***, 143*, 455-459.

40. Whiteman, M.; Cheung, N. S.; Zhu, Y. -.; Chu, S. H.; Siau, J. L.; Wong, B. S.; Armstrong, J. S.; Moore, P. K. Hydrogen Sulphide: A Novel Inhibitor of Hypochlorous Acid-Mediated Oxidative Damage in the Brain? *Biochemical and Biophysical Research Communications* **2005***, 326*, 794-798.

41. Mitsuhashi, H.; Yamashita, S.; Ikeuchi, H.; Kuroiwa, T.; Kaneko, Y.; Hiromura, K.; Ueki, K.; Nojima, Y. Oxidative Stress-Dependent Conversion of Hydrogen Sulfide to Sulfite by Activated Neutrophils. *Shock* **2005***, 24*, 529-534.

42. Whiteman, M.; Armstrong, J. S.; Chu, S. H.; Siau, J.; Wong, B.; Cheung, N. S.; Halliwell, B.; Moore, P. K. The Novel Neuromodulator Hydrogen Sulfide: An Endogenous Peroxynitrite "Scavenger"? *Journal of Neurochemistry* **2004***, 90*, 765-768.

43. Geng, B.; Chang, L.; Pan, C.; Qi, Y.; Zhao, J.; Pang, Y.; Du, J.; Tang, C. Endogenous Hydrogen Sulfide Regulation of Myocardial Injury Induced by Isoproterenol. *Biochemical and Biophysical Research Communications* **2004***, 318*, 756-763.

44. Mishra, P. K.; Tyagi, N.; Sen, U.; Givvimani, S.; Tyagi, S. C. H_2S Ameliorates Oxidative and Proteolytic Stresses and Protects the Heart Against Adverse Remodeling in Chronic Heart Failure. *American Journal of Physiology* **2010***, 298*, H451-H456.

45. Zhao, W.; Zhang, J.; Lu, Y.; Wang, R. The Vasorelaxanteffect of H_2S as Anovelendogenous Gaseous K_{ATP} Channel Opener. *EMBO Journal* **2001***, 20*, 6008-6016.

46. Kiss, L.; Deitch, E. A.; Szabo, C. Hydrogen Sulfide Decreases Adenosine Triphosphate Levels in Aortic Rings and Leads to Vasorelaxation via Metabolic Inhibition. *Life Sciences* **2008***, 83*, 589-594.

47. Jiang, B.; Tang, G.; Cao, K.; Wu, L.; Wang, R. Molecular Mechanism for H_2S-Induced Activation of K_{ATP} Channels. *Antioxidants & Redox Signaling* **2010***, 12*, 1167-1178.

48. Ali, M. Y.; Ping, C. Y.; Mok, Y. Y.; Ling, L.; Whiteman, M.; Bhatia, M.; Moore, P. K. Regulation of Vascular Nitric Oxide *in vitro* and *in vivo*; A New Role for Endogenous Hydrogen Sulphide? *British Journal of Pharmacology* **2006***, 149*, 625-634.

49. Kubo, S.; Doe, I.; Kurokawa, Y.; Nishikawa, H.; Kawabata, A. Direct Inhibition of Endothelial Nitric Oxide Synthase by Hydrogen Sulfide: Contribution to Dual Modulation of Vascular Tension. *Toxicology* **2007***, 232*, 138-146.

50. Hosoki, R.; Matsuki, N.; Kimura, H. The Possible role of Hydrogen Sulfide as an Endogenous Smooth Muscle Relaxant in Synergy with Nitric Oxide. *Biochemical and Biophysical Research Communications* **1997***, 237*, 527-531.

51. Goubern, M.; Andriamihaja, M.; Nubel, T.; Blachier, F.; Bouillaud, F. Sulfide, The First Inorganic Substrate for Human Cells. *FASEB Journal* **2007***, 21*, 1699-1706.

52. Whitfield, N. L.; Kreimier, E. L.; Verdial, F. C.; Skovgaard, N.; Olson, K. R. Reappraisal of H_2S/Sulfide Concentration in Vertebrate Blood and its Potential Significance in Ischemic Preconditioning and Vascular Signaling. *American Journal of Physiology* **2008***, 294*, R1930-R1937.

53. Wintner, E. A.; Deckwerth, T. L.; Langston, W.; Bengtsson, A.; Leviten, D.; Hill, P.; Insko, M. A.; Dumpit, R.; Vanden Ekart, E.; Toombs, C. F.; Szabo, C. A Monobromobimane-Based Assay to Measure the Pharmacokinetic Profile of Reactive Sulphide Species in Blood. *British journal of pharmacology* **2010***, 160*, 941-957.

54. Guidotti, T. L. Hydrogen Sulfide: Advances in Understanding Human Toxicity. *International Journal of Toxicology* **2010***, 29*, 569-581.

55. Kamoun, P. Endogenous Production of Hydrogen Sulfide in Mammals. *Amino Acids* **2004***, 26*, 243-254.

56. Wallace, J. L.; Caliendo, G.; Santagada, V.; Cirino, G.; Fiorucci, S. Gastrointestinal Safety and Anti-Inflammatory Effects of a Hydrogen Sulfide–Releasing Diclofenac Derivative in the Rat. *Gastroenterology* **2007***, 132*, 261-271.

57. Mundargi, R. C.; Babu, V. R.; Rangaswamy, V.; Patel, P.; Aminabhavi, T. M. Nano/Micro Technologies for Delivering Macromolecular Therapeutics using Poly(DL-Lactide-co-Glycolide) and its Derivatives. *Journal of Controlled Release* **2008***, 125*, 193-209.

58. Uhrich, K. E.; Cannizzaro, S. M.; Langer, R. S.; Shakesheff, K. M. Polymeric Systems for Controlled Drug Release. *Chemical Reviews* **1999***, 99*, 3181-3198.

59. Nair, L. S.; Laurencin, C. T. Biodegradable Polymers as Biomaterials. *Progress in Polymer Science* **2007***, 32*, 762-798.

60. Jing, F.; Hillmyer, M. A. A Bifunctional Monomer Derived from Lactide for Toughening Polylactide. *Journal of the American Chemical Society* **2008***, 130*, 13826-13827.

61. Fiore, G. L.; Jing, F.; Young, V. G., Jr.; Cramer, C. J.; Hillmyer, M. A. High Tg Aliphatic Polyesters by the Polymerization of Spirolactide Derivatives. *Polymer Chemistry* **2010***, 1*, 870-877.

62. Castillo, J. A.; Borchmann, D. E.; Cheng, A. Y.; Wang, Y.; Hu, C.; Garcia, A. J.; Weck, M. Well-Defined Poly(lactic acid)s Containing Poly(ethylene glycol) Side Chains. *Macromolecules (Washington, DC, U. S.)* **2012***, 45*, 62-69.

63. Uygun, M.; Tasdelen, M. A.; Yagci, Y. Influence of Type of Initiation on Thiol-ene "Click" Chemistry. *Macromolecular Chemistry and Physics* **2010***, 211*, 103-110.

64. Chu, C. M.; Gao, S.; Sastry, M. N. V.; Yao, C. F. Iodine-Catalyzed Michael Addition of Mercaptans to α,β-Unsaturated Ketones Under Solvent-Free Conditions. *Tetrahedron letters* **2005***, 46*, 4971-4974.

65. Manaka, A.; Sato, M. Synthesis of Aromatic Thioamide from Nitrile Without Handling of Gaseous Hydrogen Sulfide. *Synthetic Communications* **2005***, 35*, 761-764.

66. Gupta, A. P.; Kumar, V. New Emerging Trends in Synthetic Biodegradable Polymers - Polylactide: A Critique. *European Polymer Journal* **2007***, 43*, 4053-4074.

67. Kiesewetter, M. K.; Shin, E. J.; Hedrick, J. L.; Waymouth, R. M. Organocatalysis: Opportunities and Challenges for Polymer Synthesis. *Macromolecules* **2010***, 43*, 2093-2107.

68. Nederberg, F.; Connor, E. F.; Moeller, M.; Glauser, T.; Hedrick, J. L. New Paradigms for Organic Catalysts: The First Organocatalytic Living Polymerization. *Angewandte Chemie, International Edition* **2001***, 40*, 2712-2715.

69. Otsuka, H.; Nagano, S.; Kobashi, Y.; Maeda, T.; Takahara, A. A Dynamic Covalent Polymer Driven by Disulfide Metathesis Under Photoirradiation. *Chemical Communications* **2010***, 46*, 1150-1152.

70. Runge, M. B.; Mwangi, M. T.; Miller, A. L. I.; Perring, M.; Bowden, N. B. Cascade Reactions using LiAlH4 and Grignard Reagents in the Presence of Water. *Angewandte Chemie, International Edition* **2008***, 47*, 935-939.

71. Mwangi, M. T.; Runge, M. B.; Hoak, K. M.; Schulz, M. D.; Bowden, N. B. A Materials Approach to Site-Isolation of Grubbs Catalysts from Incompatible Solvents and m-Chloroperoxybenzoic Acid. *Chemistry - A European Journal* **2008***, 14*, 6780-6788.

72. Crank, J. *The Mathematics of Diffusion;* Clarendon Press: Oxford, 1970; .

73. Shah, M. R.; Noble, R. D.; Clough, D. E. Measurement of Sorption and Diffusion in Nonporous Membranes by Transient Permeation Experiments. *Journal of Membrane Science* **2007***, 287*, 111-118.

74. Watson, J. M.; Zhang, G. S.; Payne, P. A. The Diffusion Mechanism in Silicone Rubber. *Journal of Membrane Science* **1992***, 73*, 55-71.

75. Tamai, Y.; Tanaka, H.; Nakanishi, K. Molecular Simulation of Permeation of Small Penetrants through Membranes. 1. Diffusion Coefficients. *Macromolecules* **1994***, 27*, 4498-4508.

76. Tamai, Y.; Tanaka, H.; Nakanishi, K. Molecular Simulation of Permeation of Small Penetrants through Membranes. 2. Solubilities. *Macromolecules* **1995***, 28*, 2544-2554.

77. Mwangi, M. T.; Schulz, M. D.; Bowden, N. B. Sequential Reactions with Grubb's Catalyst and AD-mix-α/β Using PDMS Thimbles. *Organic Letters* **2009***, 11*, 33-36.

78. Miller, A. L.; Bowden, N. B. Site-Isolation and Recycling of PdCl2 using PDMS Thimbles. *Journal of Organic Chemistry* **2009***, 74*, 4834-4840.

79. Miller, A. L. I.; Bowden, N. B. A Materials Approach to the Dual-Site Isolation of Catalysts Bonded to Linear Polymers and Small, Ionic Molecules for use in One-Pot Cascade Reactions. *Advanced Materials* **2008***, 20*, 4195-4199.

80. Miller, A. L. I.; Bowden, N. B. Room Temperature Ionic Liquids: New Solvents for Schrock's Catalyst and Removal using Polydimethylsiloxane Membranes. *Chemical Communications* **2007***, 20*, 2051-2053.

81. Mwangi, M. T.; Runge, M. B.; Bowden, N. B. Occlusion of Grubbs' Catalysts in Active Membranes of Polydimethylsiloxane: Catalysis in Water and New Functional Group Selectivities. *Journal of the American Chemical Society* **2006***, 128*, 14434-14435.

82. Lee, J. N.; Park, C.; Whitesides, G. M. Solvent Compatibility of Poly(dimethylsiloxane)-Based Microfluidic Devices. *Analytical Chemistry* **2003***, 73*, 6544-6554.

83. Balmer, T. E.; Schmid, H.; Stutz, R.; Delamarche, E.; Michel, B.; Spencer, N. D.; Wolf, H. Diffusion of Alkanethiols in PDMS and Its Implications on Microcontact Printing (μCP). *Langmuir* **2005***, 21*, 622-632.

84. Banerjee, S.; Asrey, R.; Saxena, C.; Vyas, K.; Bhattacharya, A. Kinetics of Diffusion of Water and Dimethylmethylphosphonate Through Poly(dimethylsiloxane) Membrane Using Coated Quartz Piezoelectric Sensor. *Journal of Applied Polymer Science* **1997***, 65*, 1789-1794.

85. Runge, M. B.; Mwangi, M. T.; Bowden, N. B. New Selectivities from Old Catalysts. Occlusion of Grubbs' Catalysts in PDMS to Change their Reactions. *Journal of Organometallic Chemistry* **2006***, 691*, 5278-5288.

86. Schaefer, T.; Di Paolo, R. E.; Franco, R.; Crespo, J. G. Elucidating Interactions of Ionic Liquids with Polymer Films using Confocal Raman Spectroscopy. *Chemical Communications* **2005***, 20*, 2594-2596.

87. Madhavan, N.; Weck, M. Highly Active Polymer-Supported (salen)Al Catalysts for the Enantioselective Addition of Cyanide to α,β-Unsaturated Imides. *Advanced Synthesis & Catalysis* **2008***, 350*, 419-425.

88. Harned, A. M.; He, H. S.; Toy, P. H.; Flynn, D. L.; Hanson, P. R. Multipolymer Solution-Phase Reactions: Application to the Mitsunobu Reaction. *Journal of the American Chemical Society* **2005***, 127*, 52-53.

89. Ryo, A.; Shu, K. "Microencapsulated" and Related Catalysts for Organic Chemistry and Organic Synthesis. *Chemical reviews* **2009***, 109*, 594-642.

90. Bergbreiter, D. E.; Tian, J.; Hongfa, C. Using Soluble Polymer Supports To Facilitate Homogeneous Catalysis. *Chemical Reviews* **2009***, 109*, 530-582.

91. Schmidt, B.; Patel, J.; Ricard, F. X.; Brechtelsbauer, C. M.; Norman Lewis, N. Application of Process Modelling Tools in the Scale-Up of Pharmaceutical Crystallisation Processes. *Organic Process Research & Development* **2004***, 8*, 998-1008.

92. Mueller, S.; Afraz, M. C.; De Gelder, R.; Ariaans, G. J. A.; Kaptein, B.; Broxterman, Q. B.; Bruggink, A. Design and Evaluation of Inclusion Resolutions, Based on Readily Available Host Compounds. *Journal of Organic Chemistry* **2005***, 6*, 1082-1092.

93. Cesur, S.; Gokbel, S. Crystallization of Mefenamic Acid and Polymorphs. *Crystal Research and Technology* **2008***, 43*, 720-728.

94. Murnane, D.; Marriott, C.; Martin, G. P. Polymorphic Control of Inhalation Microparticles Prepared by Crystallization. *International journal of pharmaceutics* **2008***, 361*, 141-149.

95. Otsuka, M.; Nishizawa, J. I.; Shibata, J.; Ito, M. Quantitative Evaluation of Mefenamic Acid Polymorphs by Terahertz–Chemometrics. *Journal of Pharmaceutical Sciences* **2010***, 99*, 4048-4053.

96. Pranzo, M. B.; Cruickshank, D.; Coruzzi, M.; Caira, M. R.; Bettini, R. Enantiotropically Related Albendazole Polymorphs. *Journal of Pharmaceutical Sciences* **2010***, 99*, 3731-3742.

97. Sheth, A. R.; Bates, S.; Muller, F. X.; Grant, D. J. W. Polymorphism in Piroxicam. *Crystal Growth & Design* **2004***, 4*, 1091-1098.

98. Qi, S.; Weuts, I.; De Cort, S.; Stokbroekx, S.; Leemans, R.; Reading, M.; Belton, P.; Craig, D. Q. M. An Investigation into the Crystallization Behaviour of an Amorphous Cryomilled Pharmaceutical Material Above and Below the Glass Transition Temperature. *Journal of Pharmaceutical Sciences* **2009***, 99*, 196-208.

99. Dijkstra, H. P.; Van Klink, G. P. M.; Van Koten, G. The Use of Ultra- and Nanofiltration Techniques in Homogeneous Catalyst Recycling. *Accounts of Chemical Research* **2002***, 35*, 798-810.

100. Dijkstra, M. F. J.; Bach, S.; Ebert, K. A Transport Model for Organophilic Nanofiltration. *Journal of Membrane Science* **2006***, 286*, 60-68.

101. Geens, J.; De Witte, B.; Van der Brugge, B. Removal of API's (Active Pharmaceutical Ingredients) from Organic Solvents by Nanofiltration. *Separation Science and Technology* **2007***, 42*, 2435-2449.

102. Pink, C. J.; Wong, H. -.; Ferreira, F. C.; Livingston, A. G. Organic Solvent Nanofiltration and Adsorbents; A Hybrid Approach to Achieve Ultra Low Palladium Contamination of Post Coupling Reaction Products. *Organic Process Research & Development* **2008***, 12*, 589-595.

103. Silva, P.; Peeva, L. G.; Livingston, A. G. Nanofiltration in Organic Solvents. *Advanced Membrane Technology and Applications* **2008**, 451-467.

104. Gould, R. M.; White, L. S.; Wildemuth, C. R. Membrane Separation in Solvent Lube Dewaxing. *Environmental Progress* **2001***, 20*, 12-16.

105. Patterson, D. A.; Lau, L. Y.; Roengpithya, C.; Gibbins, E. J.; Livingston, A. G. Membrane Selectivity in the Organic Solvent Nanofiltration of Trialkylamine Bases. *Desalination* **2008***, 216*, 248-256.

106. See-Toh, Y. H.; Silva, M.; Livingston, A. Controlling Molecular Weight Cut-Off Curves for Highly Solvent Stable Organic Solvent Nanofiltration (OSN) Membranes. *Journal of Membrane Science* **2008***, 324*, 220-232.

107. See-Toh, Y. H.; Ferreira, F. C.; Livingston, A. G. The Influence of Membrane Formation Parameters on the Functional Performance of Organic Solvent Nanofiltration Membranes. *Journal of Membrane Science* **2007***, 299*, 236-250.

108. Peeva, L. G.; Sairam, M.; Livingston, A. G. Nanofiltration Operations in Nonaqueous Systems. *Comprehensive Membrane Science and Engineering* **2010***, 2*, 91-113.

109. Nair, D.; Wong, H. -.; Han, S.; Vankelecom, I. F. J.; White, L. S.; Livingston, A. G.; Boam, A. T. Extending Ru-BINAP Catalyst Life and Separating Products from Catalyst Using Membrane Recycling. *Organic Process Research & Development* **2009***, 13*, 863-869.

110. Anraku, Y.; Kishimura, A.; Oba, M.; Yamasaki, Y.; Kataoka, K. Spontaneous Formation of Nanosized Unilamellar Polyion Complex Vesicles with Tunable Size and Properties. *Journal of the American Chemical Society* **2010***, 132*, 1631-1636.

111. Asatekin, A.; Gleason, K. K. Polymeric Nanopore Membranes for Hydrophobicity-Based Separations by Conformal Initiated Chemical Vapor Deposition. *Nano Letters* **2011***, 11*, 677-686.

112. Jirage, K. B.; Hulteen, J. C.; Martin, C. R. Nanotubule-Based Molecular-Filtration Membranes. *Science* **1997***, 278*, 655-658.

113. O'Donnell, J. L.; Thaitrong, N.; Nelson, A. P.; Hupp, J. T. Liquid/Liquid Interface Polymerized Porphyrin Membranes Displaying Size-Selective Molecular and Ionic Permeability. *Langmuir* **2006***, 22*, 1804-1809.

114. Snurr, R. Q.; Hupp, J. T.; Nguyen, S. T. Prospects for Nanoporous Metal-Organic Materials in Advanced Separations Processes. *AIChE Journal* **2004***, 50*, 1090-1095.

115. Chen, B.; Xiang, S.; Qian, G. Metal-Organic Frameworks with Functional Pores for Recognition of Small Molecules. *Accounts of Chemical Research* **2010***, 43*, 1115-1124.

116. Liu, D. H.; Zhong, C. L. Understanding Gas Separation in Metal-Organic Frameworks Using Computer Modeling. *Journal of Materials Chemistry* **2010***, 20*, 10308-10318.

117. Mueller, U.; Schubert, M.; Teich, F.; Puetter, H.; Schierle-Arndt, K.; Pastre, J. Metal-Organic Frameworks-Prospective Industrial Applications. *Journal of Materials Chemistry* **2006***, 16*, 626-636.

118. Thomas, K. M. Adsorption and Desorption of Hydrogen on Metal-Organic Framework Materials for Storage Applications: Comparison with other Nanoporous Materials. *Dalton Transactions* **2009***, 9*, 1487-1505.

119. Zhao, D.; Timmons, D. J.; Yuan, D.; Zhou, H. Tuning the Topology and Functionality of Metal-Organic Frameworks by Ligand Design. *Accounts of Chemical Research* **2011***, 44*, 123-133.

120. Zou, R.; Abdel-Fattah, A. I.; Xu, H.; Zhao, Y.; Hickmott, D. D. Storage and Separation Applications of Nanoporous Metal-Organic Frameworks. *CrystEngComm* **2010***, 12*, 1337-1353.

121. Perring, M.; Bowden, N. B. Assembly of Organic Monolayers on Polydicyclopentadiene. *Langmuir* **2008***, 24*, 10480-10487.

122. Lee, J. K.; Gould, G. L. Polydicyclopentadiene Based Aerogel: a New Insulation Material. *Journal of Sol-Gel Science and Technology* **2007***, 44*, 29-40.

123. Bellan, L. M.; Coates, G. W.; Craighead, H. G. Poly(dicyclopentadiene) Submicron Fibers Produced by Electrospinning. *Macromolecular Rapid Communications* **2006***, 27*, 511-515.

124. Della Martina, A.; Graf, R.; Hilborn, J. G. Macroporous Poly(dicyclopentadiene) Beads. *Journal of Applied Polymer Science* **2005***, 96*, 407-415.

125. Rule, J. D.; Moore, J. S. ROMP Reactivity of endo- and exo-Dicyclopentadiene. *Macromolecules* **2002***, 35*, 7878-7882.

126. Cowen, J. A.; Liu, H.; Xiao, P.; Imhof, R. E. Optothermal *in vitro* Diffusion Measurements Through Silicone Membranes. *Review of Scientific Instruments* **2003***, 74*, 764-766.

127. Du Plessis, J.; Pugh, W. J.; Judefeind, A.; Hadgraft, J. The Effect of the Nature of H-Bonding Groups on Diffusion Through PDMS Membranes Saturated with Octanol and Toluene. *Journal of Pharmaceutical Sciences* **2002***, 15*, 63-69.

128. Phillip, W. A.; Amendt, M.; O'Neill, B.; Chen, L.; Hillmyer, M. A.; Cussler, E. L. Diffusion and Flow Across Nanoporous Polydicyclopentadiene-Based Membranes. *ACS Applied Materials & Interfaces* **2009***, 1*, 472-480.

129. Sarveiya, V.; Templeton, J. F.; Benson, H. A. E. Effect of Lipophilic Counter-Ions on Membrane Diffusion of Benzydamine. *European Journal of Pharmaceutical Sciences* **2005***, 26*, 39-46.

130. Kovacic, S.; Krajnc, P.; Slugovc, C. Inherently Reactive PolyHIPE Material From Dicyclopentadiene. *Chemical Communications* **2010***, 46*, 7504-7506.

131. Amendt, M. A.; Chen, L.; Hillmyer, M. A. Formation of Nanostructured Poly(dicyclopentadiene) Thermosets Using Reactive Block Polymers. *Macromolecules* **2010***, 43*, 3934-3934.

132. Jeong, W.; Kessler, M. R. Toughness Enhancement in ROMP Functionalized Carbon Nanotube/Polydicyclopentadiene Composites. *Chemistry of Materials* **2008***, 20*, 7060-7068.

133. Kessler, M. R.; White, S. R. Cure Kinetics of the Ring-Opening Metathesis Polymerization of Dicyclopentadiene. *Journal of Polymer Science, Part A: Polymer Chemistry* **2002***, 40*, 2373-2383.

134. Perring, M.; Long, T. R.; Bowden, N. B. Epoxidation of the Surface of Polydicyclopentadiene for the Self-Assembly of Organic Monolayers. *Journal of Materials Chemistry* **2010***, 20*, 8679-8685.

135. Stuart, B.; George, W. O.; McIntyre, P. S. *Modern Infrared Spectroscopy;* John Wiley & Sons: New York, 1996; .

136. Vankelecom, I.; Vercruysse, K.; Moens, N.; Parton, R.; Sudhakar, J.; Jacobs, P. Solvent-free Oxidation Reactions with Ti-MCM-41 and TS-1 Catalysts Occluded in Polydimethylsiloxane (PDMS) Membranes. *Chemical Communications* **1997***, 1*, 137-138.

137. Berens, A. R.; Hopfenberg, H. B. Diffusion of Organic Vapors at Low Concentrations in Glassy PVC, Polystyrene, and PMMA. *Journal of Membrane Science* **1982***, 10*, 283-303.

138. Gupta, A.; Bowden, N. B. Separation of cis-Fatty Acids from Saturated and trans-Fatty Acids by Nanoporous Polydicyclopentadiene Membranes. *ACS Applied Materials & Interfaces* **2013***, 5*, 924-933.

139. Gupta, A.; Long, T. R.; Rethwisch, D. G.; Bowden, N. B. Retention of Palladium and Phosphine Ligands using Nanoporous Polydicyclopentadiene Thimbles. *Chemical Communications* **2011***, 47*, 10236-10238.

140. Della Martina, A.; Garamszegi, L.; Hilborn, J. G. Pore Size Modification of Macroporous Crosslinked Poly(dicyclopentadiene). *Journal of Polymer Science, Part A: Polymer Chemistry* **2003***, 41*, 2036-2046.

141. Lee, J. K.; Liu, X.; Yoon, S. H.; Kessler, M. R. Thermal Analysis of Ring-Opening Metathesis Polymerized Healing Agents. *Journal of Polymer Science, Part B: Polymer Physics* **2007***, 45*, 1771-1780.

142. Liu, X.; Lee, J. K.; Yoon, S. H.; Kessler, M. R. Characterization of Diene Monomers as Healing Agents for Autonomic Damage Repair. *Journal of Applied Polymer Science* **2006***, 101*, 1266-1272.

143. Roy, D.; Semsarilar, M.; Guthrie, J. T.; Perrier, S. Cellulose Modification by Polymer Grafting: A Review. *Chemical Society Reviews* **2009***, 38*, 2046-2064.

144. Hoekstra, N.; Lao, E. Reaction Injection Molding Tooling for Structural Reinforcement of Polydicyclopentadiene. *Annual Technical Conference - Society of Plastics Engineers* **2008***, 66*, 14-18.

145. Kirkby, E. L.; Michaud, V. J.; Manson, J. A. E.; Sottos, N. R.; White, S. R. Performance of Self-Healing Epoxy with Microencapsulated Healing Agent and Shape Memory Alloy Wires. *Polymer* **2009***, 50*, 5533-5538.

146. Mathers, R. T.; Damodaran, K.; Rendos, M. G.; Lavrich, M. S. Functional Hyperbranched Polymers Using Ring-Opening Metathesis Polymerization of Dicyclopentadiene with Monoterpenes. *Macromolecules* **2009***, 42*, 1512-1518.

147. Toohey, K. S.; Sottos, N. R.; White, S. R. Characterization of Microvascular-Based Self-healing Coatings. *Experimental Mechanics* **2009***, 49*, 707-717.

148. Mol, J. C. Industrial Applications of Olefin Metathesis. *Journal of Molecular Catalysis A: Chemical* **2004***, 213*, 39-45.

149. Mora, M. F.; Giacomelli, C. E.; Garcia, C. D. Electrophoretic Effects of the Adsorption of Anionic Surfactants to Poly(dimethylsiloxane)-Coated Capillaries. *Analytical Chemistry* **2007***, 79*, 6675-6681.

150. Sugiura, S.; Edahiro, J. I.; Sumaru, K.; Kanamori, T. Surface Modification of Polydimethylsiloxane with Photo-Grafted Poly(Ethylene Glycol) for Micropatterned Protein Adsorption and Cell Adhesion. *Colloids and Surfaces, B: Biointerfaces* **2008***, 63*, 301-305.

151. Wang, A. J.; Feng, J. J.; Fan, J. Covalent Modified Hydrophilic Polymer Brushes onto Poly(Dimethylsiloxane) Microchannel Surface for Electrophoresis Separation of Amino Acids. *Journal of Chromatography A* **2008***, 1192*, 173-179.

152. Zhu, X. Y.; Jun, Y.; Staarup, D. R.; Major, R. C.; Danielson, S.; Boiadjiev, V.; Gladfelter, W. L.; Bunker, B. C.; Guo, A. Grafting of High-Density Poly(Ethylene Glycol) Monolayers on Si(111). *Langmuir* **2001***, 17*, 7798-7803.

153. Gauthier, M. A.; Gibson, M. I.; Klok, H. A. Synthesis of Functional Polymers by Post-Polymerization Modification. *Angewandte Chemie, International Edition* **2009***, 48*, 48-58.

154. Iha, R., K.; Wooley, K. L.; Nystrom, A. M.; Burke, D. J.; Kade, M. J.; Hawker, C. J. Applications of Orthogonal "Click" Chemistries in the Synthesis of Functional Soft Materials. *Chemical Reviews* **2009***, 109*, 5620-5686.

155. Matyjaszewski, K.; Tsarevsky, N. V. Nanostructured Functional Materials Prepared by Atom Transfer Radical Polymerization. *Nature Chemistry* **2009***, 1*, 276-288.

156. McClory, C.; Chin, S. J.; McNally, T. Polymer/Carbon Nanotube Composites. *Australian Journal of Chemistry* **2009***, 62*, 762-785.

157. Sreenivasan, R.; Gleason, K. K. Overview of Strategies for the CVD of Organic Films and Functional Polymer Layers. *Chemical Vapor Deposition* **2009***, 15*, 77-90.

158. Butler, J. D.; Donald, M. B.; Ding, Z.; Fettinger, J. C.; Kurth, M. J. Phenylsulfonyl as a Directing Group for Nitrile Oxide Cycloadditions and mCPBA Epoxidations. *Tetrahedron Letters* **2009***, 50*, 5110-5112.

159. Hu, H.; Yu, M.; Li, F.; Chen, Z.; Gao, X.; Xiong, L.; Huang, C. Facile Epoxidation Strategy for Producing Amphiphilic Up-Converting Rare-Earth Nanophosphors as Biological Labels. *Chemistry of Materials* **2008***, 20*, 7003-7009.

160. Leemhuis, M.; Akeroyd, N.; Kruijtzer, J. A. W.; van Nostrum, C. F.; Hennink, W. E. Synthesis and Characterization of Allyl Functionalized Poly(α-hydroxy) acids and their Further Dihydroxylation and Epoxidation. *European Polymer Journal* **2008***, 44*, 308-317.

161. Ogrin, D.; Chattopadhyay, J.; Sadana, A. K.; Billups, W. E.; Barron, A. R. Epoxidation and Deoxygenation of Single-Walled Carbon Nanotubes: Quantification of Epoxide Defects. *Journal of the American Chemical Society* **2006***, 128*, 11322-11323.

162. Wang, S.; Qiu, J. Modification of Epoxy Resins via m-Chloroperbenzoic Acid-Epoxidized Carbon Nanotubes. *Journal of Applied Polymer Science* **2009***, 112*, 3322-3326.

163. Bagheri, R.; Marouf, B. T.; Pearson, R. A. Rubber-Toughened Epoxies: A Critical Review. *Polymer Reviews* **2009***, 49*, 201-225.

164. Thomas, J. M.; Raja, R. Catalytic Significance of Organometallic Compounds Immobilized on Mesoporous Silica: Economically and Environmentally Important Examples. *Journal of Organometallic Chemistry* **2004***, 689*, 4110-4124.

165. Hansen, H. S.; Jansson, C.; Tougaard, S. Inelastic Peak Shape Method Applied to Quantitative Surface Analysis of Inhomogeneous Samples. *Journal of Vacuum Science & Technology,* **1992***, 10*, 2938-2944.

166. Tougaard, S. Quantitative Analysis of the Inelastic Background in Surface Electron Spectroscopy. *Surface and Interface Analysis* **1988***, 11*, 453-472.

167. Tougaard, S. Inelastic Background Correction and Quantitative Surface Analysis. *Journal of Electron Spectroscopy and Related Phenomena* **1990***, 52*, 243-271.

168. Hajati, S.; Tougaard, S. XPS for Non-Destructive Depth Profiling and 3D Imaging of Surface Nanostructures. *Analytical and Bioanalytical Chemistry* **2010***, 396*, 2741-2755.

169. He, C. X.; Tabata, Y.; Gao, J. Q. Non-Viral Gene Delivery Carrier and its Three-Dimensional Transfection System. *International Journal of Pharmaceutics* **2010***, 386*, 232-242.

170. Neu, M.; Fischer, D.; Kissel, T. Recent Advances in Rational Gene Transfer Vector Design Based on Poly(Ethylene Imine) and its Derivatives. *Journal of Gene Medicine* **2005***, 7*, 992-1009.

171. Tao, Y. T.; Wu, C. C.; Eu, J. Y.; Lin, W. L.; Wu, K. C.; Chen, C. H. Structure Evolution of Aromatic-Derivatized Thiol Monolayers on Evaporated Gold. *Langmuir* **1997***, 13*, 4018-4023.